A Novel Technique for using Polymers as Optical Interconnects and Sensors for Biological Recognition

by

SEEMA DEEPAK YARDI

DEPARTMENT OF ELECTRONICS AND
COMMUNICATION ENGINEERING

Submitted
in fulfilment of the requirements
of
the degree of

DOCTOR OF PHILOSOPHY

to the

MALAVIYA NATIONAL INSTITUTE OF TECHNOLOGY JAIPUR, INDIA

August 2016

Dedicated in the name of Lord Shriganeshji,

to my father Late Prof. G. S. Pandit

& my mother Smt. Asha G. Pandit …

Acknowledgement

Abstract

Amongst various techniques of bio-sensing, such as impedance based, electrochemical, surface based, mass based, optical sensing of analytes [DNA, Bacteria, viruses] from sample solutions based; optical sensing is found to be most accurate, operating in full UV-VIS-IR range and clean method of sensing. It is important that the sensing surface can be modified, if required to suite the sensing conditions of analytes. The optical signals emitted after the interaction between analytes and reagents are very weak and need tobe transmitted to the signal processing system with signal conditioner circuits in between. As the sizes of the analytes, diagnostic micro-chips is shrinking, the accessibility of signal on chip to the outer world is becoming a difficult problem due to the standard sizes of SMP connectors. The alignment of patterned optical signal carrying waveguides with the fiber connectors in all three directions is an important point of consideration, where the loss in signal is inversely proportional to the square of the distance between the two waveguides. Optical fibers are most commonly used waveguides for carrying signals into and out of the chip in Lab-on –chip applications and communication applications. The connections of fibers at specific locations on the microchips, is a crucial task. It is definitely one of the important reasons, why the growth of diagnostic chips, optically sensitive microchips is not as it was predicted to be. It is in this regard, the bonding of fibers to patterned waveguides on chip and fiber to fiber bonding was undertaken as a research objective. Besides bonding of fibers, sensing strategy is also required to be incorporated in the scheme. Initial study had shown coupling through chain of dielectric microsphere, which was a less efficient method, ring resonator coupling, microsphere grating and rib waveguide coupling, fiber to waveguide coupling with a tapered fiber. Each of these methods required extensive processing, alignment adjustments.

The study undertaken describes use of low power laser machine for bonding fiber to the substrate and a waveguide/ another fiber. Apart from micro- structure fabrication, ablation, lithography etc., lasers find a lot of utility in various areas like precision joining, device fabrication, local heat delivery for surface texturing and local change of microstructure so on and so forth. It is pertinent to mention that the

significance of Laser processing comes owing to the small spot size and fine manoeuvrability of laser beam on various complex topologies at various length scales. This makes such processing widely applicable to the fabrication of standalone optical micro-devices like microspheres, micro-prisms, micro-scale ring resonators, optical switches etc. There is a wide utility of such systems in chemical/ biochemical diagnostics and also communications where the standalone optical devices are heavily employed although printed and patterned structures are not well explored. One of the reasons why chip based printed optical waveguides are less frequently used is the issue of joining such structures with standalone single or multimode optical fibres which otherwise form a concrete basis of the bulk transmissibility of signals in opto-electronic platforms. Diagnostics can become very easy if chip based structures are explored more in comparison to standalone optical components, owing to their high sensitivity and low volume of analytes.

In this study we have developed a strategy of joining of standalone optical fibres to each other and microchip based printed optics (developed on SU8 (M/S Microchem) through lithography) using a SU8 microdrop. The materials explored for the microdrop, required to be essentially bio-materials, having good optical properties, higher refractive index, patternable with good weldability. SU8, a transparent, negative photoresist material came up as the best material for the job. A thin film of a SU8 material formulating an extended waveguide contact has been utilized for bonding with optical fibres by precise heat delivery of a CO_2 lasing system. The laser heat transmitted is used to form a strong bond between the patterned thin film and the optical fibre, with a small SU8 micro-droplet. A similar strategy has been used by joining two optical fibers on a hard substrate [Silicon wafer / Glass] by using a SU8 micro-droplet. Optimization of various dimensional parameters of the bonded assembly has been achieved as a function of laser power, speed, cycle control, spot size so on so forth. The optimization is performed with Design of experiments (DOE) in which Response surface methodology (RSM) based on central composite design (CCD) has been used to evaluate the experimental parameters for the lasing system. Finite element heat transfer model is utilized for finding out the temperature distribution at the joint, the fibre end and the SU8 structure end and further optimization is performed by localizing the heating

zone to the joint area. Exclusive optical [RF] modelling has been performed to estimate the transmissibility of the optical fibers bonded to each other on a surface with SU8 and a similar analysis is done for the free standing waveguides patterned in SU8. Our studies indicate the formation of a Whispering gallery modes [WGM] across the micro-droplet leading to very high transmissibility of the signal. It also shows heavy dependence of the temperature scale on the joint thickness. Finite element software and photonic software are used to understand and control the WGM effect on coupling, output signal & transmission of the signal. Through this work we have thus been able to develop a method for fiber stitching to each other and also to printed optical structures in microchips with smaller confinement, reduced power and lesser time for formulating these joints. The study shows impending advantages of such coupling through microdrop, viz. a) aligned and misaligned separation can provide good coupling between two waveguides; which is not the case in other methods of coupling, where alignment in elevation, lateral, spatial is most important for controlling losses in transmission. b) The laser treated bond provides a strong bond instantly like a tagged or stitched pair of waveguides. c) The lasing action does not affect surrounding microstructures on the microchip. d) The SU8 microdrop can be functionalized, micromachined and processed to suite the bio –sensing / coupling requirements. GFP, BSA protein antigen –antibody binding is sensed, characterized and analysed with this coupler- sensor. Signal sensing and coupling are two important aspects of a system, be it electrical, optical or mechanical control signal. If both these functions are carried out effectively and efficiently by a single component, then it will be considered a multifunction unit.

This study describes successfully fabricated one such component called Laser treated SU8 microdrop. It can be used as an optical signal coupler using WGM effect. It can function as an optical signal sensor, sensing any activity or coating on the functionalized SU8 surface. Interestingly in future study it can be explored as a signal modulator, which modulates output signal with the type of binding, immobilization on the microdrop surface. Construction of the spheres is a real problem and involves Laser irradiation of fiber tip followed by chemical etching which is very low yield process. Micro-spheres are not free from vibrations and as the change of wavelength if in 'pm' level it can be very sensitive to thermal noise or

any other noise. The whole body of the Micro-sphere which is around 100-150 microns in radius needs to be immersed in the analyte thus necessitating the analyte volume to be high which is always very difficult to obtain. The solution that has been developed through this work is as following:

- SU8 microdroplet on a silicon/ glass chip for coupling of standalone optical fiber and fiber/ waveguide.

- Process of application of droplet on microchip is highly innovative and is developed in laboratory.

- Extensive COMSOL Multiphysics simulations performed for investigating the WGM phenomenon on chip.

- Further WGM used in silicon/ glass chips to study rapid GFP protein –G/ antibody binding kinetics.

The whole research work has involved interdisciplinary activities, some of the activities are:

- Analysis of problem statement on coupling between optical fibers for high transmission.

- Simulation of the problem using COMSOL Multi-physics and RSOFT photonics platforms to arrive at a good estimate of the micro-droplet shape which will be used for actual transmission of optical power.

- Exposure of the SU8 micro-droplet which is on glass / ceramic substrate to CO_2 Laser to provide Laser welding.

- Modeling and experimental realization of whispering gallery modes [WGM] inside the spherical & elliptical micro-droplet with aligned and misaligned optical fibers or waveguides.

- Analysis of absorptivity of SU8 and calculation of micro-volume of SU8 through optical imaging techniques.

- Carrying out Design of Experiment [DOE] for optimization of Laser machine parameters for laser welding of SU8 Microdrolets.

- The SU8 microdrop bonded fiber-to-fiber coupling is extensively optimized , so that it can be used as a sensitive biosensor in sensing analytes in proteolytic activity, BSA protein antigen immobilization, GFP, antigen – antibody binding.

- Design and development of an experimental test set-up for analysis of optical transmittance.

Whispering gallery modes were recognized for the first time in 19th century and described by Rayleigh for sound waves inside surface of St. Paul Cathedral dome. This technology was extended to study of Resonances inside cavity resonators: torroidal, disk, spheroidal, ring using light, based on the principle of continuous total internal reflection. Light waves are confined to circular geometries as the light after one roundtrip, returns at the same point, with same angle of incidence and with the same phase, so that they interfere constructively with themselves forming waves similar to standing waves inside these circular structures. The smaller the size of the cavity the higher is the Q-factor, higher is the power density. We have been able to stitch fibers using relatively large sized microdroplets and been able to tag the micro-droplet with laser processing.

As the SU8 micro-droplet is top irradiated with laser, the heat transfer occurs across the surface of the droplet through its bulk to the substrate (Si or Glass) along a small polar region of the droplet. Depending on the heat transfer coefficient of the substrate if the heat is not conducted away by the substrates it can result in more localized heating although there is a chance of the droplet to totally melt and develop splashes. In this process the heat also flows across the embedded fibers thus melting and partially dissolving the fiber in SU8 so that on resolidification there is strong adherence between the substrate surface and the fiber. The softening of the optical fiber takes place at a temperature of 1600-1710 deg. C. DOE and number of tests carried out on Si and glass substrate for laser based bonding lead to optimized values of laser machine parameters. The strength of the fiber, weld after the laser heat delivery and resolidification period, is qualitatively judged and is accordingly categorized. Optical fibre softening can be reached on Si or glass surface by controlling laser machine parameters.

Thermal direct bonding between the Silicon substrate and the optical fiber (without using SU8) has also been attempted but the bond strength obtained was poor due to an unnecessary spill over of the fiber melt and hence this option was ruled out. The fiber softening temperature could be estimated to be in the higher

range [1600-1710^{0}C] as compared to SU8 so that there is no degradation of the fiber material or SU8. The machining parameters for Laser machining are optimized using Design of Experiment [DOE].

The DOE performed has helped us to carry out systematic and planned method of varying system parameters to get desired output conditions, out of a set of samples. Response surface methodology (RSM) based on central composite design (CCD) used to evaluate the experimental parameters for the lasing system. The Software Design Expert 7.0, with analysis technique ANOVA is used for the parametric optimization of all machining parameters. Both Simulation and experimental results supported the WGM theory, in which the transmissibility of aligned and misaligned fibers, at spatial, lateral separation of 650 µm and 700 µm was [% Tr] > 60%. Transmissibility was checked with aligned and misaligned cases of optical fibers using SU8 microdroplet technology and simulations performed extensively were also validated through experimental data acquisition.

We have plans to apply this technology to the sensitive detection of biological analytes. Figure 4 shows a schematic describing the analyte testing part wherein the SU8 microdroplet was used to find out the binding kinetics between antigen and antibodies. We have been able to see some very preliminary level observations for changing the surface of SU8 into a biosurface which can adhere well to BSA protein and also some micro-organisms.

In this work we have further initiated the ability of high intensity fluorescent detection of micro- organisms using porous PDMS structures infiltrated with Acridine Orange which may result in sensitive detection of biological agents.

Table of Contents

List of Figures

List of Tables & Graphs

Chapter 1
Introduction

Chapter 1
Introduction

1.1   Motivation

Biochips and lab-on-chips are intensely developed into viable, multipurpose, general purpose sensing platforms for bacterial detection, with precision control on bio-chemical reactions, cell manipulation and development of techniques which are low cost, robust, simple and specific to individual analytes. The incidences are increasing where we come across contamination in food and water, personal threats of infection with hospital and places of public uses, security concerns at the national levels. These devices are studied and developed for newly observed symptoms, analytes, their detection with present and novel techniques, identification of these disease carrying or causing agents with available technologies and with a renewed approach. Thus scientists working in this area and regulatory agencies are continuosly on their toes, to provide improvements in the present techniques for accurate analysis of the samples under cnsideration.Thus it is important to develop a sensing system for these microchips which is sensitive, allows direct access to the sites of analyte conjugation, provides means of carrying the signals to and from these micro-locations. According to the trend of various reviews and literature on the detection of biological entities, more stress is given on the techniques of detection. Optical sensing is favoured because of its desirable properties of clean, contactless methodology and number of ways of interpretation of the detected optical signals. The methods proposed for signal launching and detection; largely deploy highly sophisticated, complex test setup, which makes it difficult to work with smaller setups.

Motivation of this work is to provide a means to access optical signals using novel optical inter-connects, from the high density microstructures on the chips and enable to develop diverse sensing techniques around these connectors. Following sections and chapters give elaborate details of the nature of these connectors, the material used, geometrical structure, optical properties and applications of these inter-connects. Present scenario where test and signal monitoring relies on handling of optical signals: It is observed that, there is use of

1.   SMF /MMF connectors: standard in their sizes.

2.   Microscopy.

3.   Standalone optical micro devices like optical switches, microspheres, ring resonators, microprisms.

4.   Increasing number of parallel /array like high density connections, port lines: With micro-dimensions & circuit complexity.

5.   Multilevel PCBs, microchip designs, optical network connections.

6.   Precision fabrication steps and high precision alignment set ups.

It indicates that to make the optical signal measurement or sensing suitable for small and medium system users, there is need of:

1.   Smaller fibre connectors, having lesser number of precision parts, reduced manufacturing cost and a new range of potential applications.

2.   Simpler, low cost fabrication steps and alignment requirements.

3.   Smaller size, reliability of bond and lower losses.

4.   Connectors having Biosensing feature with surface modification / functionalization possibility.

1.2   Aspects of the Optical Interconnect

1.   The interconnect must provide connection between on-chip and off-chip optical waveguides, between two waveguides.

2.   The optical interconnect must be essentially low cost, simple and robust.

3.   Along with signal coupling, signal sensing feature must be incorporated.

4.   The material used for such interconnects must be biocompatible and possess excellent optical properties

5.   The material can be functionalized to suite immobilization of biological analytes.

6.   Provide signal amplification to specific range of optical wavelengths.

1.3   Enhanced Coupling and Biosensing

A sensor, transducer signal in a system is generally weak and need boosting, particularly when it is the biological signal which is being sensed. The optical interconnect will be highly beneficial if it can selectively enhance the microsignal. Signal coupling is another issue, which takes lot of time, alignments and adjustments

to transmit signal with minimum losses across the joint. The proposed interconnect will be extremely valuable if it can help reduce the task of waveguide alignment to some extent and still grant enhanced coupling.

1.4   Scope of our Work

In a typical laboratory environment, where tests and signal monitoring relies on handling of optical signals; use of SMF /MMF connectors, Microscopy or standalone optical micro devices like optical switches, microspheres, ring resonators, microprisms; is most commonly observed. SMF/ MMF connectors are standard in their sizes and most suitable, where frequent connections and disconnections are needed and the dimensions of the work platform housing all optical circuits or networks, is not an important consideration. With the advent of technology, the scaling down feature is observed in almost every field. The circuit sizes are decreasing and the complexity of the circuits leads to increasing number of parallel /array like high density connections, port lines, making the signal handling even more critical. In case of multilevel PCBs, microchip designs, optical network connections, the size of connectors is a crucial design consideration. It is important for such connectors to have low cost, low losses and ease of operation. Optical fiber outer diameter is 125μm whereas the standard ferrule size for fiber connectors varies between 1.25mm to 12.5mm. Therefore smaller fiber connectors, having lesser number of precision parts, may lead to reduced manufacturing cost and provide with a new range of potential applications.

Splicing is another method of joining two fibers, where the fibers can be just held together [mechanical splice] or permanently joined [fusion splice] using heat. Heat is provided by electric arcs, gas flames or CO_2 Lasers. Size of mechanical splice is large and fusion splice needs protector tube for the bare fiber joint. Both types of splicing mechanisms use precision alignment of fibers in X-Y-Z plane.

Another area where the signal coupling becomes difficult, is coupling optical fiber to on chip waveguides of smaller feature size. To address these issues number of signal coupling methods including use of prisms, fiber gratings, vertical taper structures, microspheres with tapered fibers are considered. All these methods need additional precision fabrication steps or high precision alignment set ups.

3

In our work we have conceptualized a simple method of coupling two waveguides [spaced and aligned suitably], using SU8 microdroplet; strengthening the bond using localized precision heat transmission using CO_2 laser. Further the microdroplet is used to sense biochemical activities occurring in the evanescent field zone of its functionalized surface. Thus this coupling method is a permanent coupling method, with number of advantages like stability of bond, reliability of connection, low cost, smallest size [droplet size of diameter 200µm], possibility of connections of multiple fiber and fiber arrays in high density applications, lower losses, less overheads of precision alignment, detachable fiber bonded assembly for flexibility of operation, ease of installation, potential use in number of biosensing applications with proper surface modification so on and so forth.

To outline the Specific objectives of this work:

1. To develop a means for high efficiency optical coupling between optical fibers and printed waveguides for effective transmission of optical signals.

2. To provide means to access optical signals using novel optical interconnects, from the high density chip based optics.

3. To explore alternate polymer materials for both interconnect and sensing.

4. To explore the development of small forces sensing from biological systems and biodiagnostics. (This is more a material exploration with ideas for future directions).

1.5 Future Scope

1. To use elliptical microsleeves of different dimensions, sizes, materials; verify them with simulation software and experiments; use these devices as optical couplers, sensors of biological entities.

2. To get smaller (diameter < 350 microns) SU8 droplets over the two fibers or fiber-waveguide-fiber, may provide improved and optimized solutions for signal transmission and sensing of biological entities.

3. Contact angle of the droplet must be nearing 90° to get a near spherical droplet.

4. Both labelled and label free techniques may be used on Laser exposed and UV exposed microdroplets.

5. A range of porous PDMS - AO materials of differing physical, chemical, optical properties can be produced by varying concentrations of curing agent and Acridine Orange (AO) in polydimethyl Siloxane (PDMS) gel.

6. Experimenting, usage of the Porous PDMS –AO material as wound dressing strip, opto-biosensor, filter or as an implant.

7. To explore the change in the image contrast by looking at the fluorescent PDMS.

8. To study nanolevel locomotory motions of the organisms.

1.6 Organization of the Thesis

The nature of our work, as discussed in subsequent chapters is multidisciplinary. It involved tasks that need knowledge and understanding of diverse range of branches of Science and Engineering. Along with modeling of the problem, extensive experimental work of varied nature and characterization was carried out to achieve the goals. Starting with problem formulation, some of the major activities can be listed as photonic simulation of signal coupling, process of laser heat transmission, simulation of temperature conditions at the time of heat transfer, optimization of process parameters, testing of optical signal, surface modification for biosensing, experimental test setup for sensing biological analytes, fabrication of microstructures, micromachining, use of biomaterials and characterization using high end instrumentation. Thus it was necessary that each major task be separately discussed in a chapter.

In chapter 2 we present the review on different coupling techniques used to transmit optical signal between two optical waveguides. Theoretical discussion on Dielectric microspheres, whispering gallery modes [WGM] phenomenon inside a curved surface is important to highlight applications of microspheres as resonators, biosensors, active and passive photonic devices. Based on the research problem, a novel method of signal coupling between two optical waveguides using elliptical microsleeve is presented. Two simulation softwares COMSOL Multiphysics and RSoft were used to model this bond and explore polymeric materials suitable for the waveguides and the microsleeve. Simulation results supported the possible efficient coupling between optical fiber and polymer waveguide. Chapter 3 discusses implementation aspects of the model conceptualized and simulated in chapter 2.

Photoresist material SU8 with its excellent optical properties is selected as a microdroplet material, to couple the signal and bind the waveguides to substrate and eachother. A model based on laser heat transmission to strengthen the bond by first melting SU8 and then resolidifying it, uses finite element method, COMSOL Solid heat transfer module. Another model is based on optical signal coupling between these bonded waveguides, experiencing WGM inside the curved surface for specific excitation wavelength. Laser machine parameters are optimized on the basis of simulation results and Design of Experiment [DOE] methodology used for the same. Experimental results indicated strength of the coupling bond and measure of optical transmittance across the bond.

In chapter 4, we present review on interaction of biomolecules, various biological entities, with surfaces of a range of different substrate materials. Focus of this study is on A. solid polymeric materials, their sensitivity and specificity towards select analytes. Surface modification and functionalization techniques are discussed to make these material surfaces suitable for the chemical- biochemical actions and reactions required for interacting with the target analytes. As SU8 material is the microdroplet bond material, as discussed in chapter 3, a review on surface modification techniques of SU8 is presented. Next before implementing these techniques on a small SU8 microdroplet, they were used to check surface sensitivity of thin SU8 film to biomolecule protein BSA, with methods like Laser exposure, UV exposure, chemical treatment, acid treatment.

Based on the results UV exposure was selected as a simple and robust method for SU8 microdroplets to immobilize BSA proteins. Also SU8 microdroplet bonding two optical fibers was surface treated for protein immobilization. Characterization of GFP tagged E-coli cells immobilized on UV exposed SU8 microdroplets and as SU8 microdroplet coupler, sensor was done using microscopy.

In chapter 4 B. a new bio material is presented. It is a porous PDMS and AOD material of reddish color and spongy appearance, suitable in filters, band-aids, sensors. Fabrication procedure involves soft lithography technique. With variations in the proportions of constituting materials, conditions of post treatment; a wide range of materials with desired properties and applications can be realized.

Each chapter is concluded with the results of the simulation or experimental work and references.

Chapter 2
Software Simulation:
Polymer Waveguide Coupling
using Elliptical Microsleeve

Chapter 2

Software Simulation: Polymer Waveguide Coupling using Elliptical Microsleeve

2.1 Introduction

Integrated Optics & photonics have intrigued researchers, scientists and application engineers equally for a long time, because of their excellent set of properties and features, innumerable applications encompassing the entire universe. Both the terms broadly deal with quantum mechanical theory, linear, non linear optics, optical engineering, optical communication, simulation and application softwares, branches of science and technology dealing with optics or optics related applications. The operating range of optical frequencies is wide enough to accommodate Ultra violet-Visible –Infrared [UV-VIS-IR] spectrum. Search is always on, for technologies, designs for better quality components, devices, circuits and circuit solutions, providing integration capability, scaled down features, tunability and stable performances in applications ranging from spacecraft engineering, communication engineering, spectrometry, micromachining and bio-sensing. Several approaches are directed towards the development of communication links of high performance laser sources, high efficiency waveguides and high sensitive detectors along with anlog and digital signal conditioning or processing functions. Integrated optics besides compactness also help address issues of losses, cost, alignment, handling of optical signals at various stages of the system under consideration. The area of Integrated Optical Circuits [IOC] which needs further exploration and cost effective approach is signal coupling between external signal carrying, off chip optical fibers, fiber ribbons and on chip waveguide like structures. The large disparity between dimensions of single mode fibers and the on-chip waveguide micro-structures needs tobe handled with critical and precise setup to minimise losses and signal degradation. Thus chip level signal alignment and coupling needs sophisticated instruments and alignment equipments.

In this work of simulation using photonic softwares, some of the important points related to optical signal coupling are considered:

1.   Tapered fibers can be used with the on-chip waveguides using novel elliptical microsleeve structures.

2.   Single fiber, fiber ribbon or array of fibers can be connected to corresponding waveguides

3.   The coupling strategy though used for polymer waveguide material, can be extended and tested for variety of substrate and waveguide materials.

4.   Optical fibers can become part of the IOC with proper pretreatment and on chip support provided by the microsleeve.

5.   Simulation conditions cover boundary conditions like perfect matched layers, perfect conductors etc.

6.   The resultant modal and electric field patterns show the coupling beween two waveguides at desired frequency, occurrence of whispering gallery modes at regular spectral intervals, effective refractive indices, Q-factor, eigen modes.

The photonic simulation softwares, RSOFT Fullwave FDTD [Finite difference time domain] module and COMSOL Multiphysics software with RF module are used to demonstrate elliptical microsleeve supported coupling between an optical fiber and waveguide in an IOC environment. The operating frequency range is in THz covering VIS –IR spectra. Also importance of whispering gallery mode resonators [WGR] and WGR based devices in confinement of light in smallest volume, providing high power density has levitated this humble coupling concept into a versatile WGM phenomenon.

2.2   Whispering Gallery Mode [WGM]: Basic principle

A bent single mode waveguide, upto a certain limit becomes multimodal; if its core width is increased, same as a straight waveguide. Beyond that the inner dielectric interface becomes irrelevant and the outer dielectric interface guides the bent mode, these are whispering gallery modes [WGM]. This phenomenon occurs in monolithic resonators with curved geometrical shapes like cylinder, ring and sphere. Conventional resonators used two or more mirrors, [5] to recirculate optical power, by way of reflection between the highly reflecting, low loss mirrors; to improve resolution, pathlength or to maintain oscillations. Although high Q quality and finesses were features of these resonators, they suffered from low stability due to

vibrations at the low operating frequencies, large size and difficulty in assembly, overall complexity and extremely high costs. Also there were hurdles in the process of miniaturization of such devices. So the focus shifted to devices with curved, polygonal surfaces supporting circulating light with total internal reflection. The circular modes in these monolithic resonators, with high index contrast at the boundaries, low losses, high –Q, pathlength of curvature in multiples of the wavelengths, were called whispering gallery modes. Surface imperfections and material dispersion once controlled, fabrication of these high performance transparent structures became simpler and cheaper. Due to their small sizes and volume, stability was good and on chip integration was possible.
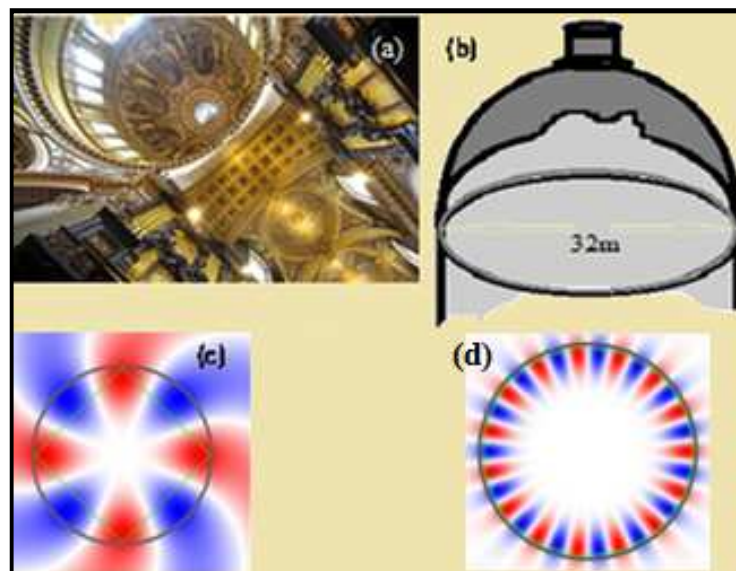
Fig. 2.1 Whispering gallery modes (a) dome structure inside St. Paul Cathedral (b) Schematic of the gallery (c) and (d) whispering gallery modes represented by eigenmode profiles.

In 1912 Lord Rayleigh experienced the phenomenon of sound waves in the form of small whispers, travelling in an oval shape domed St.Paul Cathedral [figure 2.1 (a)] to have reached a longer distance and clearly heard. Thus the term got the name whispering gallery waves and the signal modes called whispering gallery modes. Figure 2.1 shows the St. Paul Cathedral dome like structure and the gallery where this phenomenon was first observed. Optical signal when inserted at a critical angle inside a curved surface, it is completely supported by and propagated along the curved wall of the structure by total internal reflection. Curved surfaces like

micro-spheres support modes with radial, axial and polar fields which demand complicated analysis. Further modifications in the spherical structure like in case of ellipsoidal, hemispherical structures the analysis becomes even more complex. Inside the curved surface a resonance like condition occurs when after one roundtrip, the waves return with the same angle of incidence, at the same point and with the same phase, to form a constructive interference similar to standing waves.

The performance of WGM resonator is best analysed with the following parameters:

1.   Optical path length $L = C_E * n_{eff}$ 2.1

$$= \eta * \lambda_r$$

$$C_E = \pi \left[3(a_1 + b_1) - \sqrt{10\, a_1 b_1 + 3(a_1^2 + b_1^2)} \right]$$

Where C_E is circumference of ellipse with a_1, b_1 as major and minor radii, n_{eff} is effective refractive index of waveguide material, η is mode number of the resonator, λ_r is wavelength at resonance.

2.   Free spectral range [FSR]...2.2

$\upsilon_{FSR} = \upsilon_x - \upsilon_{x+1}$ …….. υ_x frequency of x mode

$\quad = C/(2\Pi r * neff)$ Hz …… C is speed of light

3.   Finesse is a quantity which relates FSR with resonance linewidth or it can be considered interms of sharpness of the resonance curve

F $= 2\Pi (\upsilon_{FSR} /\delta\omega)$ 2.3

$\quad = 2\Pi * Q(\upsilon_{FSR} /\omega_r)$

4.   Q-factor which is the ratio of time averaged energy in the cavity to the energy loss per cycle.

Q $= \omega_r *$ (stored energy / power loss) ….. ω_r angular resonance frequency

$\quad = \omega_r /\delta\omega$ 2.4

$\quad = \omega_r * \tau$ ....τ characteristic decay time

$\quad = \eta * F$

$$= (\eta * \upsilon_{FSR}) / \delta\upsilon \quad ..... \quad \delta\upsilon$$ is full width half max of spectra [see figure 2.2]
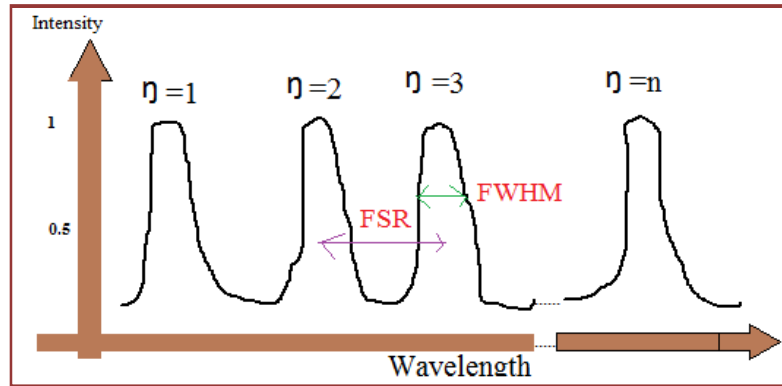
Fig. 2.2 Free spectral range [FSR] and Full width half max [FWHM] for a WGM for modes 1,2..n inside a resonator.

2.3   Simulation using Photonic Software

Any scientific or engineering problem however simple or complicated is best visualized with simulation. There are number of photonic softwares available for dealing with various aspects of photonics, like time domain analysis, beam propagation analysis, frequency domain analysis etc. Softwares like RSoft, Lumerical solutions purely deal with photonics, whereas COMSOL MULTIPYSICS simulation software allows problem defining modeling, involving multidisciplinary problems. It provides coupled physics concept with effect of two or more physical conditions, strongly or weakly coupled on the model under consideration. The Model Builder provides GUI for integrated environment, flexibility in material selection and improved functionality. In this work COMSOL version 4.3 RF module is used for solving the issue of coupling between optical fibers and waveguides using elliptical microsleeve of polymer material. A condition of whispering gallery modes is observed for the selected geometry and input signals. RSOFT fullwave FDTD software is integrated CAD [computer aided design] tool and simulation software which is based on finite difference time domain [FDTD] technique. Within a given index structure and known source of excitation, it can calculate time and space based electromagnetic fields in a broad range of photonic structures. In this work, the simulation is based on the ring resonator concept.

2.4   Coupling Methods

As mentioned previously one of the most critical aspect of design of integrated optics circuits [IOC] is signal coupling from off chips sources to on-chip microstructures and off chip detectors. Optical fibers are normally connected to the test jigs of an optical setup using SMF [single mode fiber] or MMF [multimode fiber] connectors. With ever decreasing feature sizes, the space constraints on chip designs make it impossible to use these connectors for multiple input output connections. The topic of signal coupling is also crucial, from the point of view of size disparity between fibers and waveguides on chip. A great deal of work is done to achieve high efficiency coupling between the fiber and waveguide, by guided means where the light is confined to the optical fibers and waveguides or unguided means where prisms, microlenses are used to concentrate light on the waveguide. Silicon-on-insulator [SOI] devices are known for manufacturability with available technologies, ultra compactness, strong confinement of light and transparency at 1550nm wavelength of optical communication. High index contrast is important for confinement of light and roughly it is defined as the ratio of difference to sum of highest and lowest refractive indices of the waveguide materials, tobe greater than 50%. Polymer materials as optical waveguides, though not having high index contrast as per definition, are very much used in recent cost effective fabrication technologies, for visible operating ranges, choice of materials and flexibility of designs. Tapered coupling with longer taper increases efficiency of coupling in case of fiber to waveguide coupling. The taper can be a vertical taper converter or a grayscale taper to match the dimensions of fiber to waveguide. Inverse tapered couplers, grating based couplers and prism couplers are some of the other types of coupling where sizes of waveguides are important criterion. In all these techniques high precision lithography technology or critical adjustments are involved. In 1990 permanent coupling of fibers to thin film waveguides was presented [12] by cementing fibers to the etched Si-grooves and using evanescent wave coupling. This method was reported tobe suitable for fiber arrays, different waveguide materials and for higher coupling efficiency. Anti-resonant reflective optical waveguide [ARROW], chemically etched tapered fibers were used [13, 14] to couple light with dielectric microsphere resonators having whispering gallery modes to achieve 98% power efficiency. With dual coupling of fused [15] microsphere for WGM

12

resonance, about 99.8% power coupling efficiency was registered. V-grooves and nickel pins [16] were used in an IOC to self align multiple waveguides.

2.5   Related Work

In a detailed review Righini et. al [1] have discussed WGM resonators and emphasized the importance of confinement of optical signal into smaller volumes, be it for photoelectronic devices or photonic devices like fibers, lasers. A new trend in dielectric WGM resonators was found to possess qualities like smaller mode volumes, narrow spectral linewidth and high power density. Along with the linear and spectral properties of WGM resonators [2,6], their applications included passive WGM based devices like filters and active WGM based devices like modulators, oscillators, lasers. Mathematical analysis and analytical approach for basic equations of WGM, excitation, equations for eigenmodes, field equations of WGM [3,4,5,7] resonators were reported along with experimental results of study of modes in dielectric resonators. For the study and analysis of wave propagation in resonators, it is important to provide conditions of perfectly matched layers [PML], like [8] for reduced reflections and increased absorption of incident waves at the boundaries. Implementation of COMSOL simulation for PML boundary conditions of axisymmetric resonators [9], photonic crystal fibers [10] was reported. In an optofluidic biosensor of transmission type, fullwave simulation was used to sense shift in transmission spectrum [11] due to difference in refractive index of target fluid and biomaterial. PML design considerations improved performance parameters of the sensing layers. Role of WGM resonators as sensors for chemicals and biochemicals [17], was discussed in a review to further emphasize the versatility of the WGM resonators. Thus for the purpose of signal communication across a fiber – waveguide joint extremely precise x-y-z alignment of the two is required, with stability of the fiber and size difference between the two taken into account. Overall, the performance of the circuit mainly depends on the success of these joints which are exceedingly difficult to implement.

2.6   Optical Signal Coupling Using Polymer Elliptical Microsleeve: SIMULATION

The skills and techniques involved in completing a fiber to waveguide joint on a small chip can be listed as, 1.tapering of fiber, 2.fabrication of intermediate

microstructure as an interface between the two, 3.alignment of all three to minimize losses, 4.monitoring with high end equipment the efficacy of such a bond.

The design conceptualised in this work mainly minimizes the work on remaining three except the first where fiber tapering is essentially required. Single mode fiber is tapered to its more than core and less than cladding dimensions, aligned with the waveguide or structures on chip using microscope, after using fixing arrangements, a small, uniform, polymeric microsleeve like elliptical or spherical, drop is dispensed on the waveguide joint, to completely cover it. Then the whole assembly may be post processed for a longer shelf life. A novel WGM phenomenon is explored inside the hemispherical or semi-ellipsoidal drop, which assists in transmitting the optical signal across the bond. Simulation of these designs is carried out using RSoft and COMSOL Multiphysics software, to verify feasibility of this concept. The designs are roughly based on a ring resonator, as shown in figure 2.3 (a), which is a planner resonator, coupling signal from one waveguide to other with the special arrangement of structures.

Figures 2.3(b) (c) (d) show the arrangement of fibers with polymer waveguides or with another fiber to couple the signal across the bond. It indicated that a range of materials, along with the variation in dimensions of the two binding waveguides, gap [x-y or x-z] between the two can be explored. Whispering gallery modes are known to exist at the inside surface of a curved object when excited appropriately.
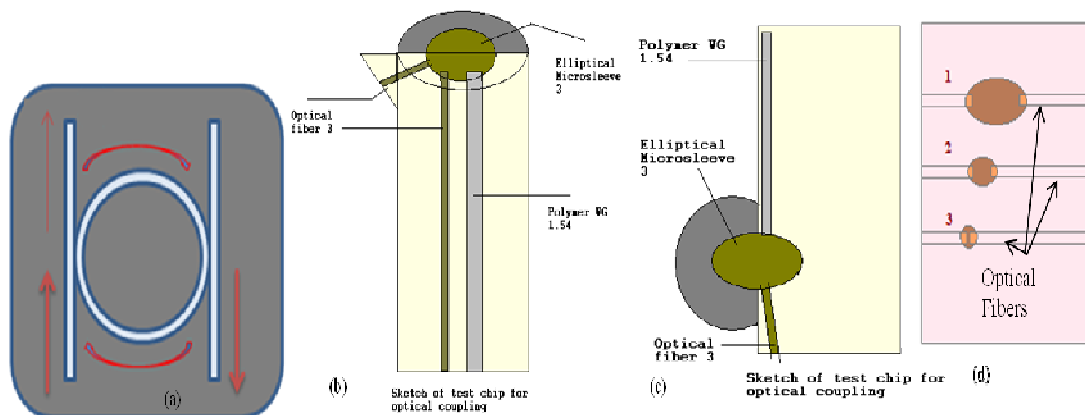
Fig. 2.3 Schematic diagram of (a) Ring resonator (b) (c) (d) designs of elliptical microsleeve bond.

The elliptical microsleeve is expected to support signal coupling with the WGM phenomenon. WGM is characterized for high – Q values and confinement of circulating energy inside a cavity.

The light propagation through an optical fiber, elliptical microsleeve and through a polymer waveguide is explored over a range of optical signal wavelengths.

COMSOL simulation platform executed designs shown in figure 2.4 (b) (d) with boundary conditions viz. electric field, perfect magnetic conductor [PMC], perfect electric conductor [PEC] and domain condition, perfect matching layers [PML] to get appropriate simulating conditions and control dispersive, reflective outer region. RF module of COMSOL supported the model demonstrating WGM inside the microsleeve, with governing equations [equation (2.5) to (2.9)] from the electromagnetic wave physics and frequency domain study.

$$\nabla X (\mu_r^{-1}.\nabla X E) - K_0^2 \left(\varepsilon_r - \frac{j\sigma}{w\varepsilon_0} \right) E = 0 \dots\dots\dots\dots\dots\dots\dots\dots\dots\dots 2.5)$$

$$\nabla X (\mu_r^{-1}.\nabla X E) - K_0^2 \varepsilon_{r0} E = 0 \dots\dots\dots\dots\dots\dots\dots\dots\dots\dots\dots(2.6)$$

Where ω= angular frequency of the incident signal, σ = conductivity [S/m], $\varepsilon_r = ($ n-ik$)^2$ is relative permittivity [F/m] (where 'n' is real part and 'k' is complex part of the refractive index of the material), μ_r is relative permeability [H/m] (both ε_r and μ_r are with respect to the permittivity and permeability of free space, ε_0 and μ_0 respectively), K_0 is the wave number of free space represented by the following:

$$K_0 = \omega\sqrt{\varepsilon_0\mu_0} = \frac{\omega}{c_1} [\ rad.m^{-1}] \qquad\qquad \dots\dots\dots\dots(2.7)$$

Where c_1 = Speed of light in vacuum [3 x 10^8m/s·]:

$$Q_0 = \frac{f_{0r}}{\Delta f} \qquad \dots\dots\dots\dots\dots\dots\dots\dots..(2.8)$$

Where Q_0 is quality factor, f_{0r} is resonance frequency, Δf is 3-db bandwidth at resonance.

Q_0 can be calculated from complex eigen-frequency value, W_r as

$$Q_0 = \frac{Re(W_r)}{2|Im(W_r)|} \qquad (2.9)$$

RSoft simulation using fullwave analysis is implemented for design of figure 2.3 (c). The design ensures proper simulating conditions with perfectly matched layer and material conditions in this 2-D model. A range of frequencies falling in the optical spectrum are utilized to observe signal coupling and WGM effect between two waveguides bonded by an elliptical microsleeve.

2.7 Result and Analysis

2.7.1 Simulation results showing ring resonator, microsleeve coupling and WGM in the frequency range of 1-5THz.
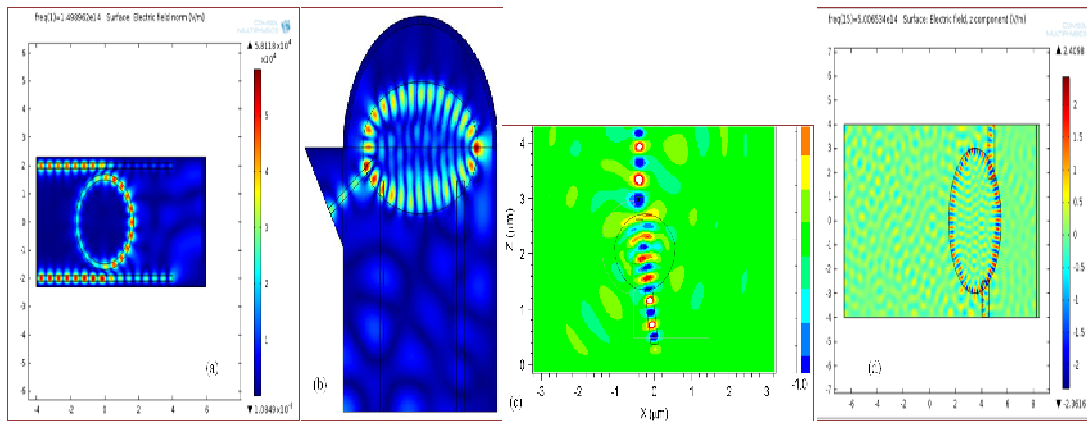
Fig. 2.4 Simulation of (a) optical ring resonator (b), (d) electric field and WGM inside two models of elliptical microsleeve (c) signal coupling and propagation.

2.7.2 Table 2.1 Calculations at WGM condition

Sr. No.	Refractive Index			Major axis multip-lier	Frequency of WGM [THz]	Frequency of coupling [THz]	Q factor	Decay time τ[ps]
	Input waveguide	MS	Output wave guide					
1	3	3	1.54	1.5	159.722	162.75	2576.17	2.567
2	1.46	1.67	1.67	1.5	458	458	1145	0.397

As shown in Table 1, the Q- factor and decay time of the WGM energy stored inside the microsphere and waveguide assembly having refractive indices 3-3-1.54 for the input waveguide –microdroplet-output waveguide respectively, are comparable to that with R.I. of 1.46-1.67-1.67 [Silica optical fiber-SU8-SU8]. Inside SU8 microdroplet the energy circulates for a slightly lower period during the WGM condition of case 2 at frequency of resonance [low R.I. contrast].

16

2.7.3 Graphs 2.1 [A & B] of total energy inside the elliptical microsleeve resonator vs Frequency over full spectrum.
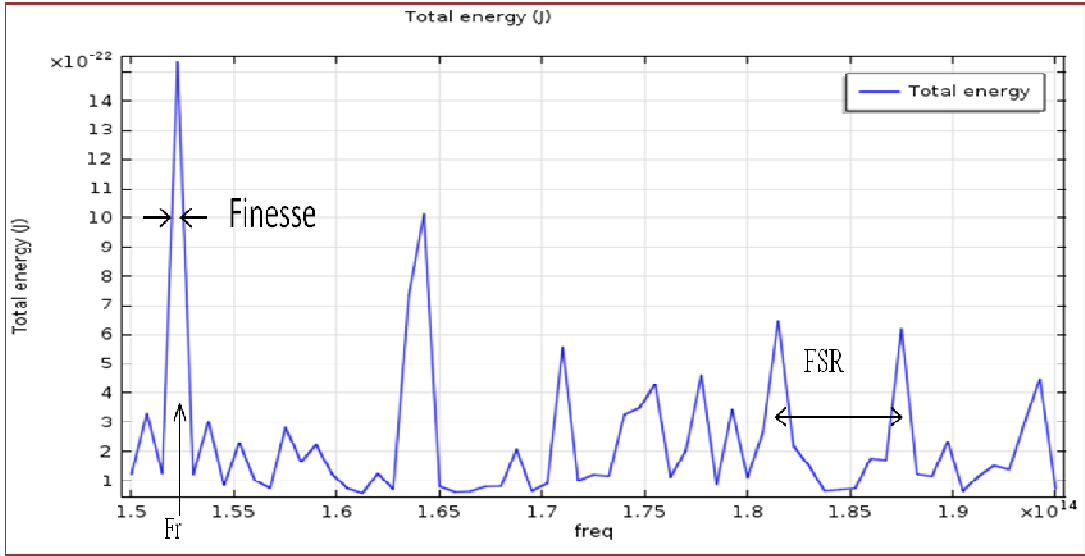
2.1 A. High contrast performance: Peak resonance at [153.75e12Hz], FSR = 0.55THz.
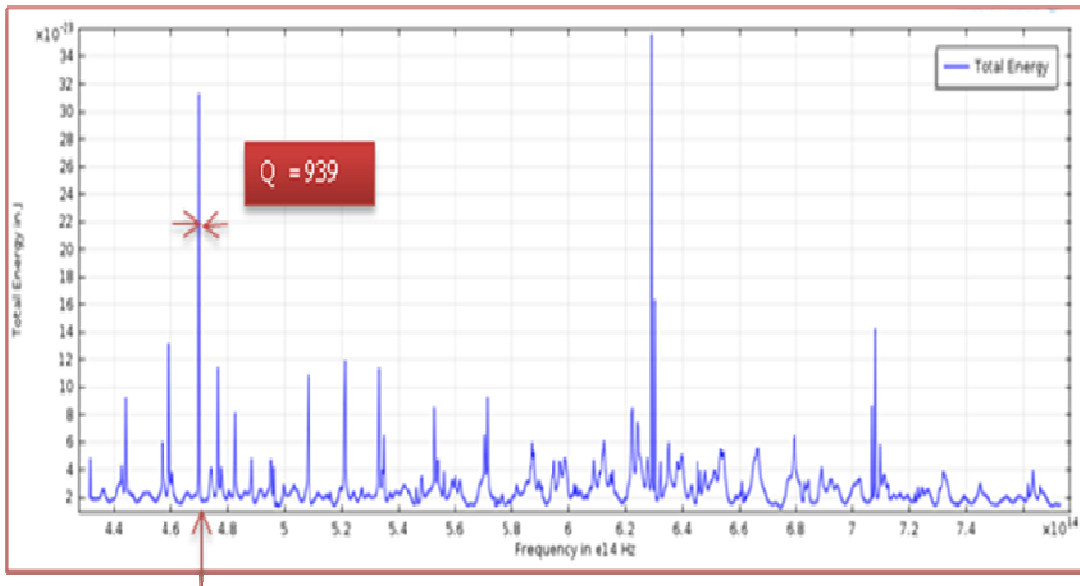
2.1 B. Total energy profile inside the SU8 microdroplet over the full visible spectrum [430 THz to 770 THz]

2.7.4 Graph 2.2 of Energy density time average value inside the elliptical microsleeve resonator [low index contrast] vs Frequency, 0ver 2.061THz range, Peak resonance at 458THz [655nm], Q –factor = 1145.

17
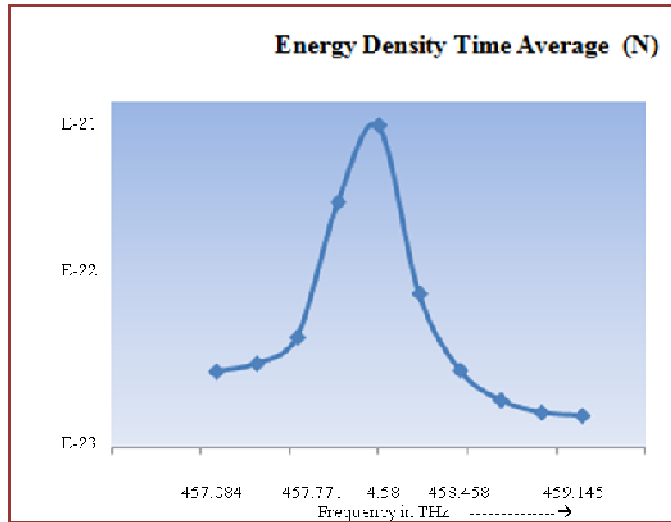
Graph 2.2 Enrgy Density Time Average Value
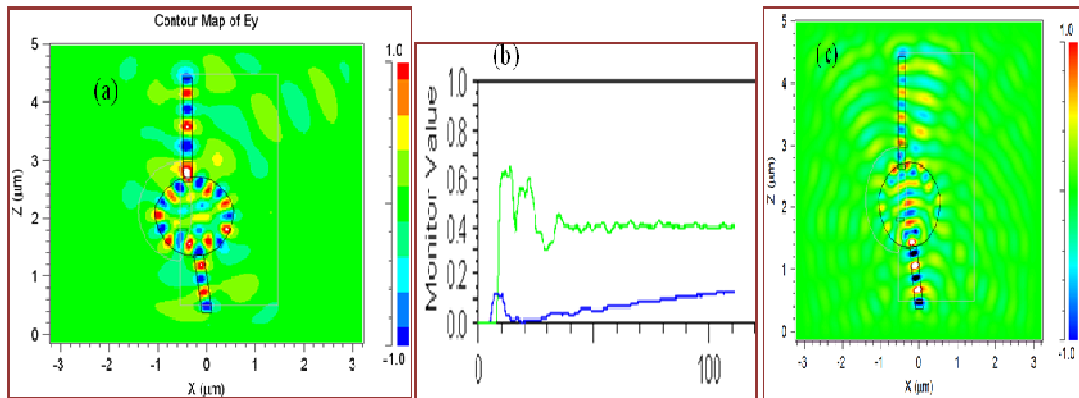
Fig. 2.5 Signal coupling and WGM at wavelength (a) Large contrast: 2.6μm [115.25THz] with (b) power graph (c) Small contrast: 515.15 nm [582THz] [RSoft]
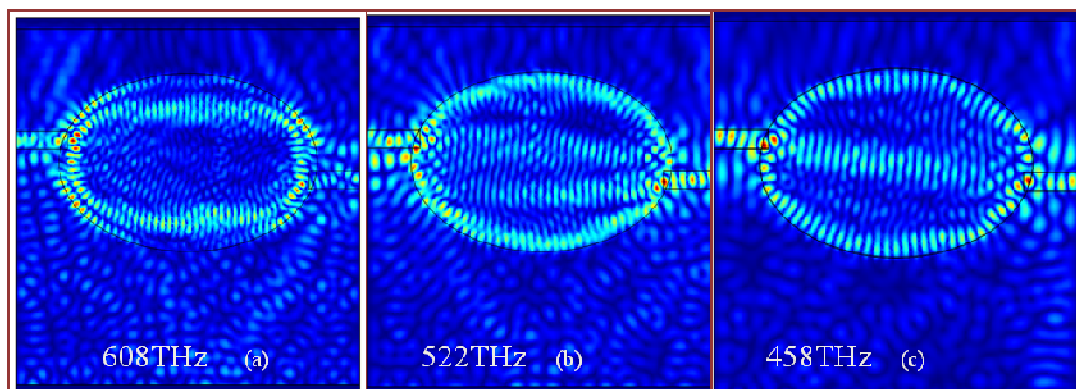
Fig. 2.6 Signal coupling and WGM at wavelength (a) 493nm [608THz] (b) 574.7nm [522THz] (c) 655nm [458 THz] with Low Contrast. [COMSOL]

18

2.8   Future Scope

Once the concept of elliptical microsleeve coupling and its feasibility is verified using the simulation softwares, the coupling can be experimentally verified using elliptical microsleeves of different dimensions, sizes, materials. Future scope is to use this device as an optical coupler as well as a sensor of biological entities.

2.9   Conclusion

Both RSoft and COMSOL Multiphysics software supported the 2D –models of elliptical microsleeve based coupling of optical fibers and waveguides. There was high efficiency coupling and WGM phenomenon observed for certain wavelengths. The performance was checked interms of the simulation graphical results, Q-factor, electro-magnetic fields, coupling efficiency. Results in Table 1 show that in case 2, WGM at 458THz, in the polymer waveguide and optical fiber tagged by polymer microdroplet assembly, Q-factor = 1145, decay time 0.3978 ps. Thus it can be concluded that polymeric waveguides and microsleeve can be used to couple two optical waveguides.

Reference

1.   G.C. Righini, Y.Dumeige, P. F'eron, M. Ferrari, G. Nunzi Conti, D. Ristic, S.Soria, "Whispering gallery mode microresonators: Fundamentals and applications", *Rivista Del Nuovo Cimento 34 7 (2011).*

2.   A.B.Matsko, A.A. Savchenkov, D. Strekalov, V.S.Ilchenko, L.Maleki, "Review of applications of whispering gallery mode resonators in photonics and non-linear optics", IPN progress report (2005).

3.   M.L.Gorodetsky, A.E.Fomin," Geometrical theory of whispering gallery modes", Physics –Optics (2005).

4.   A.N.Oraevsky, "Whispering gallery waves", *Quantum Electronics, (2002).*

5.   A.B. Matsko, V. S. Ilchenko, "Optical resonators with whispering gallery modes – part I: Basics", IEEE JSTQE, 12 1 (2006).

6.   A.B. Matsko, V. S. Ilchenko, "Optical resonators with whispering gallery modes part II: Basics", IEEE JSTQE 12 1 (2006).

7.   M.Ornigotti, A. Aiello, "Analytical approximation of whispering gallery modes in anisotropic ellipsoidal resonators", Physics.optics (2011).

8.   S.G. Johnson, "Notes on perfectly matched layers [PML]", Book.

9.   M.Imran Cheema, A.G. Kirk," Implementation of PML to determine the quality factor of axisymmetric resonator in COMSOL", *COMSOL Conferenc, Boston,* (*2010*).

10.   Pierre Viale, S. Fevrier, F. Gerome,H. Vilard, "Confinement loss computations in photonic crystal fibers using novel perfectly matched layer design", *COMSOL Multiphysics user's Conference ,Paris,* (*2005*).

11.   Furlani, Biswas, Litchinitser, "WGM-Fullwave simulation of an optofluidic transmission mode biosensor", *COMSOL conference Boston,* (*2009*).

12.   D.J. Albares, T.W. Trask, "Optical fiber to waveguide coupling technique", *Technical report* (*1990*).

13.   J.P.Laine, B.E.Little, D.Lim, H.A.Haus, "Novel techniques for whispering gallery mode excitation in silica nanosphere", OSA, IPR (1999).

14.   J.P.Laine, B.E.Little, D. Lim, H.A.Haus, "Microsphere resonator mode characterization by pedestal antiresonant reflecting waveguide (ARROW) coupler", *IEEE Photonics Technology Letters, 2000.*

15.   M.Cai, K. Vahala, "Highly efficient optical transfer to WGM by use of symmetrical dual coupling configuration", *Optics letter 2000, OSA.*

16.   M.de Labachelerie, N.Kaou,"A micromachined connector for the coupling of optical waveguides & ribbon optical fibers", *Elsevier; Sensors & Actuators, 2001.*

17.   Yuze Sun, Xudong Fan,"Optical ring resonators for biochemical and chemical sensing", (2011).

Chapter 3
Laser Heat Transmission for High Efficiency Bonding of Two Optical Fibers Using SU8 Microdroplet

Chapter 3
Laser Heat Transmission for High Efficiency Bonding of Two Optical Fibers Using SU8 Microdroplet

3.1   Introduction

Lasers are versatile in their applications including precision optical test setups, entertainment displays, micro- structure fabrication, precision joining, device fabrication, ablation, lithography, local heat delivery, optical fiber splicing, etc. In specific application areas like surface texturing and local variation in microstructure fabrication of standalone optical micro-devices like micro-scale ring resonators, microspheres, optical switches micro-prisms, etc lasers are indispensable. These standalone optical devices are widely utilized in chemical/ biochemical diagnostics systems, sensing systems and also in communications systems whereas printed and patterned structures are not so well explored. One of the reasons for this gap might be, the issue of joining these structures with standalone single or multimode optical fibres which otherwise provide total transmissibility of signals in opto-electronic platforms. Diagnostics can become very easy, flexible, adaptable to new situations if chip based structures are explored more in comparison to standalone optical components because of their high sensitivity, stability and low intake volume of analytes.

In this chapter we have explored and conceptualized a strategy of joining optical fibres to microchip based printed optics using a SU8 micro-drop. The fibers are placed straight in close proximity, with proper consideration of gap and alignment between the two. The adjoining fiber ends are covered with a small SU8 microdroplet which is carefully and precisely exposed to Laser beam for specified period and with optimum power. The heat transferred to the microdroplet locally melts the SU8 and then solidifies again to form a solid bond. Long monomers of SU8 are cross linked and hardened, with the laser exposure and subsequent chemical reactions. SU8 has low absorbance in the mid Infra Red [MIR] range. Hence laser power control is the key to strong and perfect bond formation. The technology developed is presently analysed and evaluated on optical fiber to fiber bonds on

glass or silicon wafer. It can be a directly implemented in an application where coupling process between optical fibre and extended contact of SU8 thin film optical waveguide, utilizes precise heat delivery of a CO_2 lasing system on a SU8 micro-droplet. Optimization of some physical/dimensional parameters of the bonded assembly was possible with the control of laser frequency, speed, power, spot size and cycle control. The optimization is performed with Design of experiments (DOE) technique, in which Response surface methodology (RSM) based on central composite design (CCD) is used to evaluate suitable experimental parameters for the lasing system. Study of temperature distribution at the fiber joint, SU8 droplet and SU8 structure end was possible with finite element heat transfer model. Consequently further optimization was carried out by focussing the heating zone to the joint area. Exclusive optical [RF] modelling is performed to estimate the optical transmission property of the optical fibers bonded to each other on a substrate with SU8. Our studies indicate the possibility of formation of Whispering gallery modes [WGM] at the inside surface of the micro-droplet leading to very high transmissibility of the optical signal. It also shows that, the thickness of the joint, on heating might control the temperature at the spot. Thus through this work we have been able to develop a novel method for fiber stitching to each other and also to printed optical structures on microchips with reduced power, smaller confinement and lesser time for forming these joints.

Various aspects of this work are discussed from sections 3.2 to 3.10, to introduce different processes and concepts on the basis of which this work is developed.

3.2   Lab-on-Chip

Lab-on-a-chip [LOC] integrates one or many diagnostic or laboratory operations on a singlechip of compact, small size. It handles smaller volumes of samples and deals with its transport from one section to other. Thus dispensing of measured quantities of specific chemical, reagent in specific port, setting time, stir/mixing the same and subjecting it to the sensing section are some of the operations LOC does as a regular feature. Thus all the required laboratory sample handling equipments are scaled down and cramped into a square millimeter size chip. Also it is important that the sequence of events and analysis is maintained. It

finds applications in point-of-care diagnostics, low cost global health diagnostic kits, diagnostic tools, immunoassays. Merits of LOC are many including 1.Compact size, fast response and smaller volumes of fluids, smaller heat capacities, low cost 2.Fast analysis and improved process control 3. Analysis with high throughput 4.Disposable, low cost chips, better quality control, redesignable platform.

A few demerits are 1. Cleaning, predicting effects of previous reactions on the chip material is difficult 2. Precision engineering accuracy decides accuracies and performance parameters of the device. 3. Scale down principle may not be applicable to sensors, detectors and sources.

Lab-on-chip technology when used in diagnostics, it is designed to monitor microorganisms in the environment, count cells and other molecules in the sample, separate required biological entity from sample for future investigations. Figure 3.1 (a) shows a typical microfluidic system on a palm size chip. It conducts around 1000 reactions in this small area [Lab-On-Chip]. Normally a programmable microfluidic chip mixes and stores samples, the LOC shown in figure 3.1 (b) mixes, stores, heats and senses the samples. This chip consists of an electronic control region and microfluidic section [Purdue University News]. Thus sensing is an important aspect of LOC design which still relies on add-on instrumentation like microscopes.
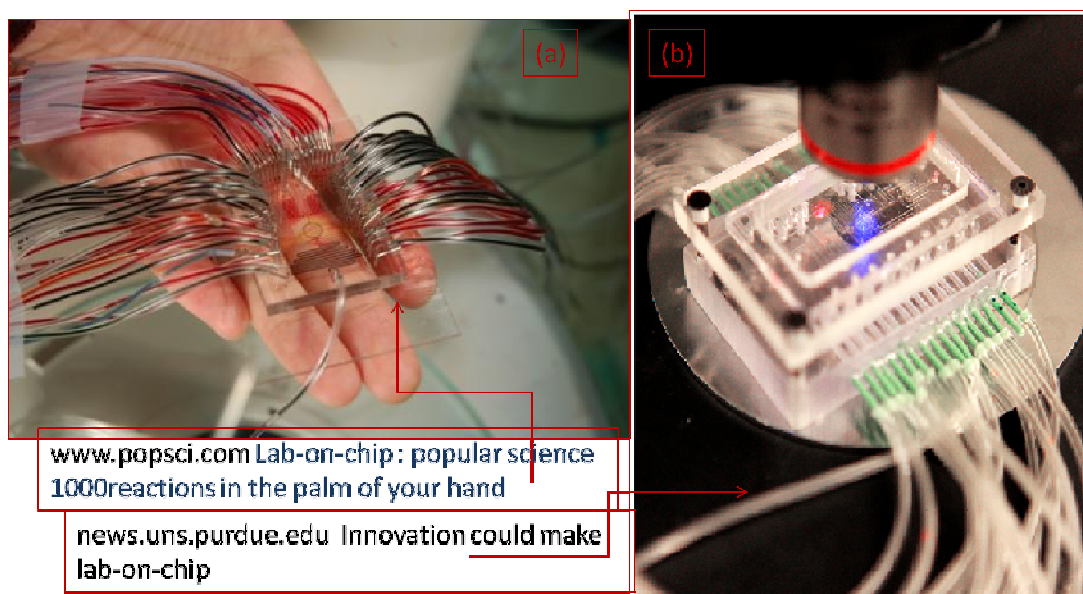
Fig. 3.1   Images of two categories of lab-on-chips.(a) microfluific chip [Lab-On-Chip] (b) Microfluidic system with multipurpose programmable controller chip [Purdue University News].

3.2.1 Merits of Miniaturization

A few of the benefits of micro-miniaturization are accounted as 1.Reduced overall power consumption, 2.Compact size, shape, smaller weight 3.Rapid interaction between components 4.Optimized material, solution, reagent usage 5.Specificity in operations and design.

3.2.2 Limitations of Miniaturization

1. Reduced reliability 2. Stability is compromised 3. Poor serviceability after manufacturing 4. Increased design complexity may lead to poor performance 5. Increased cost due to improved R and D engineering.

3.3 Methods of Microfabrication

Microfabrication essentially means fabricating devices with one of the feature sizes in micrometer range. Previously this phenomenon was dominated by Si based systems. Current status is that a range of new materials are being explored to reduce the cost of material, process and complexity of the endeavour. Microfabrication has a source from steady and compelling need of miniaturization in every field of life, be it manufacturing, automotives and electronic goods, defence and military, medicine and diagnostics, communication systems. Some of the microfabrication technologies are employing laser machining, photolithography, soft lithography amongst many.

3.3.1 Laser Micromachining

Modern Laser machines have computer controlled movement of the beam. A software defined pattern, along with pulse frequency, speed, time and intensity of beam control, can monitor the depth of exposure, damage due to polymerization or nucleation of the material. The laser beam can be of CW or pulse type. It is the wavelength and power of laser beam which decide end use of the machine. Based on wavelengths there are three main types of lasers: Excimer Laser [193nm, 248nm, 308nm, 351nm], Nd: YAG laser [1064 nm, 532nm, 473nm], CO_2 laser [10.6µm]. The selection of wavelength depends on desired minimum feature size, transparency of the material to the wavelength and optical properties of the material. Smallest feature size or resolution of the laser machine is ideally double the wavelength in

24

nm. For a CO_2 minimum feature size is 21.2μm. Besides laser based 2-D, 3-D microfabrication using a range of polymer materials; for materials like glass, wood, some soft metals it can be utilized to make moulds or dies for soft lithography, masks for photo-lithography. Lasers find applications in thermotherapy, medicines [soft, micro surgery, cancer treatment], defence, manufacturing [cut, drill, weld, rapid prototyping].

3.3.2 Photolithography

Photolithography is selective exposure of a photosensitive/ resist material coated on a substrate, to the Ultra Voilet [UV] light source, development of the photo exposed material in a developing solution to realize desired features on the substrate. Resolution of the mask decides smallest feature size. Positive photoresist delink and weaken when exposed to UV rays whereas negative photoresist link and harden when subjected to UV exposure. Prebaking and postbaking are essential procedural steps to chemically control other ingredients of the photoresist. After development in the developer solution the unbonded material is etched away. Masking is done using hard [pattern printed on transparent sheet] or soft masks [Computerized black and white pattern]. Two high resolution image producing lithography wavelengths are 365nm and 436nm. It is mostly recognized for its use in fabrication of highly complex electronics integrated circuits.

3.3.3 Soft Lithography

Soft lithography according to definition is the technology involving molds, masks, stamps to replicate structures very often in elastomeric materials. Feature sizes of micro and nano are possible with this technique. It has merits of lower cost, suitability in 2D as well as 3D surfaces, can achieve smaller feature sizes of 6-10nm appropriate in biotechnology, more methods of pattern transfers or replication are available to suit specific applications. In replica molding, PMMA or PDMS is normally used as replica mold or mask for the prepolymer. After making a bubblefree, clear composition with the curing agent the polymer gel is poured in a suitable container along with the replica mold or mask. The assembly is then cured by heating or exposing it to UV rays.

3.4   Types of Optical Signal Coupling

Optical fiber –fiber, fiber to waveguide, thinfilm waveguide to waveguide and fiber –to-thin film waveguide are four possible optical signal coupling conditions. There is a large disparity between dimensions of single mode fiber [SMF-10µm] and the silicon-on Insulator [SOI very small cross-section] waveguide. In-plane and out-of plane mode transformation couplers are used to to match the fiber and waveguide [1]. The coupling is very inefficient if the two are not properly matched. With gray scale technology the input waveguide can be tapered. Grating coupler and photonic crystal coupler are two other coupling methods. Signal coupling using asymmetric GRIN lens was tested with a coupling loss of 0.3db. Optical coupling loss can be affected by multimode to single mode fiber coupling, fiber mismatch, launch conditions while launching light into the fiber, quality and type of test, reference chords being used.

Loss due to fiber mismatch is caused by the fiber characteristics and not due to joining techniques used. Fiber mismatches are due to (a)difference in numerical aperture [NA] (b) Core/cladding concentricity error (c) Core diameter mismatch [4] (d) Linear gap between two fibers/ waveguides.

$$NA_2 = n_2 \sin\Theta_2 \hspace{5cm} (3.1)$$

$$\text{Coupling Loss} = -10 \ [NA_1/ NA_2]^2 \hspace{3cm} (3.2)$$

$$\text{Coupling Loss} = -10 \ [D_1/ D_2]^2 \hspace{3.5cm} (3.3)$$

$$I_2 = I_1 \ e^{-Ad} \quad \text{Beer -Lamberts law} \hspace{3cm} (3.4)$$

$$I_2(\lambda) = I_1(\lambda) \ e^{-A(\lambda)d} \quad \text{Beer Lambert law as function of } \lambda \hspace{1cm} (3.5)$$

Where n_2 is refractive index of second fiber core in the joint, Θ_2 is the maximum cone of light half angle for the amount of light to enter or exit, NA_1, NA_2 Numerical apertures of first and second waveguide, D1, D2 are diameters of two fiber cores, I_1 is intensity of light at the input of first fiber, I_2 intensity of light at the output of second fiber, d is the gap or thickness of material in between input and output fibers/ waveguides, *A* is the coefficient of linear attenuation [if scattering is ignored, it can be equated to absorption coefficient in cm^{-1}], λ is wavelength in nm, $A(\lambda)$ is Coefficient of linear attenuation which is function of wavelength, $I_2(\lambda)$, $I_1(\lambda)$ are ouput and input light intensities which are functions of λ, see figure 3.2 .
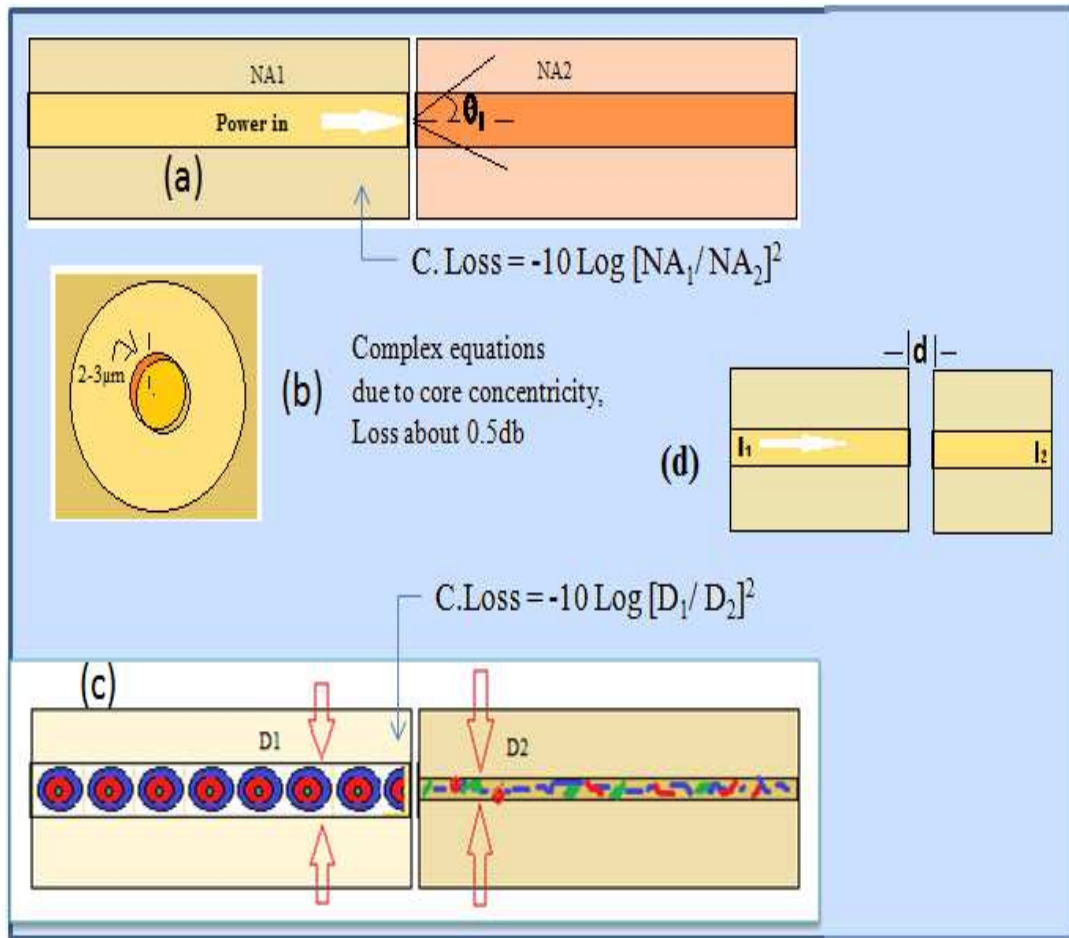
Fig. 3.2 Schematic diagrams of fiber coupling and causes of losses (a) Fibers with different Numerical apertures (b) Core concentricity (c) Core diameter mismatch ($D_1 > D_2$) (d) Linear gap between two fibers/ waveguides.

3.4.1 Tapered signal coupler

The inequality between single mode fiber and Silicon-on-insulator [SOI] waveguides dimensions is prominent and cause of coupling losses. Figure 3.3 (a) Shows schematic diagram of a tapered coupler [31] used to couple optical signal from fiber to SOI waveguide with minimum coupling losses. The light is confined to the bottommost layer of the stacked tapered coupler which had highest refractive index. Linear taper confines and guides the light to the narrow waveguide. Figure 3.3 (b) SEM image showing coupler stack layers with parabolic index profile.
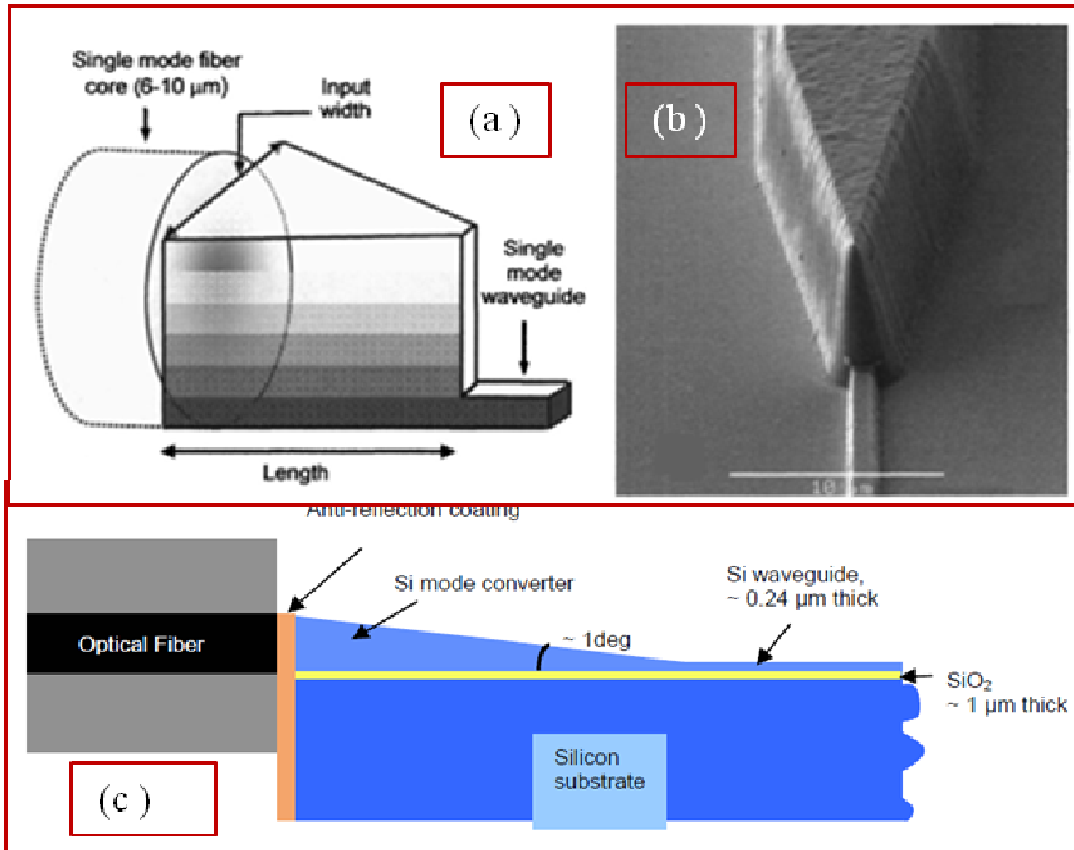
Fig. 3.3 Techniques used to minimise coupling losses (a) schematic diagram of a tapered coupler [Ref. 2] used to couple optical signal from fiber to SOI (b) SEM image showing coupler stack layers with parabolic index profile (c) SOI waveguide and mode converter cross section[Ref. 3].

In Figure 3.3 (c) a 3-D adiabatic taper used to couple single vertical mode from single mode fiber to SOI waveguide. It is called [2] mode converter and for achieving vertical taper grayscale photolithography technique is employed.

3.4.2 Grating coupler

Another efficient optical coupling technique of single mode fiber coupling with SOI waveguide is by using shallow etched diffractive waveguide grating coupler [3]. The waveguide / grating [see figure 3.4 (a) and (b)] thickness, fill factor, coupling strength are optimized to match the modes, to minimize the reflection, minimize coupling loss, enhance efficiency of coupling.
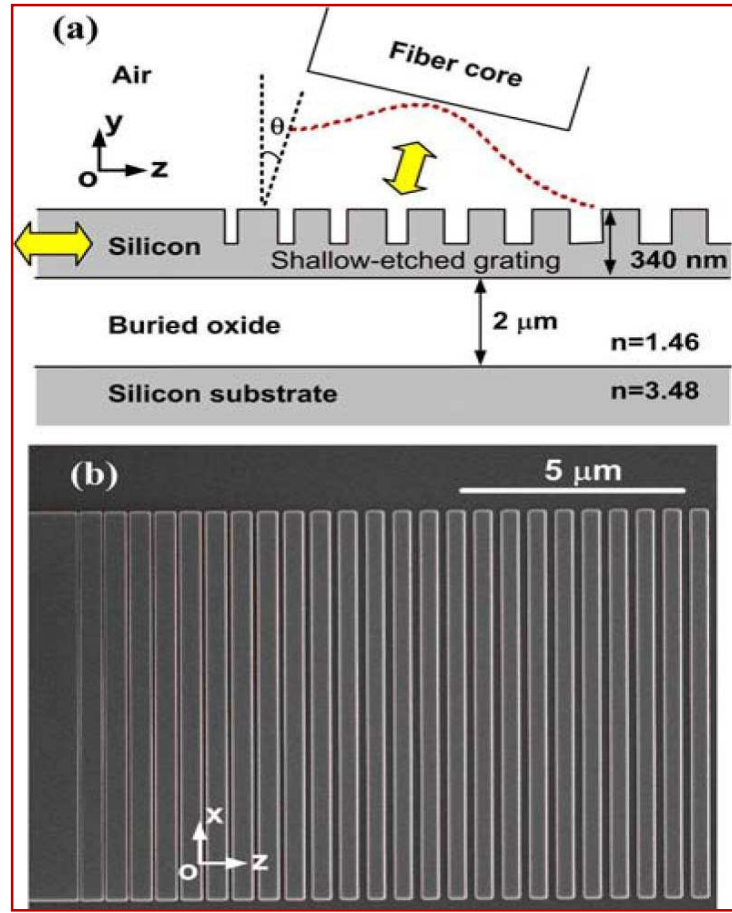
Fig. 3.4 Coupling between optical fiber and SOI waveguide (a) schematic of waveguide diffractive grating coupler (b) SEM image of varied coupling strength grating coupler [4].

3.4.3 Optical Fiber Splicing

One of the oldest methods of fiber coupling is fiber splicing. In this method heat is used to join to ends of fiber. These fiber ends are preformed before aligning and joining. The objective of this joint is to have minimum coupling loss, scattering and reflection at the splice. Heat is given locally at the splice using gas flame, electric arc or current carrying heat source and CO_2 laser [see Figure 3.5]. 1. Fibers are preformed by first stripping the coating with a fiber stripper or dipping in sulfuric acid or flowing hot air over the fiber. 2 Fibers are cleaned with isopropyl alcohol. 3.Fiber cleaving in which fiber endface is cut with mirror like finish [90° at the face], is important to minimize losses at the splice. 4. Fibers are aligned in x-y- z in plane and then fused together. Sometimes a splice protector tube is provided around the fiber to strengthen the joint and protect it.

29

3.5 Epilog Laser machine

In this work, a mini laser machine is employed for some unconventional functions and operations. Epilog mini/ HELIX Laser, Model 8000, Class 3R laser product with International Standard IEC 60825-1 and CO_2 laser source. It operates with maximum 35W power and graphics software CorelDraw. Raster engraving operation is high resolution dot matrix printing with laser beam. Vector cutting is with hairline thickness outline, continuous path following.
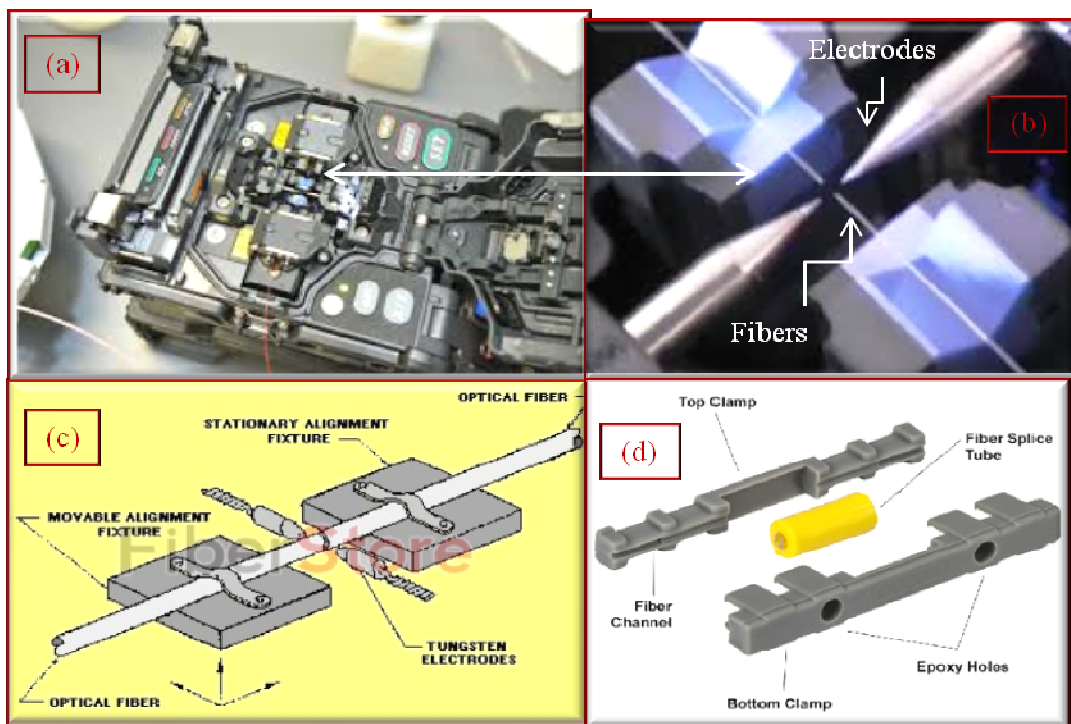
Fig. 3.5 Various optical fiber-to-fiber splicing techniques (a) Electric arc: Image from en.wikipedia.org (b) Electric arc: Enlarged view, Image from www.fiber-optic-tutorial.com (c) Schematic diagram of Arc fusion of two optical fibers. Image from www.tpub.com. (d) Mechanical-fiber-to-fiber splice, Image from www.Thorlabs. com

This machine was used for glass, PMMA, Si, SU8, Silica materials for cutting, drilling holes, making moulds, masks, melting optical fiber tip to make silica microspheres, strip cladding layer of optical fiber, melt and crosslink SU8 material at microspots.

Laser exposure was carried out on a EPILOG WIN32 laser machine with 32 Watts power and total working platform of size 2ft x1ft. The path of the Laser head

was pre-programmed using Corel draw (CorelDRAW Graphics Suite X5) which was subsequently converted into a machine readable file of format '.dwf' or '.cdr'and imported into the EPILOG machine.

3.6   SU8 as bonding material

In photolithography technology epoxy based SU8 photoresist is used to selectively make structures out of a plain Silicon substrate. It is also used to produce structures of high aspect ratio. It is dissolved in Gama Butyrolacton [GBL] an organic solvent, quantity of which in SU8 decides, viscocity and feature thickness of SU8 structure. Thus this negative photoresist is basically a photopatternable, microfabrication and micromachining material. Its highest absorbtion is at 365nm near UV wavelength. Hence UV processing is observed in 350 to 400nm near UV range. It also has very high optical transmission above this range. Once the SU8 film is exposed to UV rays, the exposed portion has long molecular chains of SU8 crosslinked causing hardening of the region. Once hardened, it is difficult to remove this portion from substrate. The unexposed portion has no crosslinks, so it dissolves easily in the developer solution. SU8 has very good imaging characteristics and it is a regular practice to image, cure and allow the SU8 structures to remain on the substrate. Thus the process steps involved in Photolithography for making high resolution SU8 structures are: 1.Substrate cleaning and treatment 2.SU8 spin coating with speed in RPM and time controlled according to desired thickness of film 3.Soft bake time set according to thickness of SU8 film 4.UV Exposure with 365nm wavelength [long pass filter to eliminate wavelengths below 350nm]. 5.Post exposure bake time set according to film thickness 6. Developing to etch away unbounded SU8, using SU8 developer 7.Wash with Isopropyl alcohol and dry 8.Hard bake 150˚-250˚C for 5-30 min helps in maintaining properties of SU8 9.Removal of structures from substrate is difficult.

Fabrication of optical waveguides using SU8 material for experimenting optical fiber -to-wave-guide bond following procedure and optimized parameters were used:

Substrates (Glass, Si wafer) were spin coated with SU8-2025, maintaining 1000 rpm speed of rotation, for 30 sec. Pre-baking temperature was 95°, period 4-5 min. Then photo-lithography was used using M/S Union Optics mask alignment system. The spincoated SU8 surface was exposed to UV rays for 80sec. Post exposure baking at 95°C for 5 min was carried out to harden the photoresist. The substrates were developed in a suitable developer solution (M/S Microchem Inc.) for 2-3mins.

Besides use of SU8 as a microfabrication material, it possesses some important properties which are found suitable for its use as a fiber bond material: It has 1. High bond strength, 2. Post UV exposure, chemical resistance due to crosslinking, 3. Biocompatible nature, 4. Low bonding temperature [90°], 5. Excellent optical properties 6.Transparent appearance.

3.7   Design of Experiments [DOE]

DOE is a statistical way of carrying out experimental studies in number of engineering processes. It helps in establishing a relation between process parameters and output responses to optimize the system. Thus in the fields of science and technology, DOE finds application of system optimization, development, management and validation. This is a systematic way of planning experiments, accessing and predicting the data output. Amongst various analysis techniques, ANOVA, Taguchi's methods are commonly used techniques [44].

3.8   COMSOL Simulation

Simulation softwares help plan the design parameters of a process, system, device; allow to optimize them with frequent variations and provide a data base to predict output conditions. Thus they are software DOE techniques, which provide knowledge of feasibility and performance before actually embarking upon the fabrication and experimentation. COMSOL Multiphysics software is one such software. In this simulation different physics modules handling physical parameters like flow, heat, stress and radiation can be linked together in a multi disciplinary, multiphysics environment. Effect of one physics and process can be predicted on other physics and process. It is graphical user interface software with illustrative

design models, physics and studies. COMSOL Simulations were carried out using an Intel (R) Core (TM) 2 Quad CPU, with 8.0 GB RAM and 64 bit operating system. The research work, discussed in this chapter, also involves interdisciplinary studies, laser heat transmission and optical signal transmission, behavior of optical fiber and SU8 material under these conditions.

3.8.1   Laser Heat transmission Coupling

To synthesize a fiber-to-fiber bond using SU8, COMSOL Multiphysics solid heat conduction model, as proposed in this chapter, is used. A moving laser source is simulated to provide heat transmission at the joint. It helps design parameters to achieve end temperature conditions at the microspot and at the location of bond.

COMSOL heat transfer module supports laser heat transfer model with the governing mathematical equation: It is for the circular symmetry, based on simplified heat transfer equation.

$$\rho C_P \frac{\partial T}{\partial t} = \left(\frac{k}{r_L} + \frac{\partial k}{\partial r_L} \right) \frac{\partial T}{\partial r_L} + \frac{\partial k}{\partial z_s} \cdot \frac{\partial T}{\partial z_s} + k \left(\frac{\partial^2 T}{\partial r_L{}^2} + \frac{\partial^2 T}{\partial z_s{}^2} \right) + \frac{dI}{dz_s}$$

.... 3.6)

Where z_s = distance from irradiated SU8 film/contact in m, r_L = distance from center of laser beam in m, t = interaction time in sec, k= thermal conductivity [W.m^{-1}.c^{-1}], T= Temperature in K, I = radiation intensity in Wm^{-2}.

Refractive index of SU8 is in the range of 1.668 -1.575 for wavelength range 365nm-1550nm respectively [R. Muller et.al. 43].

Table 3.1 enlists properties of SU8 relevant to this model.

Table 3.1 Properties of SU8

Thermal conductivity **k** [W.m^{-1} .c^{-1}]	0.2
Heat Capacity **Cp** [J .Kg^{-1} .c^{-1}]	1500
Density **ρ** [Kg. m^{-3}]	1200
Absorption coefficient **α** [cm^{-1}]	40

3.8.2 Effect of Heating on Optical property

Laser heat transmission affects at microlevel the structural properties of SU8 material joining the two fibers. The stress at the joint is interpreted in terms of change in optical properties at the joint.

3.8.3 Whispering gallery mode [WGM] based Optical signal coupling between two fibers

The two fibers or planner waveguides are joined using SU8 microdroplet which possess excellent optical properties and refractive index as high as 1.67 at the operating range of frequencies. Simulation results in a 2-D design show whispering gallery modes phenomenon [see chapter 2. for details] in the elliptical microdroplet with selective input wavelengths. RF model used for this support the concept that two fibers can have high efficiency coupling with WGM effect in a semicircular or elliptical joint.

3.9 Measurement of optical properties - SpectraSuite Ocean Optics software

Ocean Optics Spectrometer [Model Name: USB 4000 UV-VIS Miniature fiber optic Spectrometer, Spectra-Suite Software, Model No. USB4H02846 M/S Ocean Optics, Inc. Dunedin, FL 34698 with Halogen light source (HL-2000-HP-FHSA 034990459)] is used for optical signal measurements.

Important performance criterion of the laser heated SU8 bond is transmission efficiency of the two fibers joined together through the bond. The fiber alignment, position, dropsize taken care of, the bonded assembly is irradiated with CO_2 laser source to strengthen the bond. The device is then characterized with SpectraSuite Optics mini spectrometer software and array detector. Figure 3.6 shows the schematic diagram of the SpectraSuite optical measurement setup. Using a broadband light source, optical signal was given to input fiber and corresponding wavelength wise % transmittance was available on the SpectraSuite screen.

34
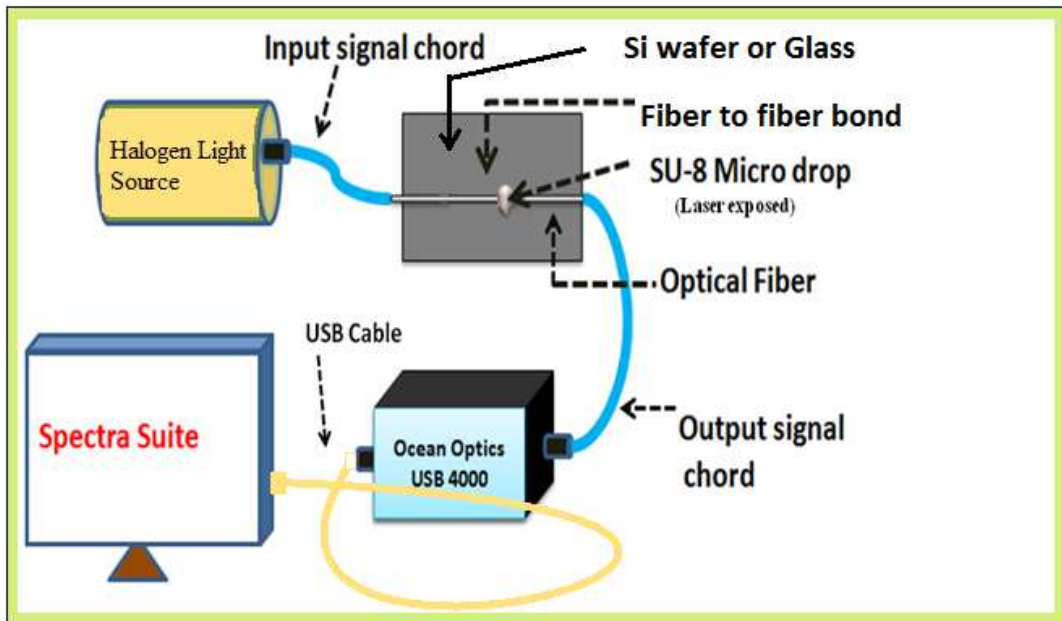
Fig. 3.6: Schematic diagram of test setup for measurement of % optical signal transmittance.

3.10   Related Work - Literature Survey

The optical electronics, opto-medical and communication industries are fast developing and transforming into planar integrated optics systems [IOS] from the individual structures like optical switches, microspheres, ring resonators, micro prisms [5-8]. Among number of other performance measuring criterion in IOS, the transmittance is important parameter, which depends on alignment, linear gap and joining of the various components of such systems [9]. IOS finds application in effectively every field of science and technology, be it optical sensing and diagnostics for chemical/ biochemical biological analytes, optical communication, medical therapeutics [10-14]. The complexity and levels of engineering in association of such systems have increased very fast and keeping with the Moore's law, in the field of communication and sensing [15]. In communication systems and sophisticated sensing systems multiple input/ output signals are required in an environment of miniaturized chip platforms. The optical signals as outcome of a reaction, intermediate signals, specific indicators need to be monitored using some kind of optical probing. In micro/ miniaturized spacial probing, use of standard optical probes and connectors is difficult. Fiber splicing is normally used for joining two fibers, it is not explored much in other regions of binding which involves chip based structures. Once the optical signal is transmitted to the right spot on the chip

35

and taken from other important test points on the mini chips, the signal can be taken over by existing connectors, splicing connectors for readers, recording systems, mini spectrophotmeters and other such testing instruments. Thus fiber bonding is an important interface between the mini and mega world of optical technology. Biomedical diagnostics as in the lab-on-chip technology heavily depend on proper input, output connecting probes for the largely used optically driven high speed strategies of signal transmission from chip to reader and need further explorations for a truly compact and independent LOC environment. Precaution and care must be taken while developing these interconnects, to ensure that a strong bond is developed between the optical fibre and the patterned structure in micro-chip architecture, so that they remain in position, occupying much less space, provide lossless transmission amongst various structures.

In this work we have conceptualized through literature survey, simulation and implemented ,verified with Design of experiments, experimental work, data, that optical fibres can be firmly bonded to substrates (both glass and silicon), to extended contacts of patterned SU8 waveguides/ other optical fiber with laser processed SU8 micro-droplets. The droplets further provide indication of characteristic whispering galleries and resultant transfer of energy modes from signal input to output sides in such an unusual optical joint. The parameters of Laser welding process are decided by the material properties like absorption coefficient, their behaviour under laser irradiation. Thus proper use of laser machining parameters is important to get a perfect, shining bond for the fiber-to-fiber or fiber-to-waveguide joint. To further elaborate the point, considering a transparent polymer film coated over absorbent/ opaque substrates which when exposed to a small laser spot with high energy density enables a much faster heat transfer to take place across the film, eventhough the film material may have high reflectivity, transmissibility and probably less absorptivity. If the substrate is thermally insulating then the absorbent substrate below the thin transparent film layer melts and transfers the heat back to the transparent film layer. This melting, solidification and re-melting at the film substrate interface create a well bonded region. The advantage offered by the laser is its ability to machine and work in a small area without affecting the surrounding material, keeping it intact. [16-19].

Literaure survey on laser assisted machining, heating provided, mathematical modeling of stationary and moving laser beam [20,21], experimental procedures [22] and computer simulation of the moving and still laser source [23, 25,28], helped predict laser assisted bonding for various materials speculating different machining conditions. A range of work is carried out for micro-fabrication of optical waveguides using photoresist SU8 material spun in a thin film on desired substrate [24]. The major problem as discussed is access to the optical signal coming out of these waveguides.

Alternate materials other than SU8 were ABS (Acrylonitrile Butadiene Styrene) polymeric material[26], PC (poly carbonate) and PMMA (Poly methyl methacrylate) have shown good quality joining strength when exposed to laser source although their optical properties may not be suitable to apply them for wave-guiding function as in case of ABS and PC materials[27]. Optical waveguides are subjected to various coupling strategies including usage of hybridized rib-like waveguides with polystyrene microsphere [29], gap filling between the fiber and waveguide using optical solder [30], to confine light in both vertical and horizontal directions, stepwise parabolic graded index profile is used for a vertically asymmetric design and combined it with a horizontal taper [31], optical fiber end with miniature waveguide grating structure [32]. The methods described in all these works are either complex in nature, accommodated outside the planar architecture of the IOC or associated with self assembly/ difficult micro-fabrication strategies, requiring one or the other form of alignment.

3.11   Laser Heat transmission Based Bonding of Optical Fibers Using SU8

In this research work, SU8 photoresist with laser heat transmission processing was used as a contact bond material to assist a high coupling efficiency amid chip bonded optical fibers. Low power CO_2 laser was used for stitching or welding of two optical fibers using SU8 micro-droplet acting as a contact pad or optical fiber solder bond for the coupling and coupled ends of the optical transmitter test set up. The coupling end of the optical transmitter was an off-chip fiber and the coupled end a well located fiber on a microchip substrate. The fiber coupled end indicates whispering gallery mode formation happening along the SU8 microdroplet ensuring good transmissibility of input signal between the two coupled fibers. The simulation models and experiments based on fiber-to-fiber interconnects gave us

clear idea of the physics of whispering gallery modes occurring in the micro-droplet. Silicon and glass, both substratres were used for evaluating the performance of these contacts. CO_2 laser based engraving system [EPILOG] was used with precise control on beam traversing pattern, power, exposure time, speed, frequency, resolution for bonding optical fibers to the IOC or LOC with an SU8 micro-droplet and % transmittance as the experimentally measured output parameter of this coupler presented the quality of the bond interms of transmissibility and strength. COMSOL Multiphysics version 4.3 based Modeling of the heat transfer process was excercised with initial scanning speed/ power, pattern and other Lasing parameters estimated before using them on the actual laser engraving machine. Design of experiments (DOE) technology was implemented to plan number of experiments, to further optimize the heat transfer control of laser machining process. The SU8 micro-droplet bond joining both the fibers exhibited whispering gallery mode (WGM) phenomenon along its circumference. With suitable positioning of fiber ends with respect to the diameter of the microdroplet, light could be transmitted between the two fibers aligned or misaligned with high efficacy. Thus we could provide with simulations and experimentation a basis to endorse high transmittance couplings in this manner between the two bonded off chip fibers.

3.11.1 Experimental procedures

SU8 photoresist polymer (M/S Micro chem. Inc.) with its inherent properties [section 3.6] was utilized as a bonding material for stitching optical fiber to Si or Glass substrate. Advantages of SU-8 over other polymers are, its chemical resistance after UV exposure due to cross linking, high bond strength, transparent appearance, suitability in bio-sensing applications due to bio-compatible nature, excellent optical properties and low bonding temperature [90ºC]. SU8 being an epoxy based negative photo resist is also photo-patternable and is used to create waveguides on microchips and thus it is possible to translate, the coupling strategy developed in this paper to patterned optical devices on microchips. It offers resistance to removal once coated on the substrate and is otherwise a very good bonding material sometimes used to bond multiple layers of microchips [33, 34].

3.11.1.1 SU8 microdrop dispensing on fibers set for bond formation

The optical fibers are aligned using a fixing ,clamping and positioning system over the substrate (Glass or Si) and a 1.05 µl in volume microdrop of SU8 2025, is dispensed over the prior set optical fibers on the substrate, which is heat treated with laser to firmly glue the two optical fibers to the substrate. The exact nature of the drop volume is set through an off-chip syringe pump with a 1ml syringe [pretreated if required] and a prior modification of the surface energy of the substrate is performed if required to generate the requisite contact angle of the dispensed SU8 fluid formulating
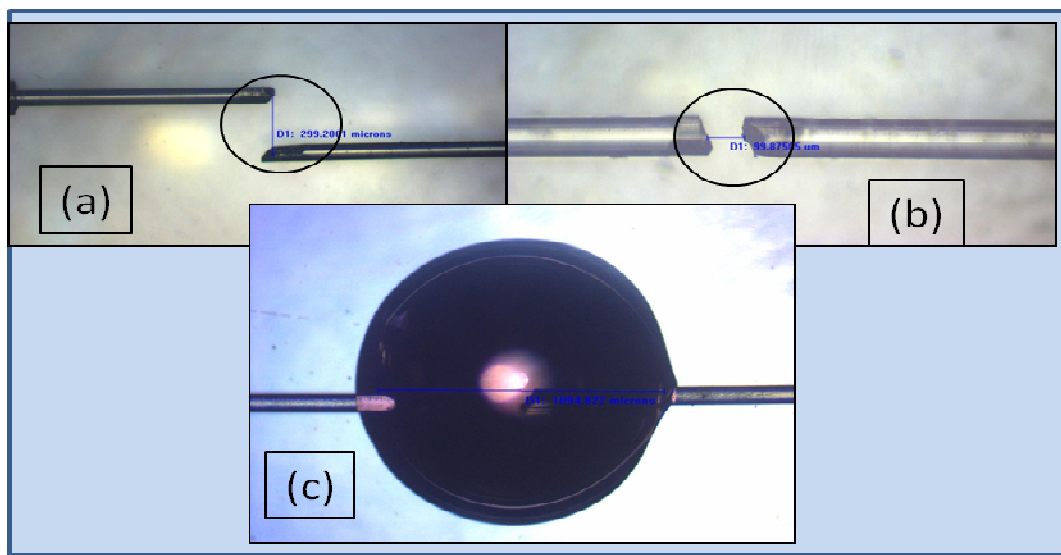
Fig. 3.7 Fibers set, aligned, spaced before and after mocrodroplet dispensing (a) Before dispensing of microdroplet at the circle position on the misaligned fibers (b) Before dispensing of microdroplet at the circle position on the aligned fibers (c) After dispensing of the microdroplet circling the fiber joint.

The droplet with the substrate surface. The substrate is moved in z-direction after adjusting the two fibers in the x or y directions accordingly to set the proper [linear and lateral] distance between them, before applying the SU8 micro-droplet and the two different states that are achieved by this process are categorized as misaligned and aligned fibers [Figure 3.7 (a) and (b)].

In a two-stage X-Y-Z fiber alignment and microdroplet dispensing, following procedure was used .The first fiber was fixed on the substrate which was

mounted and fixed on one of the XYZ stages. The other fiber was mounted on a holder near the X-Y-Z stage and carried near the previously mounted glass substrate. Once the fibers are aligned and found satisfactory, when observed under the magnifying lens the second XYZ stage containing the syringe pump with a projected syringe is aligned first in the X-Y platform with respect to the coupling region. Then the syringe pump is moved down in the - Z direction so that the droplet starts touching over the substrate at exact spot of the desired bond. The droplet adheres to the substrate and the syringe is pulled back in the –X direction to break the contact and release the droplet over the coupling region. This way the small distances between the fibers for both the aligned and misaligned cases could be easily maintained. The drop volume was recorded as 1.05 µl. Accurate laser beam exposure of the precise location and spot-size in the polar zone of the droplet could be obtained to ensure a perfect adherence at the spot to the substrate surface. SU8 grade 2025 was found to offer the right viscosity to undertake these repeated dispensing. The substrate plays a major role in offering a relatively higher level of adhesion to the SU-8 drop and the de-adherance of the drop from the needle body. Goniometric contact angle studies were conducted on the SU-8 droplet getting formulated over the silicon substrate and over the thermal grown oxide layer on surface. The contact angle formed by the droplet was approximately 101°C. This fabrication technique ensured precision dispensing of SU8-2025 without affecting the surrounding miniaturized devices or structures.

3.11.2 Laser heat treatment

To provide laser heat with a preselected and preset pattern for the laser head, CorelDraw software was used. Laser exposure was carried out by 32 Watt powered EPILOG WIN32 laser machine. The laser parameters were fully optimized using DOE technique in which a Central Composite Design (CCD) was used to fit a model by least square technique. The software tool Software Design Expert 7.0, is used for this purpose. After carrying out all experiments, images of the fabricated designs were captured with top illuminated fluorescence microscope (Nikon 80i) in the bright-field mode. Transmittances of these welded pairs were measured using test setup of Ocean Optics Spectra Suite including its software, a broadband [Halogen] light Source and array detector [UV-VIS miniature fiber optic spectrometer]. Figure

3.8 shows the effect of optimization of laser machining parameters, on the quality and appearance of the bond.

3.11.3 COMSOL Simulation for modeling Laser heat transmission

The processing problem is multi disciplinary and involves Multiphysics considerations and studies. In process modeling, finite element solid heat transfer model was used to get temperature distribution at the Air-fiber-SU8 interfaces and estimate the heat induced stress in the fiber. Using this information as preset input data in optical [RF] model, birefringence at the SU8 bonded fiber was obtained.
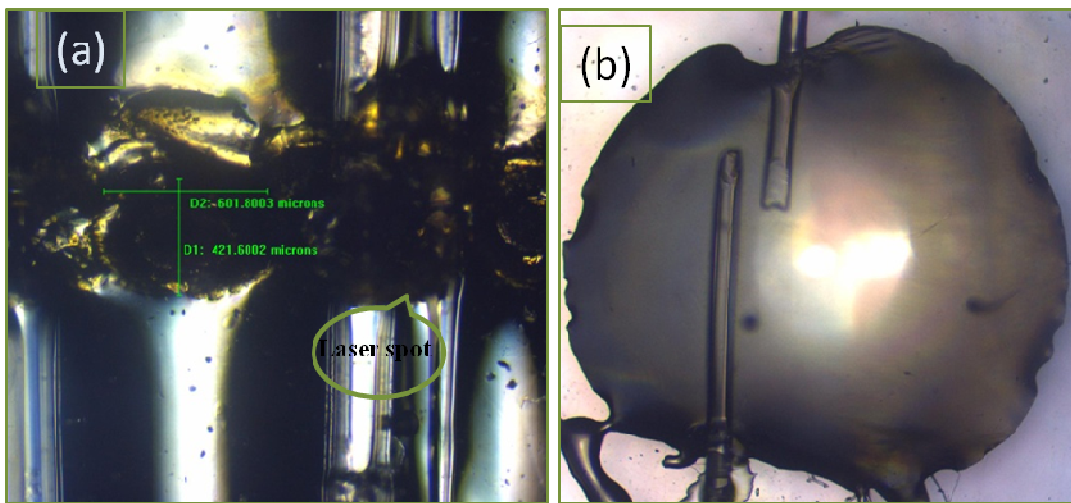
Fig. 3.8 (a) a visible spot on fiber covered with SU8 droplet after laser heat transfers without optimization of machine parameters (b) a highly optimized laser heat transmission procedure for bonding two optical fibers with SU8 microdroplet

Software COMSOL multiphysics was used to model the temperature distribution on the irradiated SU8 contact surface. 3-D model and geometry was designed to simulate laser heat transfer, on temperature at the bond, the fiber, SU8 interface and investigate effect of varying thickness of the SU8 film on the temperature. Equation (3.7) was modified to suit the simulation conditions, boundary conditions [19-20]. Mathematical model considered circular symmetry for the simplified heat conduction equation

$$\rho C_P \frac{\partial T}{\partial t} = \left(\frac{k}{r_L} + \frac{\partial k}{\partial r_L} \right) \frac{\partial T}{\partial r_L} + \frac{\partial k}{\partial z_s} \cdot \frac{\partial T}{\partial z_s} + k \left(\frac{\partial^2 T}{\partial r_L{}^2} + \frac{\partial^2 T}{\partial z_s{}^2} \right) + \frac{dI}{dz_s}$$

.................(3.7)

41

Where r_L = distance from center of laser beam in m, z_S = distance from irradiated SU8 film/contact in m, T= Temperature in K, t = interaction time in sec, I = radiation intensity in Wm^{-2}. [Section 3.8.1] Table 1 enlists the properties of SU8 which were used for thermal modeling of heat transfer across SU8 film on glass or silicon substrate.

Figure 3.9 shows temperature distribution caused by a simulated 30W laser beam traversing in circular path on the substrate over a SU8 micro-drop.

Some process constants are assumed while carrying out simulation: Reflection coefficient of SU8 = 0.3, Heat transfer coefficient [$\frac{P_L}{A-\Delta T}$] of contact: 10~260 [W/(m^2 .K)] depending on area of interaction, where P_L is laser power, A is area of interaction, ΔT is desired temperature difference on exposure.

Heat flux boundary condition with thermal heat coefficient = 260, initial temp=293.15^0 K. Thermal insulation boundary condition, heat source domain, heat transfer in solid domain, k, σ, C_p from material.

Heat source equation for moving laser: Gaussian Signal [Ref: 17-34]
Q_inL=Q0L*(1-Rc$_L$)*Ac$_L$*(1/(pi*sigX*sigY))*an1L(x,X00,sigX,y,Y00,sigY)*exp
(-Ac$_L$*abs(z))

Where X00=X0+rad*cos(omega*t) : Y00=Y0+rad*sin(omega*t) : Co-ordinates
 an1L: exp(-((a-a0)^2/(2*siga^2))-((b-b0)^2/(2*sigb^2))) analytic function
 arguments: a, a0, siga, b, b0, sigb
 sigX, sigY in μm.
 Rc$_L$ =0.3, Ac$_L$= 0.25[1/cm] Gaussian signal coefficients

The temperature scale shown on the right side of the simulation output varies from 300~900 ˚K and the snapshot of simulation were obtained at time instant 80.425 milli-seconds. If the laser heat is allowed to continue flowing in, the temperature of the spot may go sufficiently high to damage the SU8 film or material of the micro-droplet or the optical fiber. The degradation temperature of SU8 is

recorded as 380°C and should be reached for proper fusion of the melt polymer and fiber so that a firm bond can be obtained after it cools down.

3.11.4 COMSOL multiphysics simulation for modeling the whispering gallery mode (WGM):

RF module of COMSOL multi-physics tool was used for analyzing the SU8 micro-drop bonding the optical fiber to a polymeric waveguide. The governing equations in the Electro-magnetic wave frequency domain physics that was used to model the whispering gallery modes are [equations3.8-3.12] as follows:
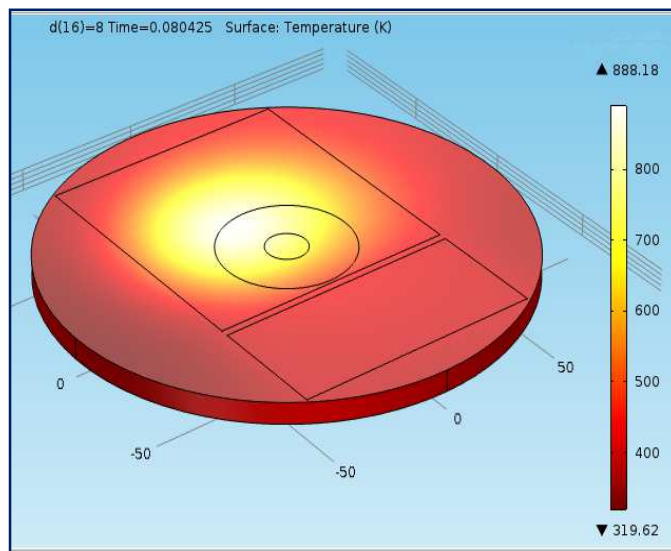
Fig. 3.9 Simulation of laser heat transmission process for a moving laser exposing along a circular path on a 10 microns thick patterned SU8 layer.

$$\nabla X(\mu_r^{-1}.\nabla X E) - K_0^2 \left(\varepsilon_r - \frac{j\sigma}{w\varepsilon_0}\right) E = 0 \quad \text{.......................................(3.8)}$$

$$\nabla X(\mu_r^{-1}.\nabla X E) - K_0^2 \varepsilon_{rc} E = 0 \quad \text{.......................................(3.9)}$$

Where $\varepsilon_r = ($ n-ik$)^2$ is relative permittivity [F/m] ('n' being the real part and 'k' being the complex part of the refractive index of the material SU8 in our case), μ_r is relative permeability [H/m], both these quantities are considered with respect to the permittivity and permeability of free space (ε_0 and μ_0 respectively) σ = conductivity [S/m], ω= angular frequency of the incident signal, K_0 is the wave number of free space represented by the following:

$$K_0 = \omega\sqrt{\varepsilon_0\mu_0} = \frac{\omega}{c_0}\ [\ rad.m^{-1}]$$ ....(3.10)

Where c_0 = Speed of light in vacuum [3**X**10^8m/s]**.**

$$Q - factor = \frac{f_0}{\Delta f}$$ ....(3.11)

Where f0 is resonance frequency and Δf the 3-db bandwidth at resonance. Q, the quality factor when cacalculated from complex eigen-frequency value W_r as

$$Q_0 = \frac{Re(W_r)}{2|Im(W_{r)}|}$$ ....(3.12)

For WGM simulation, boundary conditions were selected as perfect electric conductor [PEC], perfect magnetic conductor, electric field and the domain condition was perfectly matched layer [PML] to control dispersive outer region.

3.11.5 Fabrication of optical waveguides:

Fiber to fiber laser welding using SU8 was done with two pairs of optical fibers placed in close proximity on glass slide, Si-wafer or Si/SiO₂ substrate. The distance between each individual pair and its alignment were adjusted using microscope, X-Y-Z stage. The interfaces were covered with small drops of SU8-2025. SU8 material was also used for fabricating the optical waveguides and interconnects [detailed procedure is given in section 3.6]. These structures were suitably aligned with the, off the chip optical fibers using clamping or positioning system and SU8 micro-droplet was dispensed over the respective joints in volume of about [2.42E^{-10} m^3] 0.242 micro-liter. One-by-one the SU8 micro-droplets were then exposed to the CO₂ Laser beam of Epilog Laser Engraving Machine according to the pre-programmed pattern and select parameters of the machine. The beam diameter of this machine is around 80μm and the system emits at 10.6μm wavelength. The laser path was designed using Corel Draw and is described to move the laser head over the assembly, connecting the coupling to coupled fibers in a pre-designed layout. Each exposure of the laser is coincided with the geometric pole of the individual SU-8 micro-droplet and only a very small zone of the droplet was laser exposed. The laser power being highly focused in a small area guides the light past the whole radius of the micro-droplet all the way to the substrate over which the droplet is placed. The advantages of these laser welding processes are 1.They prepare the bonded fiber and waveguide or bonded fibers for external

44

connections in a system, 2.By varying some of the machine parameters a wide range of surface changes alongwith a bond and corresponding % transmittance can be availed.

Figure 3.10 shows (a) schematic of fiber to fiber coupling and fiber-waveguide fiber coupling on a Si substrate using SU8 microdroplets (b) optical micrographs of fiber-fiber bonded laser tagged microdroplets at different stages of optimization of Laser machining.

As the SU8 micro-droplet was top irradiated with laser the heat transfer occurs across the surface of the droplet through its bulk to the substrate (Si or Glass) along a small central zone of the droplet. As discussed before depending on the heat transfer coefficient of the substrate if the heat is not conducted away by the substrates it can result in more localized heating although there is a chance of the droplet to totally melt and develop splashes.
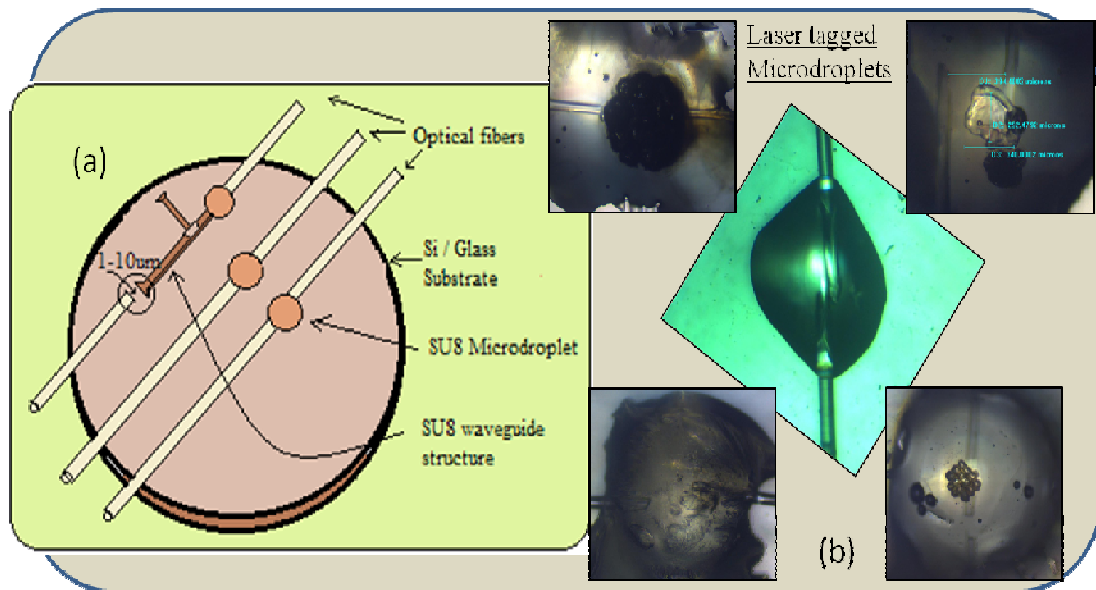
Fig. 3.10 Fiber bonding (a) the schematic diagram for coupling between two pairs of optical fibers using the SU8 microdrop along with a SU8-waveguide-fibers coupling, (b) shows various stages of optimization of laser machining with the optical micrographs of the laser tagged micro-droplet surfaces (top view) for the fiber/ fiber joints[Clockwise from top left].

The heat is also said to flow across the embedded fiber thus melting and partially dissolving the fiber in SU8 so that on resolidification there was strong adherence between the substrate surface and the fiber. The softening temperature of optical fiber is 1600-1710°C. Thus the localized and focussed laser beam is completely controllable. Post the instant of laser beam exposure, the center of the SU8 drop is solidified very fast. CO_2 laser beam has operating wavelength of 10.6μm. With optimization of speed, pattern, power, frequency of the laser machine, the controlled laser power is flown through the surface and bulk of the droplet, forming either a desired bond strength or making the inner curved surface area near the substrate functionalized for the input optical signal or by creating a sensitive surface for registering the activities just beyond the dome like surface of the semi-elliptical /semi-hemispherical surface of SU8 microdroplet.

With DOE and number of other tests carried out on Si and glass surfaces for laser heat transmission based bonding, led to optimized values of laser machine parameters. The strength of the fiber weld after exposure to laser heat and resolidifaction was evaluated qualitatively and grouped Very Good, Good, Not Good and Bad. Optical fibre softening can be reached on Si or glass surface by controlling laser machine parameters as shown in Table 3.2.

Table 3.2 Laser based bonding: % Transmittance obtained with variation in speed and power of laser beam.

S. No.	Corel Draw Pattern	% Power Speed	Weld Strength	Optical Transmittance
1.	Si + SU8 drop	100/1	Bad	-----
2.		60/1	Good	0.00209
3.		50/1	Very good	0.744
4.		40/1	Good	0.09495
5.	Direct Bonding of Fiber on glass with no SU8 material	100/ (40-80)	Good (Fiber melt)	-------

Direct bonding of optical fiber on the glass surface without SU8 thin film or drop was attempted to know % power/ speed. The bond strength was found to be poor and there was spill over of the fiber melt, so this option was not investgated in further studies. The fiber softening temperature is in the higher range [1600-1710^{0}C] than SU8. So fiber material or SU8 do not experience degradation [600~ 900 K max] in this study.

3.11.6 Measurement of % Transmittance across the coupling

Once the strategy of coupling of optical fibers is established, it can be applied and extended to microchip based waveguide like structures using SU8 micro-drop. To evaluate performance and optical characteristics of this bond, its use as a tool or probe to access optical signal from source, microchip and deliver it to desired external setup; the bonded assembly must be tested for % transmittance using an optical test setup. The laser bonded fiber-fiber and fiber-waveguide-fiber bond asemblies were optically characterized for % Transmittance measurement using Ocean Optics Spectra Suite Spectrometer in an integrated test setup, see figure 3.6.

A halogen lamp [wavelength 300-1100 nm peak measured value [R_λ] of 60000 counts (this 60000 count is considered as reference value for further discussion)] was used as light source for the input fiber chord which fed the signal to coupling fiber bonded on chip. The alignment process of the fiber and SU8 microdroplet dispensing was done using two precision XYZ stages. The ouput signal [$S_{O\lambda}$] is connected by optical fiber cable or chord to the Ocean optics USB4000 which is a UV-VIS miniature Fiber optic spectrometer. USB 4000 has 16-bit A/D convertor, a set of CCD arrays, GPIOs, enhanced electronics with increased signal-to-noise ratio. It is connected to a computer system at the USB port and Spectra-Suite spectroscopy software of Ocean Optics with advanced data capture attributes, was used to analyse signal from the array detector. The output spectra has wavelength in 'nm' on X-axis and intensity (counts) on Y-axis. It can be used to measure wavelength dependent transmittance of a sample or structure, its absorbance, reflectance and relative irradiance. Before starting with the actual measurement, reference [R_λ], dark [$D_{R\lambda}$] files referring to background subtraction must be first stored, see equation (3.13).

In order to find coupling efficiency of a sample, the transmittance of an optical signal across such a sample, coupling was numerically determined by percentage transmittance which represents the % amount of energy allowed to pass through a sample medium relative to energy passing through the reference medium.

$$\% \, Transmittance = \% \, \frac{S_{o\lambda} - D_{R\lambda}}{R_\lambda - D_{R\lambda}} . 100 \quad ....(3.13)$$

Where $S_{o\lambda}$ is signal output intensity level, $D_{R\lambda}$ is dark reference signal level (Intensity=1000 counts) and R_λ is a reference signal (taken as 60000 counts in most cases). % Transmittance is a unitless quantity as it represents ratio of two intensities. After following required steps in a wizard for transmittance measurement, a graph /spectra of wavelength dependent % transmittance was obtained on the active window of the Spectra Suite. The spectra along with the readings in notepad files were saved. The % transmittance was further measured for the cases of aligned and mis-aligned fiber bonds.

3.11.7 Measurement of absorptivity of SU8

SU8 is an optically transparent material with maximum absorbance of light at 365nm wavelength. Usually in an application of SU8 as a photoresist or microfabrication material involving photolithography, laser beam of wavelength closer to 365nm is selected. In this study based on laser heat transmission using SU8 microdroplet, role of SU8 and its properties like absorptivity at the operating wavelength is vital. The laser engraving machine used for laser based bonding application had a CO_2 laser source. It operated in the mid infra red range [MIR] with wavelength of 10.6μm. The purpose of determining the absorbance at the interface of the SU8 and the substrate was to find out about the refluxing heat which is reflected at the interface, not transmitting conductively to the sides which would aid in melting of the interface, promoting adherence of the SU8 micro-drop over Si/ glass substrate. [35] With its properties glass substrate might offer higher reflectivity and greater refluxing of the heat to the interface with minimum conductive loss as compared to Si substrate. Quantitatively the absorbance can be obtained from eq. (3.14).

$$\varepsilon = \frac{N_A . Absorption \, cross \, section}{1000.\ln(10)} \quad ....(3.14)$$

Where, N_A is Avogadro no. representing for a given material, number of constituent particles per mole. The absorption cross section was considered to be in terms of the

laser beam spot-size on the exposed substrate, assumed to be in cm^2. So an exercise was undertaken to find absorptivity of SU8 at this wavelength. A comparison of absorptivity with and without SU8 on glass/ Si was made where, Absorptivity (ε) was measured at 10.6 µm. Number of substrates of glass, Si were prepared with coating of Su8 in the form of small circles prepared for the Laser exposure. Half the Si/ glass sample substrates were kept uncoated for the exposure. Then systematically number of CO_2 laser exposures were carried out on all the four sets [Si, Si+SU8, Glass, Glass+SU8] of substrates with varying power and speed parameter of the lasing machine. The spot-sizes thus obtained were imaged and measured using Nikon epifluorescence microscope. As the glass - SU8 interface is the most heated up and high temperature zone in the whole cross-section of the droplet owing to the heat reflux back into the SU8 at the interface we thought it important to observe the absorption at this interface. Hence the absorptivity at the interface of the SU8 was subsequently calculated by using the equation (3.15).

Absorptivity of SU8=Absorptivity of Glass-Absorptivity of (Glass+SU8) …….
(3.15)

Method of averaging was used to get the final value of SU8 absorptivity.

3.11.8 Calculating the SU8 droplet Volume

The cross-sectional area [for a, b] of the SU8 micro-droplet was imaged using the Nikon epifluorescence microscope using the bright field option. Then vertical cross-section plane of the droplet, perpendicular to the plate (both major and minor axes) was imaged and measured [for h]. This was achieved by aligning the glass slide in the vertical direction perpendicular to the sample stage of the microscope. The volume of the droplet was calculated by using the expression (3.16) see Figure 3.10 (c):
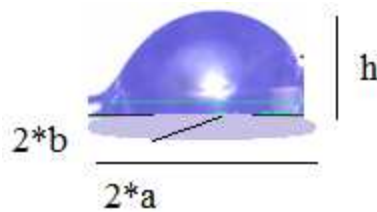
3.10 (c) Volume Measurements of microdrop

$$V = \frac{\pi}{6} * h * (3a^2 + 3b^2 + h^2)$$ ....(3.16)

Where a, b and h were the major radius, minor radius and height of the hemispherical droplet, respectively. The first job was to see the consistency in dispensing identically sized volumes and then based on this data the average interface area of the glass SU8 interface was calculated.

3.12   Result and Analysis

After considering methodologies of analysis, simulations, calculations, measurements of various quantities, following subsections present results and correlation between them.

3.12.1 Optimization of Machining Parameter

In the laser stitching experiments the lasing parameters like span time, power, pattern of lasing, speed, frequency were varied and optimization of these parameters was carried out using design of experiment (DOE) software. Table 3.2 shows the strength of the laser welding process with respect to the power/ speed percentage of maximum values. The maximum power of the laser source was 32 Watts and the maximum speed with which the beam traverses the X-Y stage of the laser machine was 15.4 cm/sec. Desired strength of the laser welded fiber bond was obtained with the parameters mentioned in row 2-5 of Table 2. Poor weld strength was obtained at row no. 1. It is observed that the optical transmittance values across such joints as mentioned in the last column of table 1 are also low in case the strength of the fiber joint is poor indicating that the coupling is inappropriate if the fiber SU8 melt pool is not properly formed due to insufficient heating of the microdroplet. It is further noticed that a power level equalizing the full power value provided insufficient bond strength. The cause of this condition may be overheating or burning of the SU8 material at the spot. This probably can be accounted for by looking into the thermal expansion coefficient of the Glass (1.1×10^{-8} / K) and SU8 (5.2×10^{-5}/ K) respectively. In the direct bonding of fiber to glass the coefficient of expansion being more or less similar demonstrated no inter-layer shear between the fiber and glass resulting in good bond strength between both. There was a spillover of melted fiber when direct bond was formulated. Out of all the combinations of power / speed parameters, experiments showed that ratio of 50% power and 1% speed correlated to the best bonding between the fiber, SU8 photo-resist and the

silicon substrate. It was also corresponding to highest transmittance. We hypothesize that if the fiber is very well bonded then the transmittance is also higher.

The DOE software tool Software Design Expert 7.0 was used with ANOVA mathematical model, Response Surface Methodology [RSM] and Cental Composite Design [CCD] fitted in the model by least square technique [See functional equations in Appendix]. Factors chosen for this single objective optimization process are lasing speed and lasing power of the epilogue machine. The DOE module was operating between the optimum machining conditions and resulting in getting greatest % of transmittance. Contour plot output from the DOE is provided in figure 3.11. It predicts the maximum transmittance level corresponding to 72% obtained at Laser power of 52.90% of maximum power and speed corresponding to 1% of maximum speed which is very close to the actual values at which the bond strength of the joint is very good as illustrated in Table 2 and reported earlier. Therefore, it can be concluded that there is a very high level of correlation between the % transmittance and good bonding strength. The % transmittance observed by way of experiments is actually a 2% higher than the DOE predicted value which may be further improved by taking more no. of observations in the model.
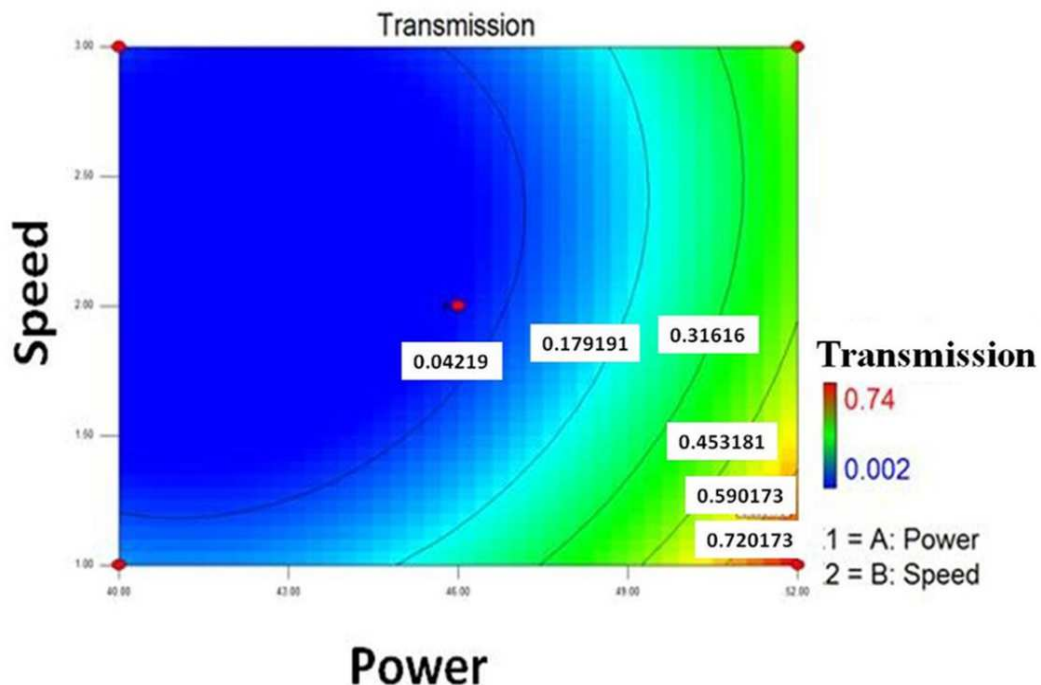
Fig. 3.11 The design of experiments [DOE] results indicating the transmission as output with speed and power as input parameters.

3.12.2 COMSOL simulations for Laser heat transfer

Simulation of the laser heat transmission process used for welding between fibers by using SU8 micro-droplet had shown time dependent variation in temperature distribution of the laser exposed area. The heat was rapidly dissipated across the micro-droplet as well as the surface. As detailed previously the heated substrate was responsible for refluxing and reflecting back the heat to the SU8 layer along the interface had it been a poor heat conductor. In fact due to the rapid temperature rise and a cross-over of the 'Tg' [glass transition temperature] value of uncross-linked SU8 2025 (50° - 65°C), it melted and then got superheated near the interface due to the heat refluxing action of the substrate [36]. This is clear in the simulation output which is reported in Figure 3.9 and Figure 3.12.
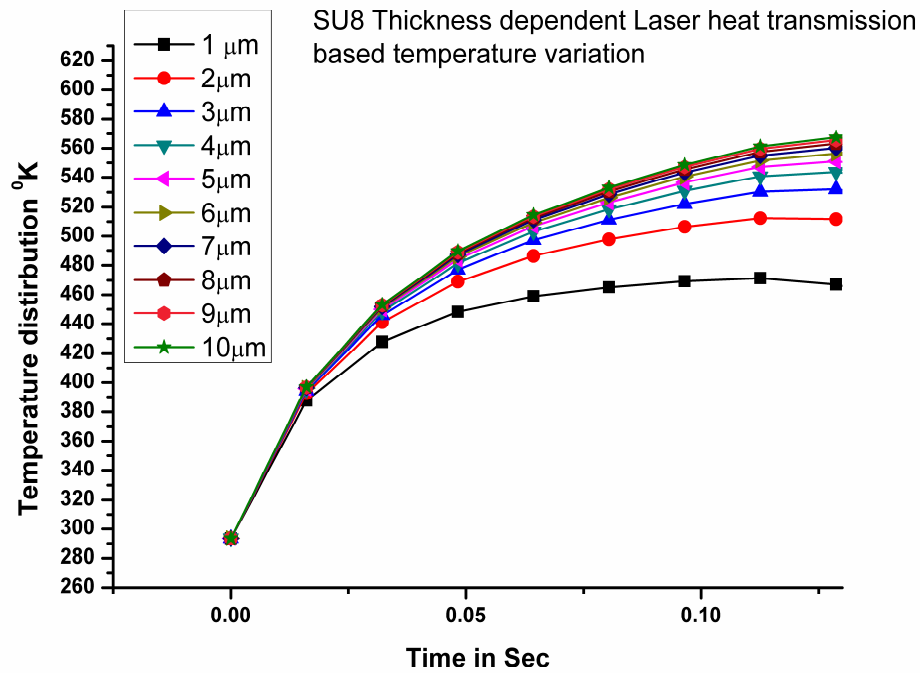
Fig. 3.12 The simulation output of bulk temperature of SU8-2025 vs. time in sec of heat treatment. [Different plots show the temperature behavior from a surface 10 micron above the interface in the SU8 layer treated as 'zero datum' towards the interface]

The temperature started rising as the Laser started radiating at time instant '0' at the micro-droplet and simultaneously heat transfer processes occured so that equilibrium was achieved in around 125 milliseconds. The equilibrating temperature is shown as 560°K (287°C) for 10 micron thickness, away from the interface [based on sectional plot of figure 3.9] and the temperature further decreased, away from the

interface towards the bulk of the SU8 material. In fact at a distance 1 micron from the interface the temperature is at a value of 470° K [197°C]. Thus very near to the Si surface, the temperature reached the melting point of SU8 but it did not go into the degradation temperature for SU8 which is about 380°C. [40] The glass being a higher reflector of incident beam shooted up to above 380°C which may degrade the SU8 in actual practice, due to very less absorbance of the substrate on beam incident side. So, we can see that as the laser processing involved similar conditions of the laser frequency, scan rate, laser power and resolution, speed as obtained in the earlier section, the exposed zone always had a molten state which solidified on removal of the Laser power. The interface therefore was found ideal for the placement of input/ output fibers. A stronger joint was formed as the fibers were aligned or misaligned as per figure 3.7 on the surface of the substrate (interface of SU8 and substrate). The model accounted for the conductivity of the wafer and if the conductivity resulting in interfacial heat loss was considered then the overall maximum temperatures achieved at the interface should be lower for Silicon substrate as the thermal conductivity of silicon will be higher than that of glass.

The birefringence estimation was performed on a combination of COMSOL modules, including structural mechanics model giving stress due to rise in laser heated material temperature [Solid heat transfer model]. This stress was monitored over a short portion of the model to find birefringence or change in effective refractive index and corresponding change in optical properties of the material. Birefringence prediction if performed starting from the interface to the bulk of the droplet, then the superheated molten state of SU8 that was formulated closer to the interface will have more refractive index homogeneity thus causing less amount of birefringence. As the distance from surface was increased then away from the hot zone as the SU8 may still be semi solid there may be large variation of refractive index causing an increase in the overall birefringence. Simulated effective birefringence data was plotted for Air/SU8/Si combination. Figure 3.13 shows the birefringence plot drawn using COMSOL multiphysics simulation software.
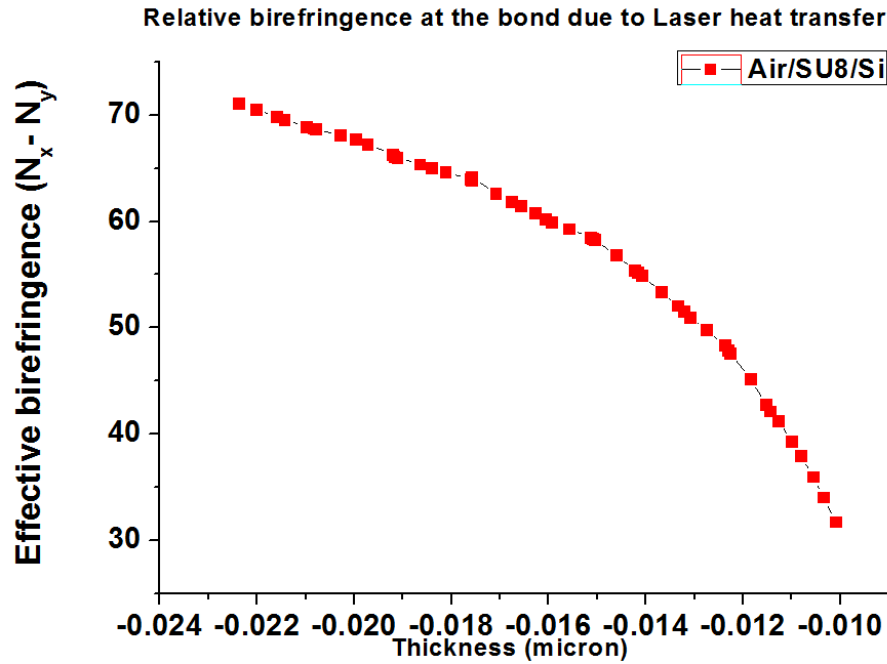
Fig. 3.13 Simulated estimation of effective bi-refringence with respect to distance from the surface for Air/SU8/Si combination.

3.12.3 Calculating microvolume and absorptivity of SU8 microdroplet

Using recorded and measured optical micrographs, minimum volume of the SU8 micro-droplets were calculated as $1.05 * 10^9$ µm^3 [As per equation 16]. Further the number of microscopic images of laser heated spots, on glass substrates, with or without SU8 coating were used for calculating the spot area of the microdroplet based on which using equations(14) and (15) the absorptivity variation for SU8 on glass and silicon was ascertained. It was observed that the absorptivity depends heavily on overall spot size and a higher spot area shows greater absorptivity. In any event glass is opaque at 10.6µm wavelength which is also the wavelength corresponding to the CO_2 laser [42]. On the other hand Si is normally opaque to UV-Vis range and is transparent at 10.6 microns wavelength. Figure 3.14 shows the absorptivity plot for SU8 on glass and Silicon substrates and it is observed that the transmittance of 'Si' at 10.6um is about 40-50 %, as compared to that of Glass which has no absorbance at this wavelength. The SU-8 over Si reflected by the blue trace in figure 3.14 show increase in absorptivity of incident laser light whereas glass reflects everything back to the medium or SU8 as illustrated in the red and black traces respectively. This provides a basis of good strength of direct bonded

54

fibers over glass substrates,eventhough the reflected light would add much reflux which may degrade the SU8 overshooting its 'Tg' and go upto the degradation temperature (380°C) value. Thus a preferable usage of Si substrates is considered by this analysis.
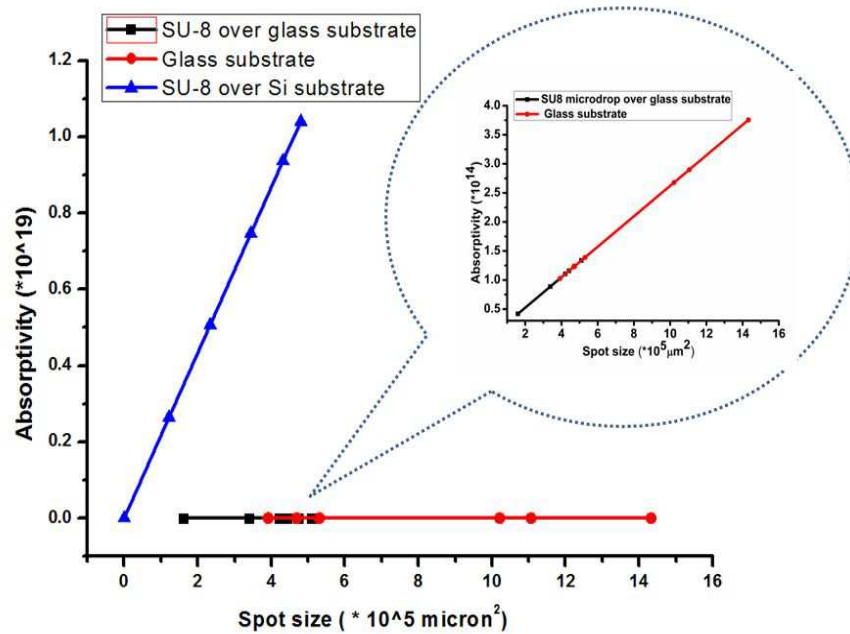
Fig.3.14 Comparison of absorptivity of SU-8 over Si and glass substrates through experimental results.

3.12.4 Simulation of WGM using COMSOL modelling

Two different aspects were studied in this 2-D model, corresponding to the aligned and misaligned cases as detailed in figure 3.7 earlier. In the aligned case the input and output fibers were aligned axially and the distance between them was varied from 1 ~5.5 microns. The geometry constructed while simulating in RF module of COMSOL that demonstrated the WGM effect most prominently happened for an ellipsoidal droplet [39] of overall diameter of 6.0 microns along the major axis and 4.0 microns along the minor axis. Therefore it was used with a refractive index =1.67 boundary of the SU8 and a refractive index = 1.46 of the optical fiber for carrying out the simulations. Initially the fibers are at the two axial ends of the microdroplet in the aligned case, so maximum distance between them is 5.5 microns, to capture the WGM based transmission of optical power inside the droplet. This was followed by a gradual movement of the output fiber towards the

input fiber (spatially fixed) upto an extent where the fiber almost touched each other. The transmissibility of the input signal in all these cases is simulated and figure 3.15 (a), (b) show output of such simulations.
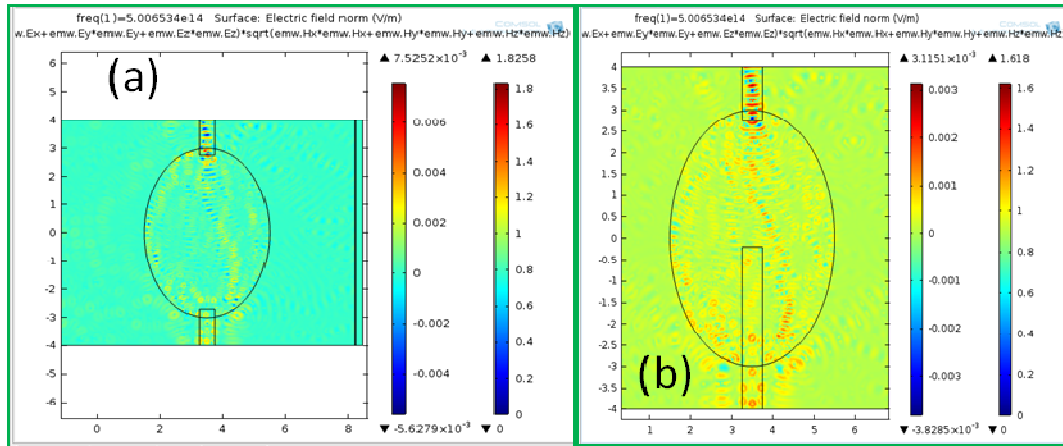
Figure 3.15 Simulation output of the aligned case with inter-fiber distance (a) 5.5µm (b) 4.8 micron.

In case of misaligned fibers, they were separated perpendicularly to their axes. The fibers were initially positioned tangentially to the ellipsoidal micro-droplet on and later manoeuvred, with input fiber fixed and the output fiber varying radially inwards. The simulation results for the same were observed and recorded. Figure 3.16 shows a bar graph with the simulation predicted % transmittances corresponding to figure 3.15.

The simulation output in the aligned case shows that as the inter-fiber distance approaches the diameter of the micro-droplet there was a tremendous increase in % transmittance between the input and output fibers almost to the extent of 100%. At other distances of separation the overall transmittance was lower than 45 % owing to scattering effects of the microdroplet material. Similarly, in the misaligned case the maximum % transmittance of 65% occured at an inter-fiber distance of 2.0 microns. This separation distance brings both the fibers close to the circumference of the ellipse. Therefore, through simulation it can be predicted that when the interfiber spacing was matched with the WGM zone in the ellipsoidal droplet, there was a sudden increase in % transmittance, even though the fibers are misaligned and at a distance from each other.
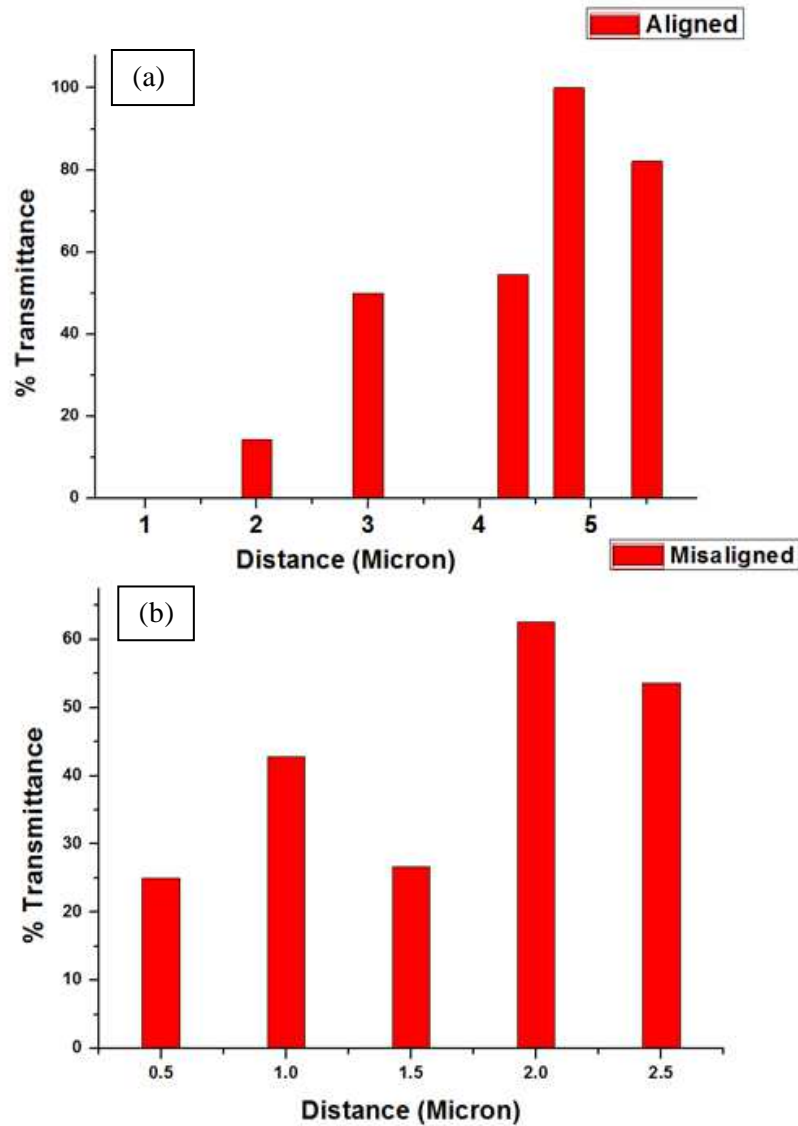
Fig. 3.16   Simulation results showing % Transmittance with respect to inter-fiber distance for (a) Aligned fiber and (b) Misaligned fiber cases.

3.12.5 Measurement of optical transmittance in a test set up

We have used the Ocean Optics SpectraSuite test setup described previously in figure 3.6 for measuring the % transmittance, using the mathematical relationship of equation (13). The transmittance study was performed for both the aligned and misaligned cases, on the similar lines to that of by simulations. The micro-drop diameter was more realistic in actual set up and in the range of 1054 microns as shown in the optical micrograph as shown in figure 3.7 (c). The inter-fiber distance in the aligned fiber case was varied from '0' to 750-microns. The fiber diameter itself was around 125 microns .When both fiber diameters and the inter-fiber

57

distance was added together to get the necessary confinement distance. The confinement distance for both the fibers in the largest separation case comes out to be similar to the drop diameter which illustrated the possibility of coupling of optical signal through WGM effect. The wavelengthwise transmitted intensity was acquired digitally and recorded with the ocean optics spectrophotometer. Experimental results of this study, for both aligned and misaligned fiber cases is shown in graphical form in figures 3.17 (a) and (b). All the graphs were recorded using the spectrophotometer and acquired with spectra-suite software. From the two graphs it can be seen that the highest transmittance occured pertaining to either a contact condition or if both fibers are near to the outer edge of the SU8 microdroplet where the transmission utilizes the WGM effect. The ~60% transmission was recorded in case of aligned fibers as they were connected end to end within the microdroplet. Full 100% transmission does not happen owing to polishing defects, lack of cleaving or mirrorlike finish of the fibers at its ends. The transmission % increased as soon as both fiber faces were brought near the outer edge of the droplet so that the WGM effect pre-dominated the transmission. The transmissibility started increasing to almost 60 % corresponding to an inter-fiber distance of 650 microns. A similar observation was recorded in the misaligned case where the maximum transmittance of 95 % was observed as the two fibers were shifted along a direction perpendicular to the axes of both fibers upto a distance of 700 microns. In the other extremity as the fibers were laterally misaligned by 10 microns the transmissibility was 80%.
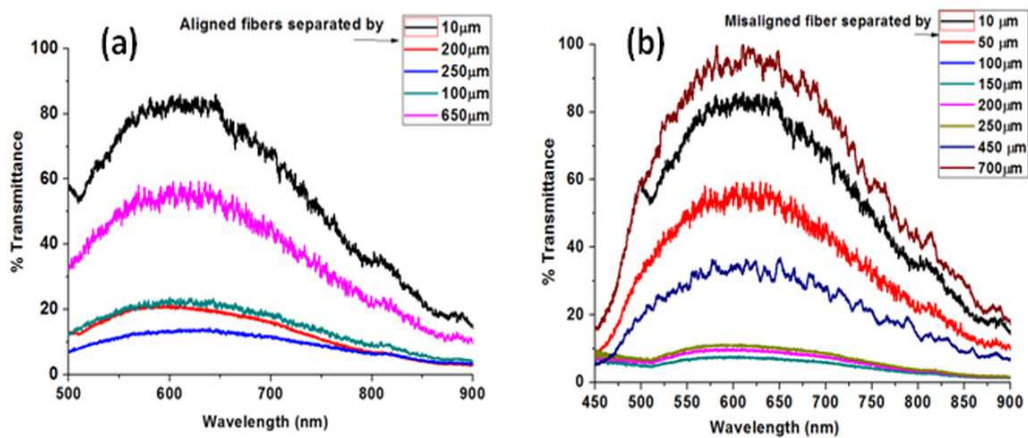
Fig. 3.17 Acquired data through spectra suite software using ocean optics spectrophotometer for (a) Aligned fibers (b) Misaligned fibers.

Therefore, in conclusion, the micro-droplet method using SU8 photo-resist and aligned fibers, followed by laser machining shown in the above work ideally offers a good methodology for optical tagging and joining of standalone optical fibers to furnish high transmittance even if the fibers were in misaligned orientation.

3.13   Future Scope

The methodology discussed above when supported by smaller (diameter < 350 microns) SU8 droplets over the two fibers or fiber-waveguide-fiber, may provide improved and optimized solutions for signal transmission and sensing of biological entities.

3.14   Conclusion

Through this work, we have attempted to explore and develop a new technique to tag optical fibers on the surface of a substrate with the aid of SU8 microdroplet and CO_2 laser source. The exposure parameters of the laser machine were optimized in such a way that the SU8 material very close to the substrate melted locally up to several layers due to heat reflux from the surface of the substrate. This melt then resolidified to ensure a good bond between the fibers, droplet and the surface. It was further ensured through heat transfer simulations that the fiber or SU8 are not degraded while getting heated. The DOE factors are lasing speed and lasing power with single objective of Transmittance. The optimization process gives optimized values of these laser machine parameters with the mathematical model set on least square techniques. Speed /power = 52/1 was obtained for transmittance of 0.792. The stitched or bonded optical fiber was then extensively evaluated for % transmittance or optical characteristics when input light was transmitted through the SU8 microdrolet to the output fiber. It was observed through simulations as well as experiments that the fibers demonstrated high transmissibility in two circumstances. One is in which the fiber is completely connected end to end. In the other configuration the fiber ends were shifted away from each other till they come very close to the outer surface of the drop where due to the WGM effect the transmissibility was found to increase. The method was further evaluated for aligned and misaligned fibers and transmissibility was found to have similar behaviour in both the cases. Thus the work ascertains that optimized laser beam exposed SU8 micro-droplet can be used to couple two or more optical fibers maintaining an overall high level of optical coupling efficiency.

Reference

1.	Book: Maria L. Calvo, Vasudevan Lakshminarayanan ,“ Optical waveguides: from theory to applied technologies”, CRC Press Taylor and Francis Group.

2.	M.B.Frish, J. Fijol, E.E. Fike, S.A. Jacobson, P.B. Keating, W. J. Kessler, J. LeBlanc, C. Bozler, M. Fritze, C. Keast, J. Knecht, R. Willamson, C. Manolatou, “ Coupling of single mode fibers to planar Si Waveguides using vertically tapered mode converters ”.

3.	X.Chen, C.Li, C.K.Y.Fung, S.M.G. Lo, H.K.Tsang , “ Apodized waveguide grating couplers for efficient coupling to optical fibers”, IEEE PHOTONICS TECHNOLOGY LETTERS 22 15 2010.

4.	Technical Support 1.800.BELDEN.1 www.belden.com

5.	Zhigang Chen and Allen Taflove, "Highly efficient optical coupling and transport phenomena in chains of dielectric microspheres", optics letters, 2006, Vol. 31, No. 3.

6.	Shih Hao Huang, Fan Gang Tseng, "Development of a monolithic total internal reflection-based biochip utilizing a micro-prism array for fluorescence sensing", Journal of Micromechanics and Micro engineering, 2005,15, 2235–2242.

7.	Amnon Yariv," Critical Coupling and Its Control in Optical Waveguide-Ring Resonator Systems", IEEE photonics technology letters,2002, vol. 14, No. 4.

8.	Stephen R. Friberg And Peter W. Smith, "Nonlinear Optical Glasses for Ultrafast Optical Switches", IEEE Journal Of Quantum Electronics, 1987, Vol. Qe-23, **No.** 12.

9.	Hirohito Yamada, Analysis of Optical Coupling for SOI Waveguides, Piers Online, Vol. 6, No. 2, 2010 165.

10.	Erik pennings, Giok - Djan Khoe, Meint K. Smit, Toine Staring, "Integrated - optic versus Microoptic devices for Fiber-optic telecommunication systems: A comparison ", IEEE Journal of selected topics in quantum electronics, vol. 2, No. 2, June 1996.

11.   Bambang Kuswandi, Nuriman, Jurrian Huskens, Willem Verboom, "Optical sensing systems for microfluidic devices; A review", Analytica Chimica Acta 60I 2007 141-155.

12.   Liang Tang, Yongjie Ren , Bin Hong , Kyung A. Kang, " Fluorphore - mediated , fiber-optic , multianalyte, immunosensing system for rapid diagnosis and prognosis of cardiovascular diseases" , SPIE, Journal of Biomedical optics, vol 11, Issue 2, 2006.

13.   Simin Mehrabani , Ashley J. Maker , Andrea M. Armani, " Hybrid integrated label - free chemical and biological sensors" , Sensors, 2014, 14, 5890 – 5928

14.   Z. Wang, N. Chocat, "Fiber-Optic Technologies in Laser-Based Therapeutics: Threads for a Cure", Current Pharmaceutical Biotechnology, Volume 11, Number 4, 2010, pp. 384-397(14)

15.   Gorden E. Moore, "Lithography and the future of Moore's law", Proc. SPIE 2440, Optical/Laser Microlithography VIII, 2 ,May 26, 1995.

16.   D.Hulsenberg, A.Hamisch, A. Bismarck,"Microstructuring of glasses", Springer Series in material science.

17.   Patent: WO 2012094737 – "Laser reinforced direct bonding of optical components".

18.   Domański R., Jaworski M.," Laser beam interaction with solid materials coated by layers with micron thickness", Archives of Thermodynamics. 1989, Vol. 10, No. 1-2.

19.   A.J.C. Grellier, N.K. Zayer, C.N. Pannell, "Heat transfer modeling in CO_2 laser processing of optical fibers",Optics Communications,1998, 152 (4-6). pp. 324-328A.

20.   Helebrant, C. Buerhop, R. Weißmann, "Mathematical modelling of temperature distribution during CO2 laser irradiation of glass", Glass Technology, 1993.

21.   G.Casalino, E.Ghorbel, "Numerical model of CO2 laser welding of thermoplastic polymers", Volume 207, Issues 1–3, 16 October 2008, Pages 63–71.

22.   S Z Shuja, B S Yibas, O Momin," Laser heating of a moving slab: Influence of laser intensity and scanning speed on temperature field and melt size", Optics and Lasers in Engineering, 01/2011; 49.

23.   Bappa Acherjee, Arunanshu Kaur, Soren mitra, Dipen Misra, "Finite element simulation of laser transmission welding of dissimilar materials between Polyvinylidene fluoride and titanium", International Journal of Engineering, Science and Technology, 2010.

24.   J.Melai, C. Salm, S. Smith, J. Visschen, J.Schmitz, "The electrical conduction and dielectric strength of SU8", Journal of micromechanics and microengineering, 2009.

25.   Rekhviashvili. et.al. "Modelling of laser pulse heating of solid dielectric with a fractal structure", American Journal of Condensed Matter Physics, 2012.

26.   M.Ilie, E. Cicala , D. Grevey, S. Maltei, V. Stoica , " Diode laser welding of ABS : experiments and process modeling ", Optics And Laser Technology 41, 5 (2009) 608-614

27.   Mirko Aden, Andreas Roesner, Alexander Olowinsky, "Optical Characterization of Polycarbonate: Influence of Additives on Optical Properties", Journal of Polymer Science: Part B: Polymer Physics, Vol. 48, 451–455 (2010)

28.   Ching Yen Ho, Moa – Yu Wen, Chung Ma, "Computer simulation for laser welding of thermoplastic polymers", International Conference on Computer Engineering and Applications, 2010.

29.   Chao Yi Tai, Bayram Unal, James S. Wilkinson, Mohamed A. Ghanem, Philip N. Barlett, "Optical coupling between a self assembled microsphere grating and rib waveguide", Applied Physics Letters,2004, Vol. 84, No.18.

30.   Tjioe, Fidelia,"Evaluation of optical solder for fiber-to-waveguide coupling in silicon photonics", http://hdl.handle.net/1721.1/45352

31.   Victor Nguyen, Trisha Montalbo, Christina Manolatou, Anu Agarwal, Ching-yin Hong, John Yasaitis, L. C. Kimerling, and Jurgen Michel, "Silicon based highly efficient fiber to waveguide coupling for high index contrast systems", Applied physics letters, 2006, Vol.88, p.081112.

32.   Shengfei Feng, Xinping Zhang, Hao Wang, Mudi Xin, Zhenzhen Lu," Fiber coupled waveguide grating structures ", Applied physics letters, 96, 133101 (2010).

33.   Santeri Tuomikoski, Sami Franssila, "Free- standing SU-8 microfluidic chips by adhesive bonding and release etching ", Sensors and Actuators A 120 (2005) 408-415.

34.   Jasbir Patel, Bozena Kaminska, Bonnie Gray, Byron Gates, "PDMS as a sacrificial substrate for SU-8 based biomedical and microfluidic applications" , Journal of Micromechanics and Microengineering 18 (2008) 095028 (11pp) .

35.   Don McMasters, M.L. Gillette, "Approximating Avogadro's number using glass beads and monomolecular film",Chemical education resources,Inc.

36.   Blanco F J, Agirregabiria M, Garcia J et al. Novel three-dimensional embedded SU-8 microchannels fabricated using a low temperature full wafer adhesive bonding. J. Micromech. Microeng. 14 (2004), 1047–1056.

37.   A. Kumar, et al. "Optimization of laser machining process for the preparation of photomasks, and its application to microsystems fabrication", J. Micro/Nanolith. MEMS MOEMS. 12(4), 041203, 2013.

38.   Richard Grzybowski, Stephan Logunov, Alexander Streltsov and James Sutherland, "Extraordinary laser-induced swelling of oxide glasses", Optics Express, Vol. 17, Issue 7, pp. 5058-5068 (2009).

39.   Seema Yardi, D.Boolchandani, Shantanu Bhattacharya, "Polymer Waveguide and Optical Fiber Coupling Using Whispering Gallery Modes in an Elliptical Micro- Sleeve", Optics in the Life Sciences Congress Technical Digest ©2013 The Optical Society (OSA).

40. Ru Feng and Richard J Farris, "Influence of processing conditions on the thermal and mechanical properties of SU8 negative photoresist coatings", J. Micromech. Microeng. 13 (2003) 80–88.

41. Installation and Operation Manual, Document Number 000-20000-300-02-201110, SpectraSuite® Spectrometer Operating Software.

42. P. Lucas, M.R. Riley, C. Boussard-Plédel, B. Bureau, Anal. Biochem. 351 [1] (2006) 1-10.

43. R.Muller, D. Cristea, M. Kusko, P. Obreja, D. Esineco, V. Damian, P.C. Logofatu, SU8 Polumer materials used in Intgrated Optic Microsystems ", Optoelectronics and Advanced materials –Rapid Communictions Vol. 4, No. 2, February 2010.

44. Sivarao, Shukor, T.J.S.Anand & Ammar, " DOE Based Statistical Approaches in Modeling of Laser Processing – Review & Suggestion ", *International Journal of Engineering & Technology IJET-IJENS Vol:10 No:04 1 101304-8787 IJET-IJENS © August 2010 IJENS I J E N S.*

Chapter 4
Interaction of Biomolecules with Solid Polymeric Surfaces of SU8 Microdroplet and Porous Fluorescent PDMS: Its Utility in Optical Bio-sensing

Chapter 4
Interaction of Biomolecules with Solid Polymeric Surfaces of SU8 Microdroplet and Porous Fluorescent PDMS: Its Utility in Optical Bio-sensing

4.1   Introduction

It is vital to associate, incessant research activity in the field of interaction of biomolecules on solid surfaces and molecular substrates; to the growth of industries like clinical diagnostics, food, pharmaceutical, biomedical, biomaterials and biotechnology. The applications and strategies of immobilisation of innumerable small, intermediate and complex biomolecules on the solid surfaces; is as diverse as the two groups of reactants involved. The nature of the required bioactive or passive surfaces may be ranging from antifouling, protein resistant, highly resistive of nonspecific adsorption of biomolecules, to extremely sensitive surface of protein microarrays. Surface modification or functionalization is required to condition the desired substrate according to the nature of handling and application of the target biomolecules.

A sensitive substrate deciphers reduced sample loss caused due to non-specific adsorption, increased performance and sensitivity, reduced possibility of contamination in the re-run of the samples using same devices, reduced inflammation or contamination in the body implants, food products. Select strategies of surface modification of hydrophobic and hydrophilic solid polymeric substrates for attaching bioactive molecules with protein resistant or protein specific antifouling surfaces are discussed in this chapter. Nature has a way of providing simple solutions to intricate problems. Researchers always come across clean, efficient and biomimmetic concepts to put forth, solutions of which bring the nature closer to our lives and also help provide steps to conserve environment in general. Over decades semiconductors have ruled the world of communication, electronics and sensing. Optical fibers made of SiO_2 were the backbone of world wide network for communication, called optical communication network. Thus dielectric materials have replaced the Cu and other metals due to scaling down technologies and need of insulating materials with low-K [dielectric constant] values in ever decreasing

feature sizes on microchips. Optical fibers made of SiO_2, offer high bandwidth, independent of the cable size, low attenuation, low electromagnetic interference, crosstalk; are light in weight, suitable for long distance communication at comparatively lower cost. Optical fibers are now available with compositions of part SiO_2 and Polymer or only polymer. Polymer optical fibers [POF] provide higher tensile strength, operate in visible range and they can be produced at a lower cost. They are widely used in industries and medical instruments inspite of having higher loss. Research is carried on, Cu wiring being widely replaced by POF. Polymers are also slowly finding their ways in optical devices like waveguides, optical components, sources and detectors. Research is carried out on functionalizing or modifying polymer surfaces to suit the conditions for sensing of biological entities. Yet there is a need to study a solid state polymer based sensor which is flexible and adaptable to the application situation.

In this chapter we have elaborately discussed prospects of bio-sensing in following materials:

A.   The ongoing work on two optical sensors in biological applications, Optical fiber and ring resonator or microspheres. In our work discussed here, we are presenting two types of SU8 microdroplets, with and without bonded fibers, being used as optical and biosensors. SU8 material is biocompatible, has excellent optical characteristics and a proven microfabrication material. The farication method, functionalization and immobilization methods are kept simple to provide a clean, biomimmetic and efficient solution to the sensing issues. Although very few characterization methods are available for 3-D structures, we have attempted to use Fluorimetry for sample solution based sensing and Spectra Suite Ocean Optics spectrometer for chip based sensing using fiber bonded microdroplets. Further both types of microdroplets can be extracted from substrate and used in most unusual and novel ways to suit the application.

Fluorescence microscopy is used wherever possible. We believe that the whispering gallery mode [WGM] phenomenon is occurring inside the elliptical or circular shaped microdroplets, based on the experiments and analysis of these devices. The devices are not perfect spheres or ellipsoids, so any mathematical,

analytical or theoretical analysis will be highly complex which need involved computing and simulating facilities.

Both labeled and labelfree sensing can be experimented with suitable pretreatment. Various experiments were carried out using different concentrations of ethanol, Bovine Serum Albumin [BSA] samples, Dye doped E-Coli and GFP tagged E-Coli cell samples. This work reviews strategies of surface modification, previously used for epoxy based, negative photoresist SU8 material and relates them to the SU8 microdroplet surface modification for waveguide bonding and optical bio-sensing application. Surface modification for protein immobilisation is explored for standalone SU8 microdroplets, which are detached and treated suitably for biosensing in sample solution, microscopy detection, can be flown in opto-micro-biofluidic channels, wells, for optical biosensing in a microfluidic reaction chamber. The surface immobilisation techniques are also applied on on- chip SU8 microdroplets used for bonding two optical waveguides on a microchip and sensing the biomolecular activities on its domelike surface.

B. In this work a novel bio-material is reported. It is a micro-porous fluorescent PDMS material with PDMS [Poly dimethyl siloxane] and Acridine Orange [AO] dye as its major constituents. PDMS is biocompatible with applications in fabrication of lab-on-chips, in bioseparation and in microfabrication. It is an artificial polymer with methyl groups and repeating silicon to oxygen bonds. Properties of PDMS material are oxygen permeability, non-toxicity and blood compatibility.

This new material is physically and characteristically dissimilar from the two combining bio-materials mixed in soft-lithography process. A range of characterization techniques, such as SEM, UV–VIS spectroscopy, Fluorescence microscopy, SpectraSuite optics signal setup, support the novel attributes of the material. Although extensive literature survey was done, it provided no references for a similar microstructure.

A   Exploring use of Biocompatible photoresist SU8 material as a biosensor

4.2   Need to Study Interaction of Biomolecules on Solid Surfaces

We are surrounded in nature by objects, materials, surfaces, liquid bodies which are susceptible to reactions with an assortment of bioactive molecules. The behaviour of these entities, which are in abundance, when they come in contact with an internal body implant or above mentioned substrates, is a reason why we need to study their interaction with these surfaces. This study has been recognized and found responsible for the steady development in the field of sensors, detectors, food packaging and processing industries, textile and pharmaceutical units, biomedical and biotechnology laboratories. Individual molecules like antibodies, peptides, enzymes, nucleic acids are included in the broad term biological entities along with complex, independent, viable biological entities like viruses, cells, spores, bacteria. Proteins and enzymes are known to have affinity towards specific targets which make it characteristic recognition behaviour. Normally oriented and randomized strategies of immobilisation are broadly considered. First is covalent strategy which provides enhanced biological activity and reduced signa - to - noise ratio, whereas second one is a covalent or other strategy which leads to reduced protein functionality and stability. The areas which are most affected due to non-specific adsorption and binding of biomolecules or colonization of microorganisms into formation of bio-films are biological implants, food packaging and hospital supplies. These are known to lose their sensitivity and performance resulting into inflammation, infection or contamination. It is of high level of importance in diagnostic devices, to know the adhesion or immobilization behaviour of proteins and DNA in varied system matrices.

Researchers need strong, robust, sensitive biomarkers in early detection of life threatening diseases. Biomarkers decipher an act of separation of cells, DNA, proteins from samples, body fluids, blood. Other methods involve controller beads, resins, filters to attract or process desired biomolecules. Surface functionalization or modification; involve processing of the surface to suit chemical interaction with specific biomolecules for its surface immobilization. Thus it is vital to know, effect

of micro-organisms, their types, behaviour in known, standard environment; specificity of the surfaces to these molecules to gain control in their detection.

4.3   Solid Polymeric Surface modification for Biomolecule Interaction

Once it is established that biomolecules bind to surfaces naturally or in chemically induced situation and cause undesired, unprecedented nuisance, if their properties are not known or behaviour not predicted in advance. It becomes essential to study them, analyse their adhesion chemistry and prepare surfaces accordingly to capture them in unknown sample matrix. Surface immobilization of specific analytes on a solid surface need modification to suite its surface chemistry with specific biomolecule. Four chemical binding or coupling strategies in connection with biomolecules are

1.   Adsorption   2.   Encapsulation

3.   Entrapment   4.   Covalent bonding

It is essential that biomedical polymers are biocompatible to have surface interaction with biological systems. Polymer materials are considered to be capable of reducing nonspecific interactions and enhancing specific adsorptions in a biological complex. A polymer –organism is best mediated by proteins which play vital role in every biological entity. Protein is a natural biopolymer and it consists of group of amino acids. Thus both protein, polymer are complex and their interaction is extremely complicated. Each amino acid or peptide residue has general backbone structure of (–NH–CαHR–CO–) in which R denotes a specific side-group structure enabling the chain to have specific functional characteristics. The amino acids may have side chains of phosphates and oligosaccharides or lipids and formulate the monomeric units of complex protein chain. Figure 4.1 shows the side chains of the 20 naturally occurring amino acids [1]. It can be seen that, typically the 'R' group is characterized into different categories such as nonpolar, polar, negatively charged or positively charged amino acids. These different functional groups make it highly amphiphilic. Three main chemical strategies which govern solid polymeric hydrophobic or hydrophilic surface interaction with proteins are adsorption, covalent bonding and absorption. The small and rigid proteins like Lysozyme, β-Lactoglobulin are more immune to structural alteration after adsorption and are regarded as 'hard' proteins [2-4].
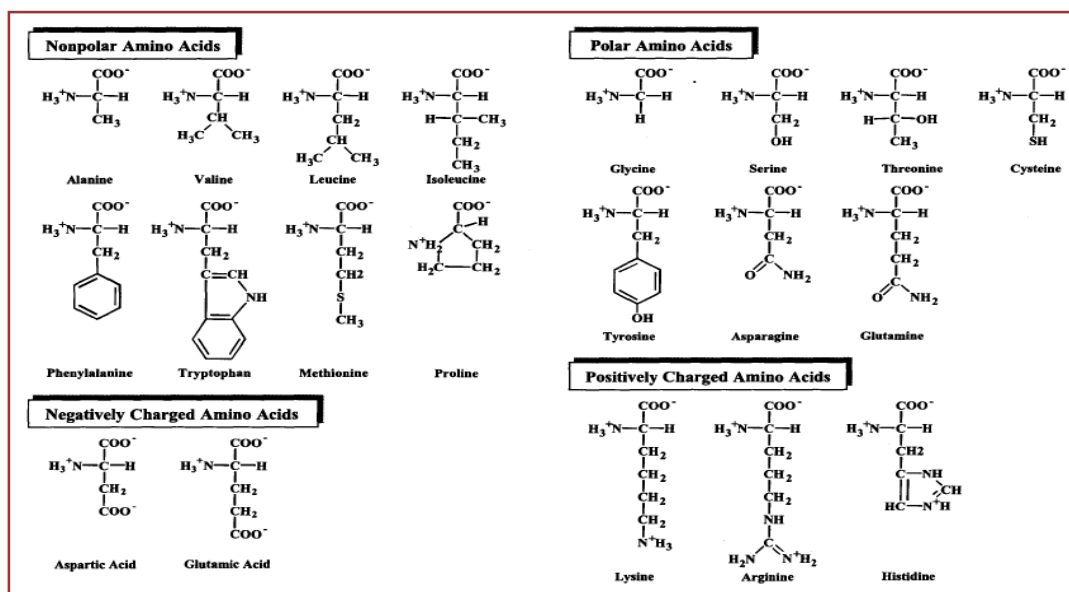
Figure 4.1: Side chains of the twenty different naturally occurring amino acid chains. [Ratner et. al. 1]

The albumin, immunoglobulins, transferrin are intermediate size proteins, more likely to undergo conformational reorientations expressing specific features of amino chains like non-polar / polar, hydrophobic/ hydrophilic or uncharged/charged nature[5]. Larger size proteins like lipoproteins and glycoproteins behave peculiarly due to presence of lipids or glycans [6].

Protein **adsorption** is a natural phenomenon with polymer surfaces, allowed by hydrophobic-hydrophilic interactions, Van Der Waal's forces, ionic interactions and hydrogen bonding. It bioactivates the surface further, to allow in some situations, coupling with bacteria, cells so that a possibility of bio-fouling or inflammation pathways is created [7-10]. Proteins observed to be more absorbent when the surface is hydrophobic than the hydrophilic surface [11-14]. The probable reason is the former surface has strong hydrophobic protein interactions and hydrophilic surface conveys strong repulsive solvation force. Polymer materials also have additional components like photoacid generators, UV stabilizers, anti-toxitants, plasticizers apart from main constituent binders, resins. As such when it interacts with protein, additional binding sites are available, causing an irrevocable change in protein molecules [15] and further adsorption reducing functionality in some domains. Protein adsorption is governed by concentration of dominant adsorbent in solvent, surface morphology, energy, polarity, charge, temperature, pH and

constituents of both reactants. Surface immobilization is the adhesion or coupling of biomolecules onto a surface resulting in partial or total loss of their mobility. Chemical and physical properties of both protein and surfaces decide the immobilization strategy. Three mechanisms viz. physical, bio-affinity and covalent immobilization broadly cover the phenomenon of surface immobilization. As discussed above random protein adsorption and physisorption occur on surfaces by ionic bonds, intermolecular forces, hydrophobic and polar interactions based on level of involvement of protein and surface. Protein adsorption by amine (positively charged) and carboxy groups (negatively charged) is called electrostatic interaction. Randomness in orientation of these interactions lack stability, consequently causing detachments when in contact with detergents or buffer.

Covalent immobilization is comparatively much stable. Protein is known to have many functional groups (-NH2, -OH, -COOH, -SH) in its amino acid side chains. These are covalently coupled to required functionalities (epoxy, carboxylic acid, amine epoxy, active ester (NHS), maleimide pyridyil disulfide, vinyl sulfone, aldehyde) of the surfaces by various interaction methods in immobilization processes [16]. This invokes heterogeneity in population of immobilized proteins.

The epoxy surface chemistry is most popularly used for its characteristic stable reactions, even in severe humid and varying pH conditions. It reacts with many nucleophilic groups and establishes strong bonds to qualify as a means to perform nominal chemical processing of the protein moieties. Covalent attachments between epoxy supports and proteins is very slow but the proteins attachment on sites nearby to the epoxy sites in the same support is very fast [17] A 2-step mechanism of rapid adsorption, then, intramolecular chemical attachment to supports with higher "apparent" concentration of epoxy functionalities is very often used for immobilization of protein molecules. Epoxy-agarose conjugates endorse negligible immobilization of proteins at low and at high ionic strengths owing to the lack of hydrophobic core for adsorption processes to start. Epoxy-amino group aided ethylene-diamine layer promotes physical adsorption of amine group and then covalent linkages by epoxy groups.

Another important group of surfaces is photoactive surfaces. Photolithography was applied in spatially-directed fabrication of oligonucleotide arrays on selective surfaces using photolabile protecting groups [18, 19]. This photo-reaction strategy is a well-organized and quick one-step reaction with no functionalization requirement of target molecules. It can be utilized for biomolecules which lacks sufficient active functional groups. The reaction needs moderate surrounding conditions and is unaffected by temperature and pH conditions. Photoactive reactions confer biocompatible surfaces. The common photo-reagents such as diazirines, arylazides and benzophenones are activated by photolysis via incident light of wavelengths ≥ 350 nm, but most of the other biomolecules are transparent. Arylazides on photolysis are converted into reactive nitrene intermediates which can be inserted into C-H bond. It provides slow binding. Diazirines upon photolysis creates reactive carbenes which act in response with proteins within microseconds forming covalent chemical bonds. An irreversible linkage between the proteins and surfaces is generated, thus enhancing the molecular immobilization. Nitrobenzyl linker provides the attachment of labile chemical groups which on UV exposure generates CO2, freed reactive groups, ketone and CO_2.

Bio-affinity immobilization is creation of biochemical affinity-bonds of a certain group of protein sequence (e.g. biotin, histidine, carbohydrate residue etc.) with the activated substrate (e.g. avidin, lectin, metal chelates etc.). It has benefit of having oriented and homogeneous immobilization of biomolecules on the surfaces. Proteins can be detached from the surface and the same surface can be reused for other purposes. Clinical and biomedical microdevices are required to be characterized to have chemically inert surfaces to avoid non-specific adsorption of proteins. Antifouling surfaces are highly protein resistant surfaces. Polymer surfaces are passivated and made resistant to adsorption of proteins or adhesion of cells with the treatment of PEG Poly (ethylene glycol).

4.4   Surface Modification Techniques of Solid Polymeric Surfaces

Solid polymeric surfaces can be modified with plasma or chemical treatment. In plasma modification there are two categories:

1.   Exposure to gas plasma for physical or chemical surface alteration

2.   Plasma deposition or polymerization to grow a film on surface by plasma phase reaction. Plasma treatment builds up an undamaged oxide thin layer on poly(dimethyl) siloxane (PDMS) with active silanol groups changing the hydrophobic surface to hydrophilic, when the process maintains high pressure, low RF power, short duration exposure [20]. Plasma polymerization is a process of deposition in an environment of plasma discharge. In this process the vapour phase develops a thin polymeric film on surface of microchannels fabricated using variety of materials. This is a solvent-free, one-step method in which virtually any dry substrate can be coated with a thin film [21-23]. Hexamethyldisiloxane (HMDSO) is used to coat open microchannels of glass for protein separation using iso-electric focussing [24].

Surface modification using chemical methods:

1.   Polymer surface silanization for covalent linkages

2.   Self assembled monolayer [SAM]

In silanization method the silanol groups are substituted on the surface by Oxygen –plasma [Silicon surface: Si-OH] method. Polymeric surfaces are silanized with the following procedure: Polymeric coated surfaces to be silanized were kept immersed in 2% (3-mercaptopropyl) trimethoxysilane (MTS) in Toluene solution, in nitrogen (N_2) atmosphere for 1-1.5 hours. They were cleaned in Toluene and dried with N_2 gas. After this MaleimidoButyryloxy-Succinimide ester in Ethanol was poured on the sample. The samples were washed with PBS (Phosphate buffer silane) three times. GMBS was included to ethanol after suspending in 50µl N, N-Dimethylformamide. The last step ensures that sufficient ethanol is present during incubation [25]. The modified surfaces were well-suited for interactions with proteins and antibodies. The reaction is shown schematically in figure 4.2.
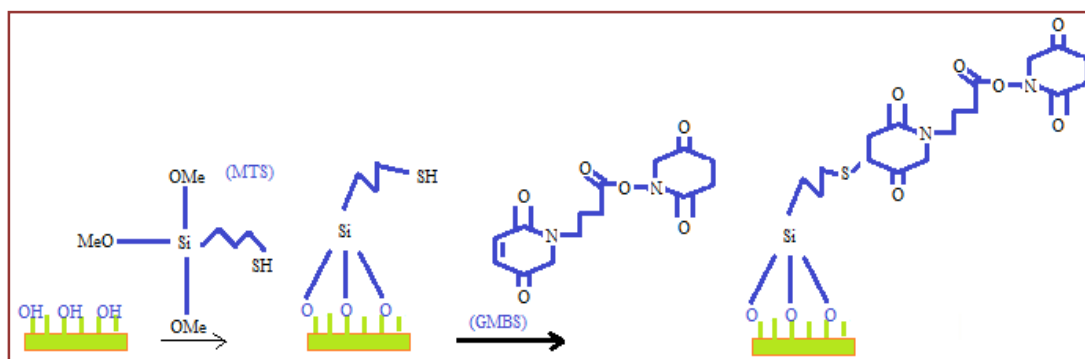
Fig.4.2 Schematic of silanization reaction on polymer surfaces. [J-J Chen et.al. (25)].

4.5.1 Need to Explore Polymeric Sensors

As per discussion in chapter 2 [Simulation of coupling elliptical microsleeve], chapter 3 [binding and Coupling with a microdroplet], chapter 4 [Interaction of solid polymeric surfaces], on various aspects of polymers used as biosensors; need of research and efforts in exploration of possibility of role of polymeric devices in the field of low cost, sensitive biosensing, seems evident. The facts that polymers can be easily doped, polymer resonators can lower losses, they were realized in microlasers, chemical sensors [75]. Polymer waveguide like microstructures make integrated devices highly efficient, with its capacity to carry light over a longer distance while enabling interaction of better quality between optical signal and the host material. Polymeric materials are available in wide range, type, cost. Fabrication of these devices is easier and optical properties are good. They are mostly biocompatible and adapt well with the application situation. Simple surface functionalization and immobilization methods are used for these materials.Hence it is pertinent to study and explore the biosensing feature of polymeric materials; SU8, a negative photoresist material in particular.

4.5.2 Related Work

It is important for researchers looking for early detection in life threatening diseases, to identify biomarkers in sensitive and robust way, for further investigations. Biomarkers involve separating DNA, Cells and proteins from blood, body fluid or other samples. Conventional methods involve beads, filters, resins amongst other controllers. They have properties to attract or process specific biomolecules. Surface immobilization of required analytes need surface modification or functionalization

to suite the chemical interaction. The chemical coupling is caused by covalent bonding, adsorption, encapsulation or entrapment. In case of solid polymeric surfaces, to be more precise, of epoxy based, negative photoresist SU8 material, M.Joshi et.al. [76] used Sulfochromic solution to remove C-O bonds and instill hydroxyl groups on the UV exposed SU8 coated surface. Amino groups were created with silanization treatment for bonding of antibodies. Wang et. al [77] used Cerium (IV) ammonium nitrate [CAN] with nitric acid or sulfuric acid on residual epoxy groups of fabricated SU8 surface for grafting hydroxyl groups by method of oxidation. In a detailed study [78] reports of interaction of proteins with polymer material surfaces were seen. Blagoi et.al. [79] compared CAN treated surfaces with bare fabricated SU8 surfaces for investigating binding kinetics of proteins. Result according to the report was, better performance of bare SU8 surfaces, making the process of protein immobilization simpler. In another paper [80] it was reported that silanization was necessary in case of positive photoresist surfaces for desired protein immobilization. Techniques of smart immobilization were discussed in a review paper [81]. After the immobilization step it was characterized by AFM , FTIR , FT-VIS-IR spectroscopy, stain and dye tests [82,83] for confirmation. Label free technique of detection of protein antigen-antibody binding was preferred over labeled technique due to sheer simplicity and rapidness of the assay. One of these techniques was refractometric which was used in detection of proteolytic activity, BSA antibody-antigen binding by noting the spectral shifts [84, 85] after each step. BSA coating protects possible adherence between substrate and analyte, this property was made use of in a novel microrobots-bioactuator to prove [86] the concept. Bare UV exposed SU8 microcubes were selectively coated by fluorescence tagged BSA layer to allow and observe attachment of specific bacteria cells to only uncoated cube surfaces. Fluorescence imaging was used to see the result. Figure 4.3 shows the resultant selective binding.

Some methods of isolation of protein, DNA for biomarkers of life threatening diseases involved functionalized microspheres, instead of conventional methods to capture specific analyte from samples. Making of cost effective, simple to dope silica microsphere was the research topic in the interest of highly specific target sensing [87].
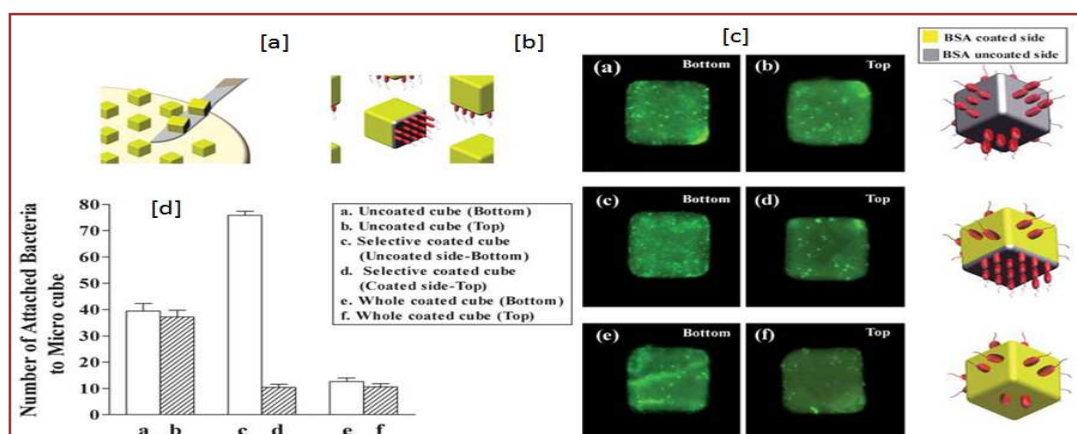
Fig. 4.3 BSA coated microrobots with bioactuators [a] Extraction of selectively BSA coated microcubes [b] Bacteria attached to bottom uncoated side [c] Fluorescent microscope images of bacteria attached to uncoated, selectively BSA coated, BSA whole coated microcubes, [d] Comparison between three configurations on the basis of number of attached bacteria. (Park et. al. [86]).

Additional features of the silica microspheres observed: light in weight to float in a sample solution, smoother, non-porous surface for effective and specific binding [See figure 4.4].
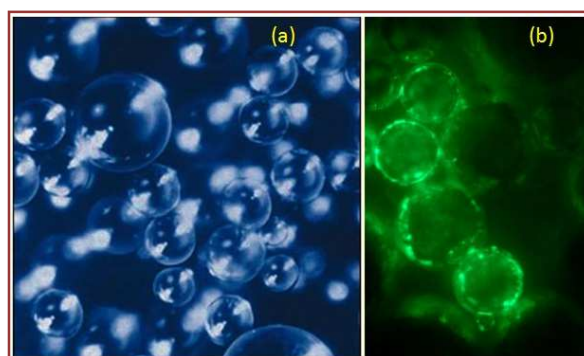
Fig. 4.4 Silica microsphere for isolating proteins (a) unconjugated silica micro-sphere (b) Protein A conjugated silica microsphere with bound mouse IgG. For visualization of bound biotinylated goat anti-mouse IgG, NeutrAvidin^{TM} conjugated to silica nano-particles doped with FAM dye is used. [Stefansson et. al. (87)]

4.6 Steps involved in fabrication of an optical biosensor connector

4.6.1 SU8 Microdroplet used as WGM Resonating sensor

Optical biosensing is considered most versatile amongst various techniques of biosensing analytes [DNA, Bacteria and viruses] from sample solutions. It is fast,

accurate, clean, stable, contact less, operating in UV-VIS-IR range. It can be categorised on the basis of type of optical signal sensed, which property of signal has changed in response to change in surrounding sample, labled or lablefree.
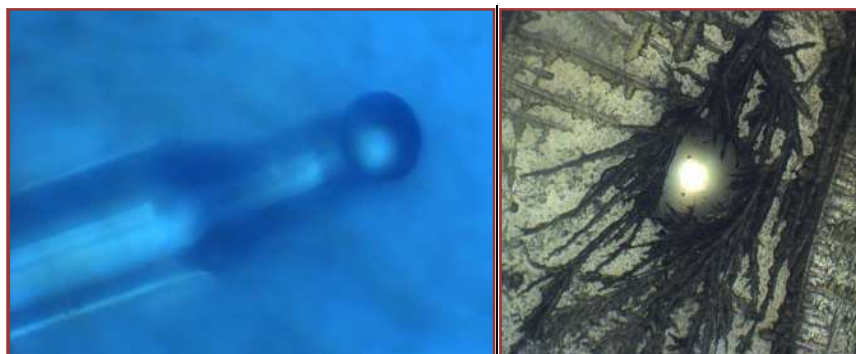
Fig. 4.5 (a) Micro-sphere developed on the tip of an optical fiber using low power Laser processing (b) Ninhydrin treated biomimetic SU8 microdroplet.

Various optical detection techniques are Fluorescence detection, change in refractive index detection, evanescent field sensing, sensing surface Plasmon resonance. Sensing or recognizing element has its material surface properties and functional groups changed to facilitate its reaction with specific analyte. Optical fibers are most commonly used waveguides for carrying signals into and out of the microchips in Lab-on -chip applications and communication applications. The connections of fibers to the microchips, at specific locations is a crucial task. Construction of the silica microsphere is a real problem and involves Laser irradiation (see figure 4.5) of fiber tip followed by chemical etching which is very low yield process. Micro-spheres are not free from vibrations and as the change of wavelength if in 'pm' level it can be very sensitive to thermal noise or any other noise. The whole body of the Micro-sphere which is around 100-150 microns in radius needs to be immersed in the analyte thus necessitating the analyte volume to be high which is always very difficult to obtain.

In this section we propose simple SU8 microdroplet [with or without bonded optical fibers] as a WGM resonating sensor. Photonic software simulation supports this concept [73]. Two optical fibers are joined on a hard substrate [Silicon wafer / Glass] by using a SU8 micro-droplet. When the wavelength and launching is right Whispering gallery modes start circulating continuously, while sensing the molecular activity at the equatorial periphery. Advantages of SU8 material besides

being an excellent microstructurable material are many, it is biocompatible, transparent, relatively inert and has very good optical properties. Radius of microdroplet is 150~250µm. Its smooth surface can be functionalized and processed to suite the signal coupling fiber bonding and biosensing requirements. It is very important that the SU8 microdroplet is a perfect hemisphere or hemi-ellipsoidal, microsphere, smaller in diameter (100-150 µm), having smoother surface, to get good sensing conditions. The optical fibers are required to be decladded or tapered further to achieve this. Efforts are on and the future goal is to get all these three conditions achieved to further improve its functionality as an optical sensor.
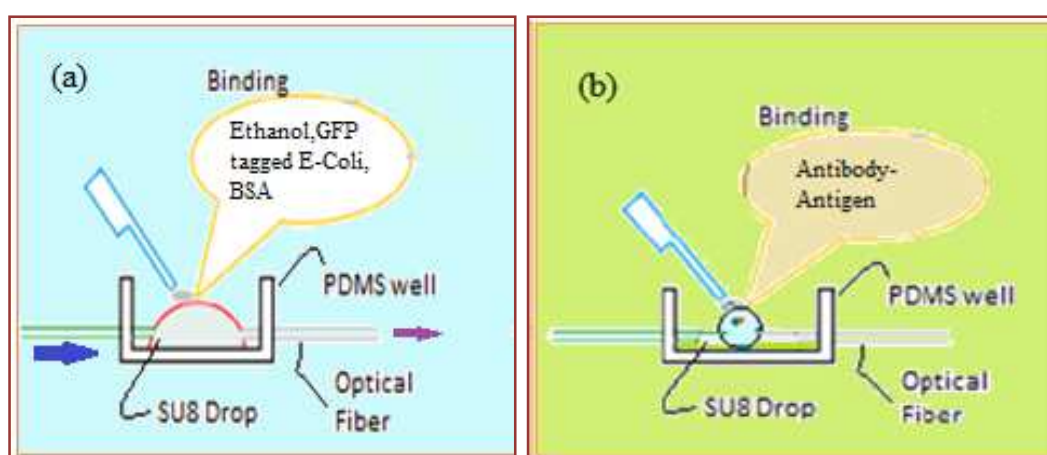
Fig. 4.6 (a) Analyte sensing using SU8 microdroplet in a PDMS well (b) Challenging goal to get a perfect SU8 microsphere.

As shown in Figure 4.6 the SU8 microdroplet can be used to find out the binding kinetics of sample solution. With WGM response sensitive to evanescent field region, in terms of variation in effective refractive index, it can be used as a refractometer.

4.6.2 Fabrication of SU8 Microdroplet Sensors [Laser or UV]

Before embarking upon protein immobilization tests on SU8 microdrop, number of experiments were carried out on spin coated SU8 layers on Si, Glass, plasma treated Si/ glass surfaces with or without UV exposure and with CO2 Laser exposure. After the fabrication, various methods of immobilization were used to find a best suited method for our purpose. Some of the methods of surface functionalization and immobilization tested were, **1.** H2SO4 [Dip test surface in

95% Sulphuric acid for 10sec, coat entire surface with BSA to incubate for 90 min, rinse with Deionised water [DIW] thrice and dry with N2 gas] **2.** MCPTS [Dip surface in mixture of 2% MCPTS in Toluene for 60 min, wash with Phosphate Buffer Saline[PBS], dip in 0.005 NDMFM in ethanol for 60 min, wash thrice with PBS, immobilize in PBS solution of BSA overnight, wash with PBS buffer] **3.** Get the SU8 surfaces UV exposed suitably.

According to the results of this exercise, it was observed that:

1. Laser treated SU8 Micro-droplets were suitable for signal coupling [Ref: chapter 3], hence they can be easily adapted to refractometric sensing of solutions under test with varying refractive indices.

2. UV exposed SU8 surfaces were functionalized suitably for protein immobilization, so protein assisted or repellent [antifouling surfaces] analyte sensing can be explored. Based on results of SU8 thin film coated surfaces, immobilization techniques were implemented on SU8 microdroplets. Fabrication, functionalization and immobilization procedures for both types of microdroplet were similar; it involved manual dispension of drop using 2.5µl micropipette. In one of the methods of dispensing, X-Y-Z stage and flow controlled dispensing pump for 1ml Syringe was used to carry out precise and controlled dispensing. Glass slides and Si wafers were cut into 1cm size to dispense SU8 microdroplets. One set of glass slides was used for UV exposure and treatment, other set for CO_2 Laser exposure as methods of surface functionalization .In UV exposure microdroplets on glass/ Si substrates were preheated at 95˚C for 5min, exposed to UV light for 80 sec, then post exposure bake was another 5min heating at 95˚C. The devices were ready for post processing. Similarly laser exposure procedure involved precise control on power /speed, center position, time to get perfect bond [Ref.: Chapter 3] and sensing.

4.6.3 Extraction of SU8 microdroplets from Substrate

The work presents possibility of both stand alone and chip based sensing scheme. The microdroplet devices can be used on the substrate or extracted to use as independent sensing component. The extraction step may be before or after immobilization, accordingly the substrates were heated at 80˚C for 24 hrs [87]. Then

carefully they were detached from substrate with the help of a knife. Extracted or attached micrdroplets with or without fiber bonding were then subjected to refractometric test [CO_2 Laser treated] or protein immobilization test [UV exposed].

4.6.4 Surface Immobilization

UV exposed bare SU8 microdroplets [87] were used for further processing. Figure 4.20 shows BSA immobilisation, microdroplet removal and stain and dye tests along with its applications. The microdroplets thus detached were tested for bonding of E-Coli cells on selectively coated and uncoated surfaces. Microdroplets in 3 groups were incubated with BSA for a period of 8 hours. First group had droplets extracted from the substrate and completely immersed in BSA solution for full coating. Second group had droplets attached and intact on the substrate. Only top dome like surface was subjected to BSA coating. Extraction step was after immobilization. Third group was kept aside; it was not incubated in BSA solution. Thus there were o6 groups; attached, extracted; fully coated, partial top coated and not coated microdroplets. These microdroplets were stored separately and marked for reference. Now they can be flown in a channel for observation of fluorescence effect under microscope. Figure 4.13 Shows images of various test results of these 3 groups. Some optical fiber bonded microdroplets were detached and placed in a 1cm^2 PDMS [Polydimethylsilicone 10:1 curing agent after desiccation, in plastic mould for 45 min in oven at 95˚] well for carrying out similar sensing experiment. Thus the hemispherical microdroplets as shown in figure 4.7, 4.10, 4.12 can be used as standalone or chip-based sensing entities.
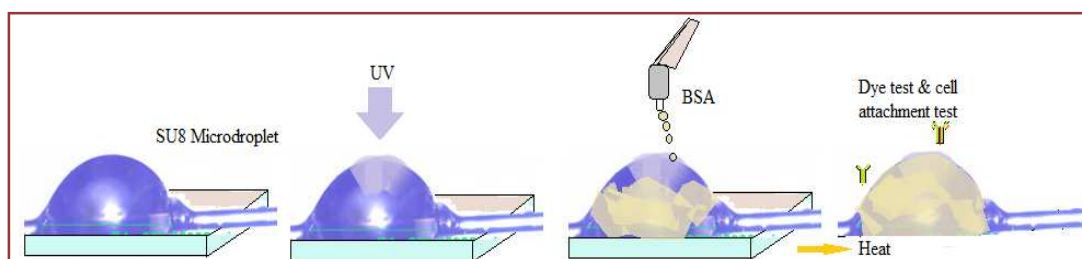

Fig. 4.7 Method of BSA immobilisation on microdroplet [with and without optical fiber] and its applications (a) Microdroplet dispensing (b) UV exposed microdroplets (c) BSA immobilised on microdroplet surfaces (d) Microdroplets detached from substrate with heat treatment and then subjected to stain & dye test.

Fiber bonded microdroplets were used to sense varying concentrations of ethanol. In another set of experiments, BSA coating, dye doped E-Coli binding, ninyhydrin test, AOD tests were carried out to check the sensitivity of the sensing device.

Further Green Fluorscence Protein [GFP] tagged E-Coli was administered on the UV exposed selectively BSA coated microdroplets to conform the protein immobilisation sensing.

4.6.5 Characterization of the Microdroplet Sensors

As mentioned previously because of the curved nature of surface, thickness in sub mm range and 3-D appearance, none of the conventional imaging or characterization schemes is suitable. Being a solid state device fluorimetry method is difficult to incorporate. Best solution was to characterize fiber bonded sensor microdroplets with microscopy and Spectra-Suite mini spectrometer test setup for measurement of light intensity with its array detector and supporting software. LED sources of suitable excitation wavelengths can be used. As mentioned above only elimentary results were obtained and spectrometer results are possible subjected to the perfect microdroplet shape, size and smoothness. The future work entails this for a perfect optical biosensor connector. The independent microdroplets were characterized for detecting fluorescence intensity on attachment of GFP [Green Fluorescence protein] tagged E.Coli on selectively BSA coated Microdroplet surfaces [87]. Number of suitable arrangements, such as use of PDMS well, Channels etc. can be thought of, for sensing purpose.

4.7 Some Elementary Results and Analysis

In view of the objective of making an SU8 microdroplet sensitive to thin layers of sample solutions in its evanescent region, surface immobilization methods were carefully selected as any chemical reactions were likely to corrode the smooth glistening surface of the SU8 microdroplet, loosing its transparent appearance. The immobilization procedures found suitable for thin films, were applied on fabricated SU8 microdroplets. The tabulated results, when analysed, it was observed that UV exposed bare microdroplets were suitable for protein immobilisation. Acridine orange dye and Ninhydrin stain tests were carried out for confirmation. Next

mobility and accessibility was checked with detachment procedure made applicable to both, with and without fiber bonded, microdroplets [Figure 4.12 & 4.13]. The detached selectively BSA coated microdroplets were allowed to separately interact with small quantity of E-Coli cell solution. The results were tabulated, for ease of understanding, the methods used for ensuring E-Coli cell binding on Microdroplet surface. The procedure is to use one fiber bonded microdroplet to detect change in concentration of Ethanol [0.025ml/ml to 0.825ml/ml]. The microdroplet acts as a whispering gallery mode resonator with BLUE [446-483nm] wavelength source. With change in concentration of sample solution in the evanescent region of the microdroplet, effective refractive index or effective radius of the device will change, causing a Blue shift [towards left of Visual spectrum [300-1100nm] or Red shift [towards right of visual spectrum] of the peak output wavelength. The equation (4.1) defining this relation is

$$\frac{\Delta\lambda m}{\lambda m} \;\; \alpha \;\; \frac{\Delta Rm}{Rm} + \frac{\Delta Nm}{Nm}$$

..........…………………………….(4.1)

where λ_m is resonant wavelength of microdroplet, R_m is radius of micro-droplet, N_m is refractive index of microdroplet under consideration. Proportionality sign of equation (1) signifies that the microdroplet is not a perfect sphere, it is deformed. The output optical signal intensity can be detected by USB 4000 array photo detector [Mini spectrometer] and supporting software. Graphical presentation of change in concentration of Ethanol vs wavelength in nm gives sensitivity of the device. Further to check BSA immobilization, E-Coli cell attachment, dye and stain test, fiber bonded microdroplet as shown in figures 4.6 can be kept in a PDMS well for sensing spectral shift due to sample solution administration.

a.   **Fabrication of SU8 microdroplets**

Fabrication of Silica microspheres using gas flame and CO_2 Laser: Initial efforts were concentrated on getting a perfect silica microsphere .Glass blowing section possessed a gas flame. Figure 4.8 (a), (b) are images of silica microspheres fabricated by melting an optical fiber tip in an extremely high temperature gas flame. Resultant microspheres were extremely round and small [diameter~ 374µm], very brittle. Using CO_2 Laser, the microspheres were fabricated.

It required high level of optimization to get moderately good, smaller [diameter ~60µm] microspheres. Fig. 4.8 (c), (d) show the microspheres.
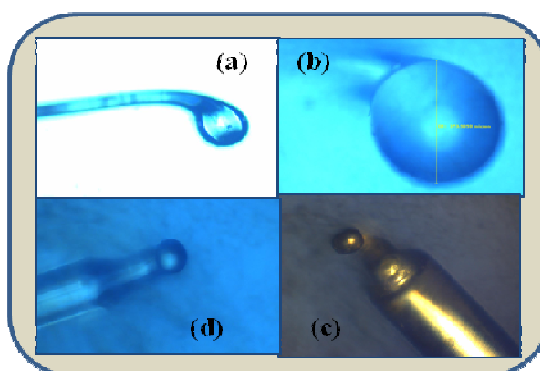
Fig. 4.8 Silica microspheres using (a) and (b) gas flame, (c) CO_2 Laser (Gold Thin film coated) (d) CO_2 Laser.

The gold thin film coating on the microsphere was deposited in a sputtering machine. It strengthened the microsphere and reduced the brittleness.

b.   SU8 Microdroplet dispensed using micropipette and syringe:

SU8 is highly viscous in nature and 1µl drop volume was initially required to be used. Using both X-Y-Z stage, dispensing pump, syringe and manual micropipette methods the droplets were dispensed. See figure 4.9.

c.   Fabrication of fiber bonded SU8 microdroplet [CO2 Laser exposure]:

As shown in figure 4.10, it was difficult to form a rounded SU8 droplet across the fiber pair because of surface energy of the SU8 and very small volumes involved. Subsequent coatings on the droplet are shown in the figure. The laser tagging ensures a strong bond between SU8 and fibers with the substrate.
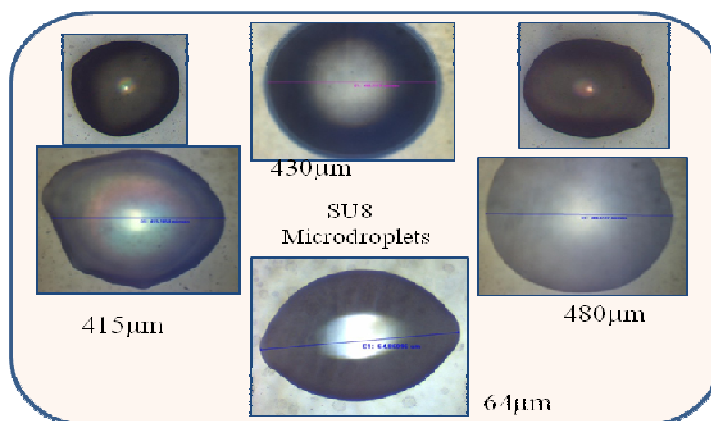
Fig. 4.9 Microdroplets dispensed using micropipette.
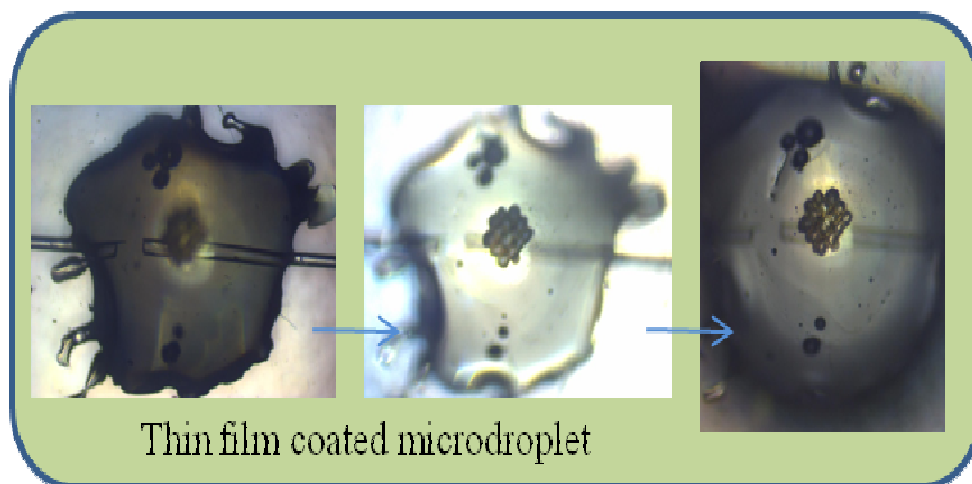
Fig. 4.10 CO$_2$ laser heat treated fiber bonded SU8 microdroplet.

d.   Fabrication of fiber bonded SU8 microdroplet [UV exposure] :

The fiber pair shown in figure 4.11 is covered with an SU8 droplet which was then UV exposed.
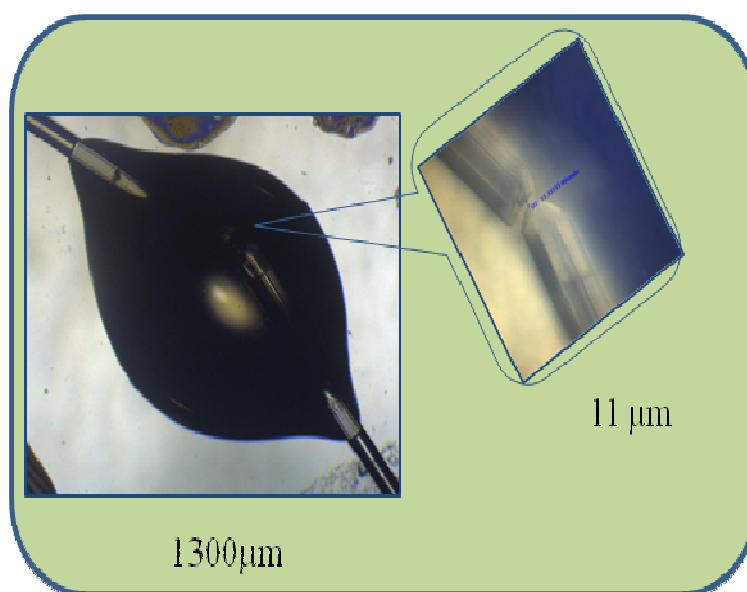
Fig. 4.11   UV exposed fiber bonded SU8 microdroplet, Inset showing fiber gap of 11µm.

e.   Extraction of SU8 microdroplets

Figure 4.12 shows pretreated and extracted SU8 microdroplets.
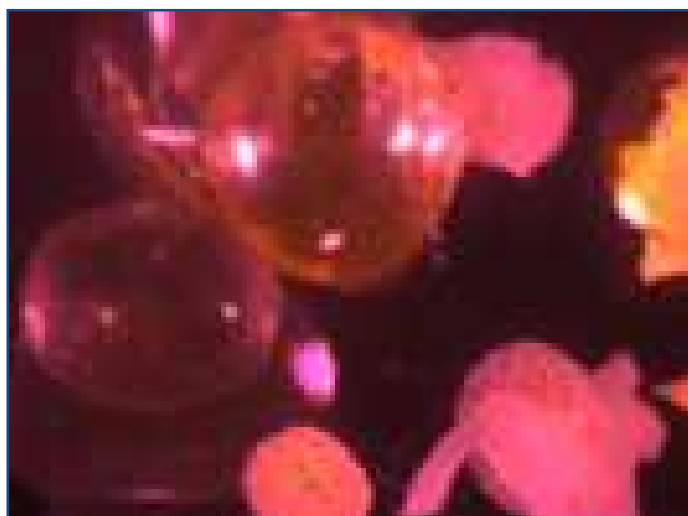
Fig. 4.12 SU8 microdroplets extracted from the substrate.

f.   Surface immobilization

Figure 4.13 tabulates the results of BSA incubation and E-Coli attachment to the selectively coated microdroplets. A2 shows E-Coli attachment to the fully BSA coated microdroplet surfaces. Its density is comparatively less than the other two. B2 shows the cell attachment at the bottom surface of microdroplet. C2 has higher density and more uniform cell attachment. This proves the point that E-Coli can attach to functionalized SU8 surfaces; BSA covering, protecting SU8 acts as a repellent for E-Coli.
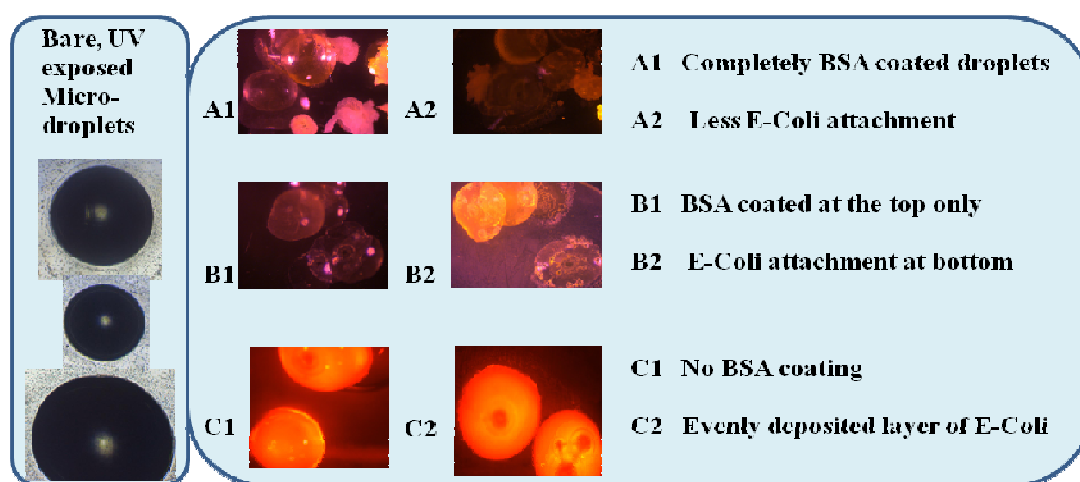
Fig. 4.13 UV functionalized bare SU8 microdroplets, selectively immobilized with BSA solution [A1,B1,C1] incubated with E-Coli cells [A2,B2,C2] observed under the microscope.

85
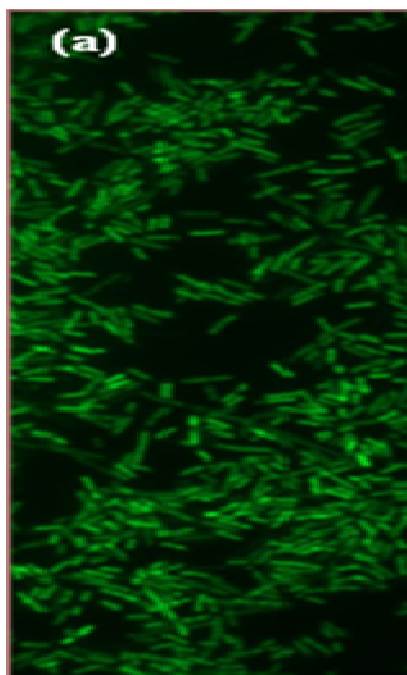
Fig. 4.14 SU8 microdroplet sensing GFP tagged E-Coli cells (a) E-Coli cells under Microscope.

See Figure 4.14. Refractive index of BSA in general is 1.355 as against 1.67 of that of SU8. Due to overnight incubation changes in effective refractive index may occur in BSA-SU8 interface, leading to higher value of intensity and spectral shift at the output.

B. Porous Polydimethyl Siloxane- Acridine Orange as Biomaterial

4.8 Introduction

A biomaterial is a structure, material or surface that interacts, functions with living organisms, biological systems. It possesses the quintessential property of biocompatibility to react with biomolecules. It is about 50 year old science and it covers disciplines, domains like medicine, tissue engineering, bio- technology, material science, surgery, therapeutics, agriculture, pharmaceuticals. Biomaterials have become very much part of our lives and for some, part of body. They imitate in a way natural functions with artificial bones, drug delivery vehicles, tissues, dentures, biosensors, organs, contact lenses, intraocular lenses, vascular grafts, heart valves, implants, pacemakers to improve life [see figure 4.15].

86
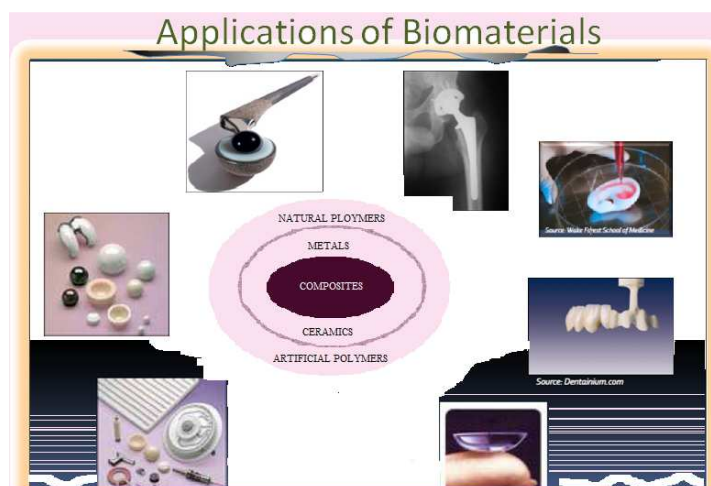
Fig.4.15 Application areas, products of biomaterials. [Ref: Dantenium.com, Water Forest School of Medicine]

Ceramic materials, metals, polymers and their composites fall in the category of biomaterials. Both [82, 88, 89], natural polymers and artificial polymers can be biomaterials. With higher proportions of carbon, oxygen and nitrogen; starch, proteins, DNA, genes, complex sugars, cellulose become natural polymers. Man made or artificial polymers with higher proportions of oxygen and nitrogen are Poly(vinyl alcohol), poly(ethylene alcohol), PTFE, PMMA, polycarbons polylactide , polyglycolide, silicones, polyurethanes .There is a reason why these artificial polymers are accepted by living organisms as biomaterials. They possess some of the following properties: 1. Biological inertness 2. Control in cell adhesion 3. Interactive functionality or bioactive feature 4. Excellent mechanical strength 5. Bio-degradable & Bio-recyclable nature 6. Bioresorbable capabilities 7. Thermal stability 8. Biodurability. Modern medical devices are produced with more than one such biomaterials mentioned above. Integrated behavioural analysis of these materials in various situations like, chemical, physical, environmental, inside or outside of a body of an organism decides its biocompatibility. Properties of these materials are mostly application specific. They carry out functions like replace, treat, augment or evaluate a tissue or organ of a body. It is observed that third generation biomaterials can provide stimulation for specific cell response [101]. Surface functionalization [section 4.3] helps in transforming these properties into desired ones [98, 100]. Proteins are important ingredient in all biological molecules. It plays primary mediating role in polymer- organism interactions. Their status on a material

substrate is known to decide the ultimate biocompatibility of the polymer device. It is important to study methods of surface functionalization of various polymer materials, immobilization of proteins on these surfaces to know its behaviour and characteristics in similar environmental situations. Polymer surfaces are passivated to minimize protein interactions which are non-specific [specific protein repelling]; in turn specific protein adsorption and cell responses are induced by staining polymer surfaces with biomolecules. "Plastic" like polymers used in paints, packaging, containers, pipes and other forms in nature are exposed to or are in contact with biological systems. They have to face problems like recycling, disposal, delivery of chemicals and pollutants, sustainability. Polycarbonate based materials are oxidation resistant and biodurable as they do not possess ether linkages, which are affected by macrophagic enzymes causing deterioration of the device. Study of biomaterials, their properties, behavior in various situation, surface modification techniques to suite application needs, thus gives the insight about a material in a specific application.

In this work a novel bio-material is reported. It is a nano-porous material with PDMS [Poly dimethyl siloxane] and Acridine Orange [AO] dye as its major constituents. PDMS is biocompatible and biodurable with applications in facial prostheses [101], fabrication of lab-on-chips, in bioseparation. It is an artificial polymer with methyl groups and repeating silicon to oxygen bonds. It is most popularly used material for bioengineering, microfabrication and bio-medical applications. Most commonly named as silicone, PDMS can be processed to easily acquire unique properties, when the methyl group is replaced with vinyl, phenyl etc. groups[102]. This will modify the organic linkages into inorganic backbone of the material. Properties of PDMS material like oxygen permeable, non toxic and blood compatible find applications [95-102] in shunts, implants, bladder stimulators, heart valves, burn dressings. With the properties of PDMS material, its tunable elastic nature and all the applications, features mentioned above, the references 95 to 102 more or less have it treated as one of the biomaterials with very bright future role to play in bioengineering. Researchers [S.M. Khare et.al. 103] have tried to use images of micropillars of dye doped PDMS to study locomotory forces of genetically modified organisms.

This new material is physically and characteristically dissimilar from the two combining bio-materials mixed in soft-lithography process. A range of characterization techniques, such as SEM, UV–VIS spectroscopy, Fluorescence microscopy, SpectraSuite optics signal setup, support the novel attributes of the material. Although extensive literature survey was done, it provided no references for a similar microstructure.

4.9 Literature Survey

Way back in 1998 in a journal paper [82] interaction between bovine serum alumin [BSA] and acridine orange [AO] was investigated. Using fluorescence spectra method, binding reaction and energy transfer effect between BSA and AO was probed. Absorption curves [300-500 nm] were interpreted to know status of AO as monomer, dimer or aggregation of AO inside a cell. Fluorescence curves [excitation 280nm emission 300-500nm] analysis was based on the forster energy transference. With this analysis distance between acceptor AO and BSA, energy transfer efficiency was found. AO fluorescent dye was introduced as cationic basic. It is a neutral, nucleophilic, proton acceptor and can penetrate into membranes of cell organs to accept protons. H^+ cationic molecules can not penetrate the membrane and cause variation in concentration. Thus the absorption and fluorescence maximas shift accordingly, to Red or Blue wavelengths. AO dye is normally used as a liquid dye solution. Solid phase AO dye solution can be an alternative and it has additional advantages such as better solubility. AO has its peak absorbance and fluorescence wavelengths blue shifted when in solid matrix [89]. Spectral characteristics were used to observe effect of solution concentration and content on absorbance and fluorescence peaks. Refractive index was measured using the dye doped polymer film and n-butyl acetate (nBA). AO was subjected to a Z-scan technique which deduced a negative non-linear refractive index.

MEMS [microelectromechanical systems] research and development activity was increasing in biomedical, clinical and therapeutics application field. Its pace was controlled by cost and limited access to silicon based microfabrication which mainly employed highly planner, expensive photolithography process. Also it invariably used a small set of materials. With commercialization and range of applications in the fields of medicine and biomedical, research community was

encouraged to find BIOMEMS applications, alternate processes, materials. Thus soft-lithography technique was developed for satisfying objective of mass production, reduced cost and use of polymer materials. Some of the prominent members of this polymer group of materials are polymethylsiloxane [PDMS], polymethylmethacrylate [PMMA], polycarbonate [PC], polyvinylchloride [PVC]. PDMS a silicon elastomer, is chemically inert, simple to handle and manipulate, can conform to submicron features in microfabrication, operates at lower cost and is thermally stable. It is most suitable for soft lithography solvent based moulding. PDMS formulations, fabricated using various processes and concentrations, were analysed [90] with SEM, goniometry, tensile testing, FTIR, chemical tests. In a detailed review, on biocomptible polymer materials, importance of protein- surface interaction is highlighted [91]. Fernandez [92] et.al. have discussed effect of porosity on PDMS cell immobilization and formation of bacterial biofilm. Further applications of these biomaterials were surveyd in the fields of tissue engineering, drug delivery, skin grafting, medical sensing, medical adhesives, textiles. Medical applications of these polymer biomaterials can be broadly classified as 1. Temperory implants: arterial stents, implantable drug delivery systems, degradable sutures 2.
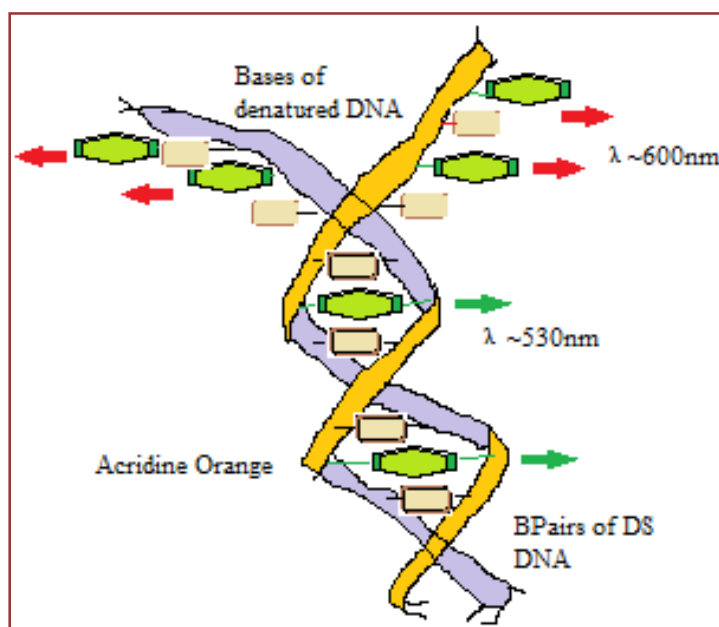

Fig. 4.16 Acridine orange interacting differentially amongst base pairs of double-stranded DNA [Green Fluorescence] and denatured DNA bases [Red Fluorescence]. [Huang et.al. [7]]

Extra- corporeal uses: ocular devices, wound dressings, catheters 3. Permanent implants: dental, orthopedic devices, sensory devices. Hydrogels [93] were prepared with biopolymers or with combination of synthetic and biopolymers for prospective biomedical applications like tool for transdermal drug delivery, dressing material for burns or cut wounds. AO differentially stain tests, double stranded DNA and denatured DNA [figure 4.16]. The dye fluoresces red (> 600 nm) when it binds to single-stranded DNA section and its binding to double-stranded DNA sections leads to green fluorescence (~530 nm) [94].

4.10   Porous PDMS- AO as a Biomaterial in Opto-Biosensing

A breathing polymer material is very much desired in recent biomedical research. PDMS [(Polydimethylsiloxane) molecular formula: $(C_2H_6OSi)_n$] is a good mould material. Characteristic optically transparent structures can be fabricated with moulding and curing. It is known as a bio-compatible material. In soft lithography the bubbles formed when PDMS base is mixed with curing agent are removed in desiccator to get a clear, white, transparent device. References, however show work on getting porous polymer structures for immobilization of cells and formation of bio films. Another biomaterial Acridine orange [(AO) molecular formula: $C_{17}H_{19}N_3$] is a metachromatic dye useful in living cell detection. Its probing capability in dead cell detection is yet to be proved. The motive and thinking behind this study was, that PDMS is a biocompatible material. AO is a fluorescent dye used in DNA, RNA cell detection. When these two were mixed together a more suitable biomaterial may be produced. Thus experiments were carried out using soft lithography technique, which produced a reddish, spongy structure with pore sizes as low as 998.8nm. This paper being first to report the material, there are no references. Spectral characteristics of waveguide like structure microfabricated with this porous PDMS– AO [PPA] material when compared with similar PDMS structure, significant variation was observed. PPA material when exposed to cell detection test it glowed under the near IR excitation signal. Varying proportion, concentration in sensitive structures of PPA may lead to a live torch effect. Further exploration of this material, having properties like porous, spongy, flexible, puffed up structure and AO content, was found to be easier to post-process. Applications in life sciences like microfilters, in-vivo/vitro sensors, biosensor, concentration detector, implants may be investigated as a future scope. It can be better analyzed as a dye doped material. The composite of PDMS/AO was developed by mixing in 10:1:1 ratio of [PDMS]

primer to curing agent and AO solution [AO powder 1mg/ml in DI water to make AO solution]. PDMS (Polydimethylsiloxane) [molecular formula: $(C^2H^6OSi)_n$] is a material often used in micro/nano fabrication, replication of microstructures and in biosensing applications. Soft lithography provides variety of ways in handling materials like PDMS, PMMA in gel form with varying proportions of their curing agents. Brittle and soft are the two possible extreme end results. It uses moulding masks on glass, Si wafer, PMMA substrate to be replicated into final structure. It is the resolution of mask, which decides the resolution of structure. Negative mask structures are made out of Si-wafer, PMMA and SU8 on Si or glass using photo-lithography and laser engraving on PMMA.

PDMS is spin coated on the mask substrate and speed, time are controlled for desired thickness. The PDMS coated structure is kept at 95ºC on hot plate (7 min) or in oven (45min). Further it is kept in oven at 200ºC for 1 hour to get stick free PDMS structure. Acridine orange [molecular formula: $C_{17}H_{19}N_3$] is a metachromatic fluorescence dye in powder form. It is mixed 1mg/ml with DI water to make a solution. It interacts with DNA, RNA and is cell permeable nucleic acid selective. For excitation maximum 502nm (DNA) and 650nm (RNA), it spectrally fluoresces with emission maximum at 525nm and 650nm respectively.

4.10.1 Experimental Procedure

Fabrication of device: Epilog Laser engraving machine was used to get negative microstructure masks on PMMA sheet. The masks are complex optical waveguide like structures with test sample channels for the biosensing application. Two pairs of mask patterns were used. Following fabrication procedure discusses steps of one of the pairs. Speed, Power of the laser machine were controlled to get high resolution, mirror finish wall structures. Following all defined procedures of soft- lithography, PDMS base was mixed with curing agent in 10:1 proportion. Half of the PDMS material was kept aside and in the other half AO was mixed with 10:1:1 proportion. After desiccation both PDMS and PDMS-AO mix were separately spin coated on two similar PMMA masks. For larger base PDMS / PDMS-AO can be molded in a suitable plastic container. The moulds were ready for heating, so a preheated oven set at 95º C was used for the purpose for 45 min curing. The devices were set and allowed to cool.

4.10.2 Instruments and tests:

Characterization of PPA material involved following procedures:

A. Physical appearance of porous PDMS AO [PPA] material was compared with the PDMS device.

B. SEM images of the device were to visualize structure at micron level.

C. Ocean Optics Spectra suite software, photodetector, LEDs [Light emitting diodes] broadband light source were used to test the device for absorbance, transmission.

D. Device was further analysed with UV-VIS spectroscopy to verify optical characteristics.

E. NIKON microscope (540nm source) with CCD camera and NIKON still camera were used to record images of a PPA device subjected to DNA detection test.

4.11   Result and Analysis

A. The PDMS and dye doped PDMS/ fluorescent PDMS / PDMS-AO devices when physically inspected, were found to be, surprisingly, totally dissimilar to each other. Figure 4.17 shows a PDMS-AO composite device. Mixing of AO and PDMS also may have caused change in effective refractive index. PPA device was porous, reddish, spongy, flexible as compared to transparent, white, set PDMS.
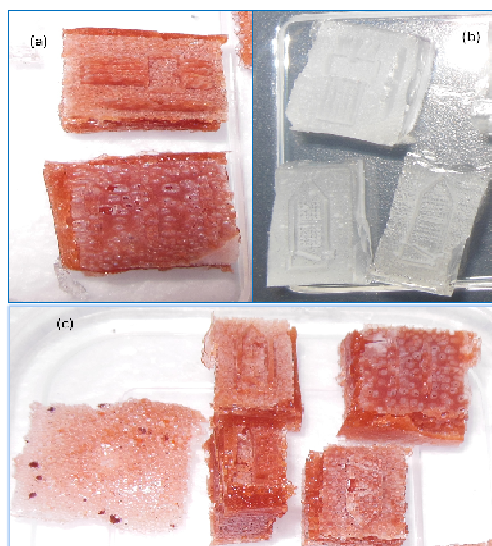
Figure 4.17 Microstructures (a) and (c) Porous PDMS Acridine Orange (b) PDMS

B.   Scanning Electron Microscope images of the devices show the micro- pores. See figure 4.18. Other SEM images are shown in Figure 4.19 (a) , (b).

C.   To characterize the device for optical properties , Ocean Optics Spectra Suite Mini Spectrometer experimental test set up was used. [SpectraSuite software, Model no. USB 4H02846 M/S Ocean Optics, Inc, Dunedin, FL 34698. Model name: USB 4000 UV-VIS miniature fiber optic spectrometer, with Halogen light source HL-2000-HP-FHSA 034990459). Figure 4.20 shows optical properties of the device when subjected to RED light Source. % transmittance was measured to a 58% at 628nm. % Absorbance was observed to 0.22 value at the same wavelength.
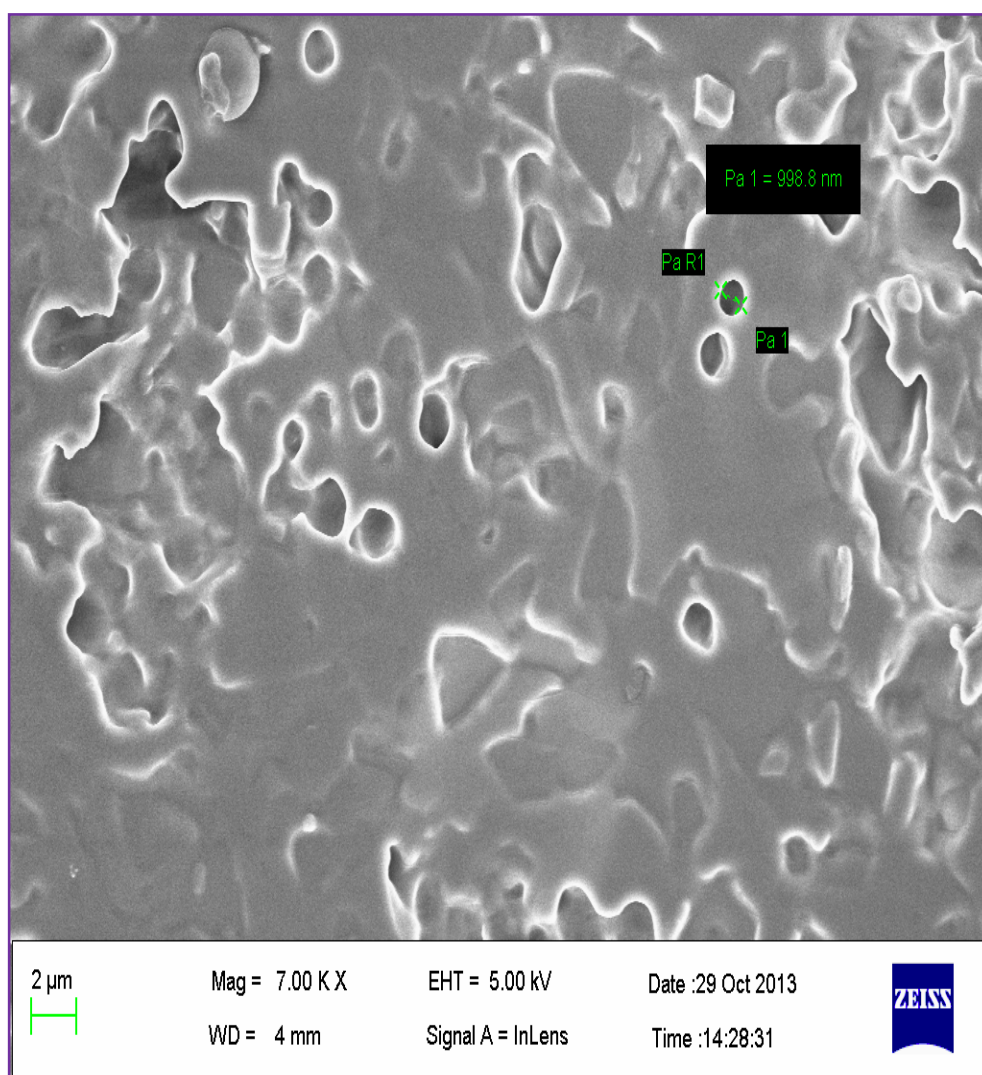
Fig. 4.18 SEM image of micropores in Porous PDMS/AO device surface.
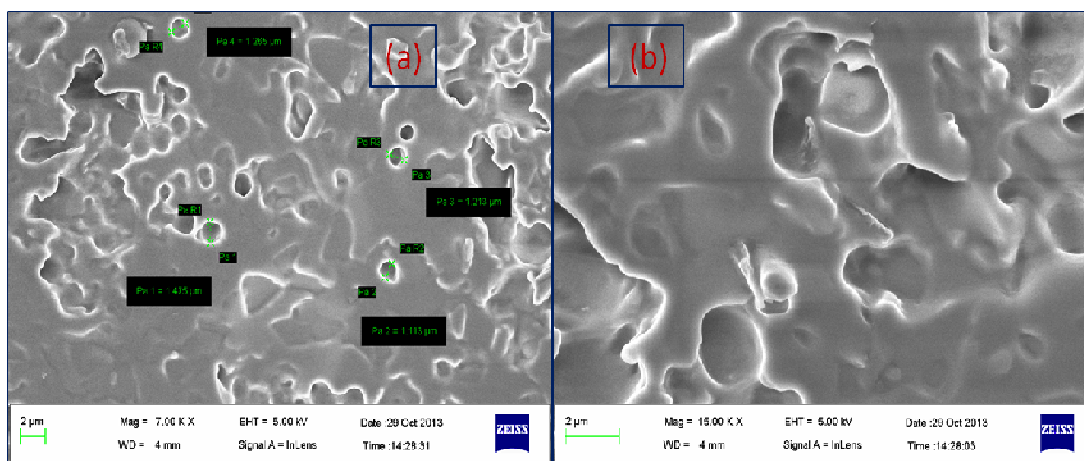
Fig. 4.19 (a) and (b) SEM images of surfaces of PPA microstructures.
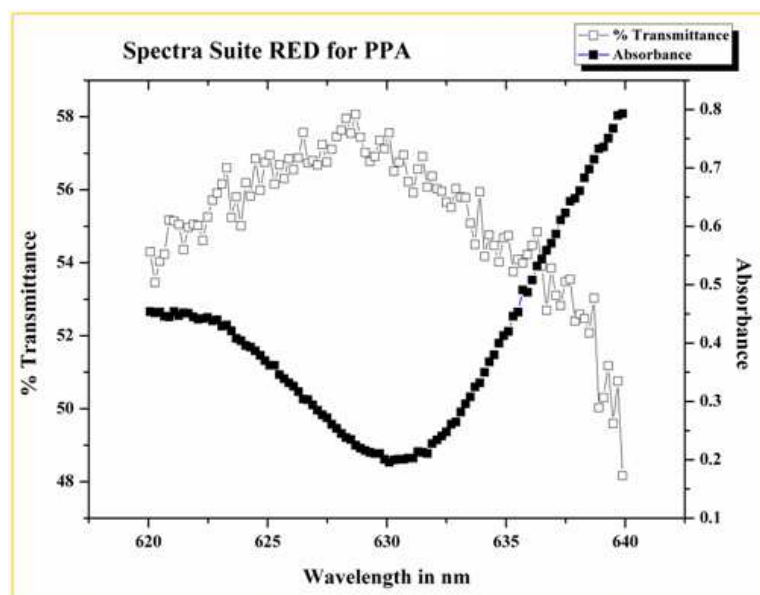
Fig. 4.20 Optical characteristics of PPA using [RED source] Spectra Suite optics test setup.

D. UV-VIS Spectometer characterization: Figure 4.21 shows the UV-VIS spectral response of the device. Peak absorbance was recorded as 0.509 at 500nm wavelength;

0.497 at 325nm

% peak Transmittance was:

38.86% at 392nm;

39 % at 634nm
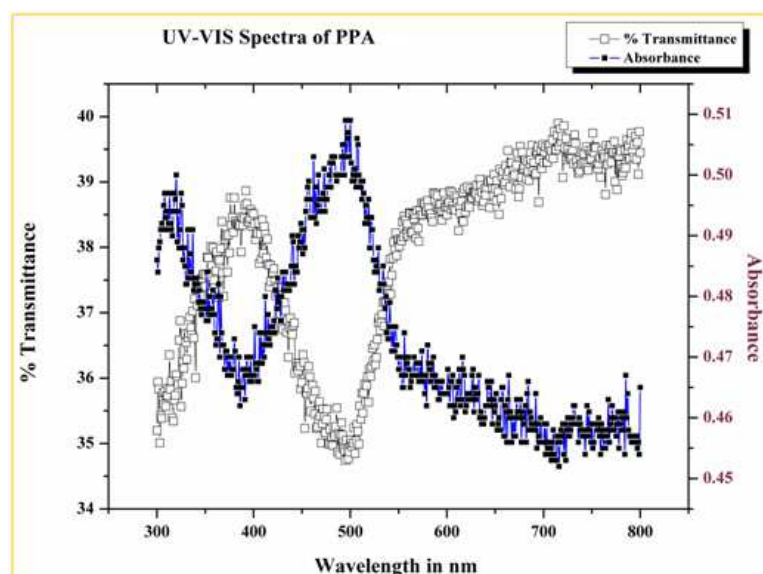
Fig. 4.21 UV-VIS spectrophotometer spectral characteristics of the PPA device [TOP first].

E.   NIKON fluorescence microscope (540nm source) with CCD camera was used to record images of a PPA device subjected to DNA detection test. Acridine orange dye tagged DNA solution was administered in the PDMS well of the PPA device. The device was placed under the 540nm filtered light source to observe fluorescence response. The image shown in figure 4.22 is recorded with a still camera [NIKON]. The device glowed under the green optical source.
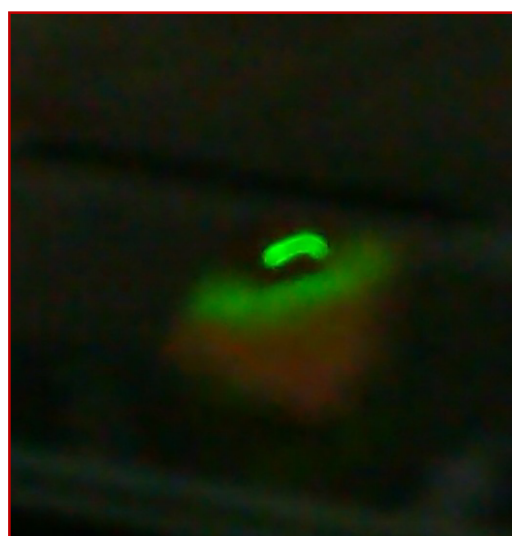
Fig. 4.22 Photo image of PPA device administered with AO tagged DNA solution, taken with NIKON still camera.

4.12   Conclusion

After extensive literature survey, on interaction of biomolecules on solid polymeric surfaces; SU8 microdroplet surface immobilisation procedure was explored with suitable, simpler and robust immobilization techniques. It was observed that UV exposed SU8 microdroplet surfaces can be prepared for protein immobilization.

In an era dominated by silica microspheres and optical fibers, polymer optical fibers and optical devices are creating some space. An attempt was made in fabricating a SU8 fiber coupler and biosensor. It is a biocompatible material and with proper functionalization it becomes suitable for the selected and specific immobilization of biological entities. Thus SU8 microdroplets with or without fiber bonding were surface functionalized, BSA immobilized and tested for antifouling property of BSA with GFP tagged E-Coli cell. Fluorimetry and SpectraSuite test setup were used for characterization of these droplets. It was observed that there is a possibility that E-Coli attaches to SU8 surface with a large density.

In B-part of the discussion, it was observed that, biomaterials are important in our lives to produce a range of biomedical articles like implants, dressings, drug delivery systems, sensors which are temporary, permanent or extracorporeal in their applications and provide immense relief, quality to life. An all encompassing study of these materials, their behaviour and properties, surface modification techniques leads to original and application specific products. In this work a novel biomaterial is produced using soft-lithography and by combining two biomaterials PDMS, AO. Its appearance (porous, reddish in colour, spongy) and properties are different from the base materials. The spongy structure had pore size of 998.8nm. Probable applications of this material may be, as dressing material for wounds, adhesives, filters, optical-biosensors, implants, detection of nanolevel locomotory motions of organisms [88].

4.13   Future Scope

It was a plan to have SU8 microdroplet diameter sizes limited to a range of ~ 80-100μm to get effective WGM inside the droplet. Also the contact angle of the droplet must be nearing 90° to get a near spherical droplet. After this both labled and

lable free techniques will be further used on Laser exposed and UV exposed microdroplets.

A range of porous PDMS - AO materials of differing physical, chemical, optical properties can be produced simply by varying concentrations of curing agent and AO in PDMS gel. With individual analysis of such materials a wide range of applications are possible. Future work involves experimenting, usage of the Porous PDMS –AO material as wound dressing strip, opto-biosensor, filter or as an implant. We wish to explore and want to change the image contrast by looking at the fluorescent PDMS. Further with the fluorescent PDMS microstructures we want to study nanolevel locomotory motions of the organisms. It is established that dye doped PDMS has much lower stiffness and is much softer than normal PDMS. Varying proportion, concentration in sensitive structures of PPA may lead to a live torch effect.

Reference

1. Ratner, Buddy D., Allan S. Hoffman, Frederick J. Schoen, and Jack E. Lemons, "An introduction to materials in medicine ", *Biomaterials Science* 484 (1996).

2. W. Norde, "Driving forces for protein adsorption at solid surfaces", Biopolymers at Interfaces, 75, p. 27–54 (1998).

3. W. Norde, "My voyage of discovery to proteins in flatland ...and beyond", *Colloids Surf B* 2008; 61:1.

4. W. Norde and C. E. Giacomelli, "BSA structural changes during homomolecular exchange between the adsorbed and the dissolved states", *J. Biotechnol.* 79, 259-268 (2000).

5. J. D. Andrade, V. Hlady and A. P. Wei, "Adsorption of complex proteins at interfaces", *Pure Appl. Chem.* 64, 1777-1781 (1992).

6. J. D. Andrade and V. Hlady, "Plasma protein adsorption: The big twelve", *Ann. NY Acad. Sci.* 516, 158-172 (1987).

7. S. Kalasin and Santore M. M. "Non-specific adhesion on biomaterial surfaces driven by small amounts of protein adsorption", *Colloids Surf., B* 73, 229-236 (2009).

8. U. M. Elofsson, M. A. Paulsson and T. Arnebrant, "Adsorption of β-lactoglobulin A and B: Effects of ionic strength and phosphate ions", *Colloids Surf., B* 8,163-169 (1997).

9. M. Wahlgren, U. Elofsson," Simple models for adsorption kinetics and their correlation to the adsorption of b-lactoglobulin A and B ", *J. Colloid Interface Sci.* 188, 21-129 (1997).

10. C. Janiak, " In order to sustain the gaze: Removing protein from contact lenses", *Chemie. in Unserer Zeit Volume: 35, 348-354 (2001).*

11. H. Noh and E. A. Vogler, "Volumetric interpretation of protein adsorption: mass and energy balance for albumin adsorption to particulate adsorbents with incrementally increasing hydrophilicity", *Biomaterials* 27**,** 5801–5812 (2006).

12. J. Israelachvili and H. Wennerstrom, "Role of hydration and water structure in biological and colloidal interactions", *Nature* 379, 219–225 (1996).

13. W. Norde, "Adsorption of proteins from solution at the solid-liquid Interface", *Adv. Colloid Interface Sci.* 25, 267-340 (1986).

14. C. A. Haynes and W. Norde, "Globular proteins at solid /liquid interfaces", *Colloids Surf., B* 2**,** 517-566 (1994).

15. J. D. Andrade, V. Hlady, "Protein adsorption and materials biocompatibility: A tutorial review and suggested hypotheses", *Adv. Polymer Sci.* 79, 1–63 (1986).

16. F. Rusmini, Y. Zhong and J. Feijen, "Protein Immobilization Strategies for Protein Biochips", *Biomacromolecules* 8, 1775–1789 (2007).

17. C. Mateo, O. Abian, G. Fernandez-Lorente, J. Pedroche, R. Fernandez-Lafuente and J. M. Guisan, "Epoxy sepabeads: a novel epoxy support for stabilization of industrial enzymes via very intense multipoint covalent attachment ", *Biotechnol. Prog.* 18, 629-634 *(*2002).

18. S. P. Fodor, J. L. Read, M. C. Pirrung, L. Stryer, A. T. Lu and D. Solas, Light-directed, spatially addressable parallel chemical synthesis. *Science* 251, 767–773(1991).

19. K. R. Bhushan, Light-directed maskless synthesis of peptide arrays using photolabile amino acid monomers.*Org. Biomol. Chem.* 4, 1857–1859 (2006).

20. S. Bhattacharya, A. Datta, J. M. Berg and S. Gangopadhyay, Studies on Surface Wettability of Poly(Dimethyl) Siloxane (PDMS) and Glass Under Oxygen-Plasma Treatment and Correlation With Bond Strength Plasma-modified Surfaces, *J. Microelectromech. Sys.* 14, 590-597 (2005).

21. H. Yasuda, "Plasma polymerization", Academic Press, 432 (1985).

22. P. K. Chu, J. Y. Chen, L. P. Wang and N. Huang, "Plasma-surface modification of biomaterials", *Mater. Sci. Eng., R* 36, 143–206 (2002).

23. C. M. Chan, T. M. Ko and H. Hiraoka, "Polymer surface modification by plasmas and photons", *Surf. Sci. Rep.* 24, 1–54 (1996).

24. M. Loughran, S. W. Tsai, K. Yokoyama and I. Karube, "Simultaneous iso-electric focusing of proteins in a microfabricated capillary coated with hydrophobic and hydrophilic" , *Curr. Appl. Phys.* 3, 495–499 (2003).

25. Jiun-Jeng Chen, Kimberly N. Struk, and Anthony B. Brennan, " Surface Modification of Silicate Glass Using 3-(Mercaptopropyl)trimethoxysilane for Thiol–Ene Polymerization ", *Langmuir*, 2011, 27 (22), pp 13754–13761.

26. S. Keller, G. Blagoi, M. Lillemose, D. Haefliger, A. Boisen, "Processing of thin SU-8 films", J. Micromech. Microeng. 18 (2008) 125020 (10pp).

27. Z. Wang , M. Stangegaard, M. Dufva, J.P.Kutter , A. Wolff, " A simple hydrophilic treatment of SU8 surfaces for cell culturing and cell patterning ", Int. Conf. on Miniaturized Systems for Chemistry and Life Sciences 2005 USA.

28. M.Joshi, R. Pinto, V. R. Rao, S. Mukherji, "Silanization and antibody immobilization on SU-8 ", Applied Surface Science 253 (2007) 3127-3132.

29. Y. Wang, J. Pai, H. Lai, C. E. Sims , M. Bachman , G. P. Li, N. L. Allbritton, "Surface graft polymerization of SU-8 for bio-MEMS applications", J. Micromech Microeng. 17 (2007) 1371-1380.

30. H.Chen, L.Yuan, W. Song, Z. Wu, D. Li, "Biocompatible polymer materials: Role of protein – surface interactions", Progress in Polymer Science 33 (2008) 1059 – 1087.

31. G. Blagoi, S. Keller, A. Johansson, A. Boisen, M. Dufva, "Functionalization of SU8 surfaces with IgG proteins", Applied Surface Science 255 (2008) 2896-2902.

32. M. Holgado, C.A. Barrios, F.J. Ortega, F.J. Sanza, R. Casquel, M..F. Laguna, M.J. Banuls, D. Lopez-Romero, R. Puchades, A. Maquiera, " Label-free biosensing by means of periodic lattices of high aspect ratio SU8 nanopillars ", Biosensors and Bioelectronics 25 (2010) 2553-2558.

33. D. Kim, A. E. Herr, "Protein immobilization techniques for microfluidic assays", Biomicrofluidics 7, 041501(2013).

34.   X. Feng, Z. Lin, L.Yang, C. Wang, C. Bai, " Investigation of the interaction between acridine orange and bovine serum albumin ", Talanta 47 (1998) 1223- 1229.

35. S.J.Park, H. Bae, J. Kim, B. Lim, J. Park, S. Park, " Motility enhancement of bacteria actuated microstructures using selective bacteria adhesion ", Lab on a Chip.

36. Mendel Friedman, "Applications of the Ninhydrin reaction for analysis of amino acids , peptides and proteins to agricultural and Biological sciences ", J. Agric. Food chem., 2004, 52 (3), pp 385-406.

37. Book: M. Zourob, A. Elwary, A. Turner , " Principles of Bacterial Detection : Biosensors , Recognition Receptors and Microsystems ", Springer 2008.

38. X. Fan, I.M. white, Review: "Optofluidic Microsystems for chemical and biological analysis", Nature Photonics, 2011.

39. C. Chou, H.Wu, C. Yu, Y. Chang, B. Hsieh , " Fiber –optic biosensor for antigen / antibody kinetic assays ", SPIE Newsroom

40. O. S. Wolfbeis," Fiber –optic chemical sensors and biosensors", Anal. Chem. 2004, 76, 3269 – 3284.

41. S.C.HER, C-Y TSAI, "Strain measurement of fiber optic sensor surface bonding on host material", Trans. Nonferrous Met. Soc. China 19(2009) s143-s149.

42. Bryant, Lange, "Fusion splice".

43. M.L.Chabinyc, D.T.Chiu, J.C.McDonald, A. D.Stroock, J.F. Christian , A.M. karger, G. M. Whitesides, " An integrated fluorescence detection system in Poly(dimethylsiloxane) for microfluidic applications", Anal. Chem. 2001, 73,4491-4498.

44. http://www.nrl.navy.mil/accomplishments/materials/fiber-optic-sensors.

45. K.T.V. Grattan, Dr. T. Sun," Fiber optic sensor technology: an overview", Sensors and Actuators 82 (2000) 40-61.

46. B. Lee," Review of the present status of optical fiber sensors", Optical Fiber Technology 9 (2003) 57-79.

47. M. Mahdkhani, Z.Bayati, "Application and development of fiber optic sensors in civil engineering", WCEE, 2008, China.

48. L.C. Shriver-Lake, A. W. Kusterbeck, F.S. Ligler, "Ch.5: Environmental Immunosensing at the naval research laoratory".

49. S. Ko, S. A. Grant, "A novel FRET –based optical fiber biosensor for rapid detection of Salmonella typhirium", Biosensors and Bioelectronics 21 (2006)1283-1290.

50. M.E. Bosch, A.J. R. Sanchez, F.S. Rojas, C.B. Ojeda ,Review " Recent development in optical fiber biosensors", Sensors 2007, 7, 797-859.

51. A. Leung, P.M. Shankar, R. Mutharasan, "A review of fiber optic biosensors", Sensors and Actuators B 125 (2007) 688-703.

52. X. Fan, I.M. White, S. I. Shopova, H. Zhu, J.D. Suter, Y. Sun , " Sensitive optical biosensors for unlabeled targets : a review ", ANALYTICA CHIMICA ACTA 620 (2008)8-26.

53.   T. Liu, Y. Zhao, Z. Zhang, P. Zhang, J. Li, R.Yang, C.Yang, L. Zhou , " A fiber optic biosensor for specific identification of dead Escherichia coli O157:H7", Sensors and Actuators B 196 (2014) 161-167.

54.   F. Vollmer, S. Arnold, "Whispering –gallery – mode biosensing: label-free detection down to single molecules" , Nature methods 5, 7, 591-596, (2008).

55.   S. Chemburu, K. Fenton, G.P.Lopez, R.Zeinldin, Review," Biomimetic silica microspheres in biosensing", Molecules 2010, 15, 1932-1957.

56.   X. Fan, I.M. White, S. I. Shopova, H. Zhu, J.D. Suter, Y. Sun , " Sensitive optical biosensors for unlabeled targets : a review ", ANALYTICA CHIMICA ACTA 620 (2008)8-26.

57.   J.P. Laine, B.E. Little, D. Lim, H.A. Haus, "Novel techniques for whispering- gallery-mode excitation in silica microspheres", OSA (1999).

58.   M.Cai, K. Vahala, "Highly efficient optical power transfer to whispering – gallery modes by use of a symmetrical dual coupling configuration", OPTICS LETTERS, OSA, 25, 4, (2000).

59.   A.N. Oravsky, Review: "Whispering –gallery waves", Quantum electronics 32 (5) 377-400 (2002).

60.   N. M. Hanumegowda, I.M.White, C. J. Stica, B. C. Patel, H. Oveys , X. Fan , " Development of label-free microsphere optical resonator bio/ chemical sensors ", Proc. Of SPI 6004, 600401 (2005).

61.   N. M. Hanumegowda, C. J. Stica, B.C. Patel , I. White, X. Fan ," Refractometric sensors based on microsphere resonators ", APPLIED PHYSICS LETTERS 87, 201107 (2005).

62.   I.M. White, N.M. Hanumegowda, H. Oveys, X. Fan , " Tuning whispering gallery modes in optical microspheres with chemical etching " ,OSA, OPTICS EXPRESS 13, 26, 10754-59 (2005).

63.   M.Noto, D. Keng, I. Teraoka, S. Arnold, " Detection of protein orientation on the silica microsphere surface using transverse electric/ transverse magnetic whispering gallery modes ", Biophysical Journal 92, 4466-4472 (2007).

64. I. M. White, X. Fan, "On the performance quantification of resonant refractive index sensors", OSA, OPTICS EXPRESS 16,2 , 1020-28 (2008).

65. S. Arnold, D. Keng, S.I. Shopova, S. Holler, W. Zurawsky, F. Vollmer, " Whispering gallery mode carousel – a photonic mechanism for enhanced nanoparticle detection in biosensing ", OPTICS EXPRESS , OSA, 17,8, (2009).

66. M.I. Cheema, A.G. Kirk, "Implementation of the perfectly matched layer to determine the quality factor of axisymmetric resonators in COMSOL", COMSOL conference, Boston, (2010).

67. J.Zehnpfennig, G. Bahl, M. Tomes, T. Carmon, "Surface optomechanics: calculating optically excited acoustical whispering gallery modes in microspheres", OPTICS EXPRESS, OSA , 19, 15 (2011).

68. M. Ornigotti, A. Aiello, "Analytical approximations of whispering gallery modes in anisotropic ellipsoidal resonators", OSA, (2011).

69. L.Huang, Z. Guo, "Biosensing in a microelecrofluidic system using optical whispering –gallery mode spectroscopy", AIP, Biomicrofluidics 5, 034114 (2011).

70. Seema Yardi, D. Boolchandani, Shantanu Bhattacharya, "Polymer waveguide and optical fiber coupling using whispering gallery modes in an elliptical micro-sleeve ", Optics in the Life Sciences Congress Technical Digest © 2013 The Optical Society of America (OSA)

71. J. Ward, O. Benson, "WGM microresonators: sensing, lasing and fundamental optics with microspheres", Laser photonics 5, 4, 553-570 (2011).

72. A. B. Matsko, V. S. Ilchenko, "Optical resonators with whispering gallery modes – Part I: Basics", *IEEE Journal of selected topics in Quantum Electronics, 12, 1 (2006).*

73. V.R. Dantham , S. Holler, V. Kolchenko, Z. Wan , S. Arnold, " Taking whispering gallery –mode single virus detection and sizing to the limit ", *Applied Physics letters 101, 043704 (2012).*

74. D. Farnesi, A. Barucci , G.C. Righini , S. Berneschi, S. Soria , G. N. Conti, " Optical frequency conversion in silica-whispering gallery mode microspherical resonators ", *PRL 112, 093901 (2014).*

75. J.R. Schwesyg, T. Beckmann, A,S. Zimmermann, K. Buse , D. Haertle, " Fabrication and characterization of whispering –gallery –mode resonators made of polymers ", *OSA, OPTICS EXPRESS 17 , 4, 2573-2578 (2009) .*

76. M.Joshi, R. Pinto, V. R. Rao, S. Mukherji, "Silanization and antibody immobilization on SU-8 ", *Applied Surface Science 253 (2007) 3127-3132.*

77. Y. Wang, J. Pai, H. Lai, C. E. Sims , M. Bachman , G. P. Li, N. L. Allbritton, "Surface graft polymerization of SU-8 for bio-MEMS applications", *J. Micromech Microeng. 17 (2007) 1371-1380.*

78. H.Chen, L.Yuan, W. Song, Z. Wu, D. Li, "Biocompatible polymer materials: Role of protein – surface interactions", *Progress in Polymer Science 33 (2008) 1059 – 1087.*

79. G. Blagoi, S. Keller, A. Johansson, A. Boisen, M. Dufva, "Functionalization of SU8 surfaces with IgG proteins", *Applied Surface Science 255 (2008) 2896-2902.*

80. V.S. Goudar, S. Suran, M.M. Varma, "Photoresist functionalisation method for high-density protein microarrays using photolithography", *Micro & Nano Letters (2012) 7, 6, 549-553.*

81. D. Kim, A. E. Herr, "Protein immobilization techniques for microfluidic assays", *Biomicrofluidics 7, 041501(2013).*

82. X.Feng, Z. Lin, L.Yang, C. Wang, C. Bai, " Investigation of the interaction between acridine orange and bovine serum albumin ", *Talanta 47 (1998) 1223- 1229.*

83. H. Mansur, R. Orefice, M. Pereira , Z. Lobato, W. Vasconcelos, L. Machado, "FTIR and UV-vis study of chemically engineered biomaterial surfaces for protein immobilization ", *Spectroscopy 16 (2002) 351-360.*

84. N.M. Hanumegowda, I.M. White, H. Oveys, X. Fan ,"Label-free protease sensors based on optical microsphere resonators", *Sansor Letter 3, 1-5 (2005)* .

85. M. Holgado, C. A. Barrios, F. J. Ortega, F. J. Sanza, R. Casquel, M.F. Laguna, M.J. Baňuls, D. Lopez-Romero, R. Puchades, A. Maquieira, Review " Label-free biosensing by means of periodic lattices of high aspect ratio SU-8 nano-pillars ", *Biosensors and Bioelectronics 25 (2010) 2553-2558.*

86. S.J. Park, H. Bae, J. Kim , B. Lim, J. Park , S. park , " Motility enhancement of bacteria actuated microstructures using selective bacteria adhesion ", *Lab Chip (2010) 10 1706-1711.*

87. S. Stefansson, D. Adams, C. Tang, "Sample preparation using buoyant silica microsphere*", 6th EDRN workshop, MD (2009).*

88. S.M. Khare, A. Awasthi, V. Venkatraman, S.P.Koushika, "Colored polydimethylsiloxane micropllar arrays for high throughput measurements of forces applied by genetic model organisms", *Biomicrofluidics 9(1):014111.February 2015 DOI: 10.1063/1.4906905.*

89. eng Feng, Z. Lin –Jin Yang , C. Wang , C.-Li Bai, " Investigation of the interaction between acridine orange and bovine serum albumin ", *Talanta 47 (1998) 1223-1229.*

90. V.S. Sukumaran, a. Ramalingam, "Spectral characteristics and non-linear studies of acridine orange dye", *Physics Letters A 34(2005) 454-458.*

91. A.Mata, A.J. Fleischman, S.Roy, "Characterization of Polymethylsiloxane (PDMS) properties for biomedical micro-nanosystems", *Biomedical Microdevices 7:4 (2005) 281-293.*

92. H.Chen, L.Yuan, W.Song, Z.Wub, D. Li," Biocompatible polymer materials: Role of protein –surface interactions", *Progress in Polymer Science 33 (2008) 1059-1087.*

93. M.R.Fernandez, M.G. Casabona, V.N.Anupama, B. Krishnakumar, G.A. Curutchet, D.L. Bernik, " PDMS based porous particles as support beds for cell immobilization : Bacterial biofilm formation as a function of porosity

and polymer composition ", *Colloids and Surfaces B: Biointerfaces, 81,1 (2010), 289-296.*

94.   N. Saha, A. Saarai, N.Roy, T.Kitano, P. Saha,"Polymeric biomaterial based hydrogels for biomedical applications", *Journal of Biomaterials and Nanobiotechnology (2011) 2, 85-90.*

95.   X. Huang , H. D. Halicka, F. Traganos, T. Tanaka , A. Kurose, Z. Darzynkiewicz, "Cytometric assessment of DNA damage in relation to cell cycle phase and apoptosis ", *NIH PA 2005 38(4).*

96.   Abbasi F, Mirzadeh H, Simjoo M , " Hydrophilic interpenetrating polymer networks of polydimethyl siloxane (PDMS) as biomaterial for cochlear implants ",*J Biomater Sci Polym Ed 2006 ; 17(3) ; 341-55.*

97.   Van Dyke M E, Clarson S J , Arshady R, " Introduction to polymeric biomaterials ", *Silicone biomaterials, PBM series, 2003 : (1) ; 109- 135.*

98.   Ratner B D , Hoffman A S, Schoen F J , Lemons J E , " An introduction to materials in medicine ", *Editors. Biomaterials Science, 2nd Ed. London: Elsevier Academic Press; 2004.*

99.   Biomaterial Tutorial: Felix Simonvsky, "Polymethylsiloxanes (PDMS)", *University of Washington Biomaterial Engineering.*

100.   Book : Stuart L. Cooper , C H Bamford , Teiji Tsuruta , T Suruta, " Polymer Biomaterials in Solution, as interfaces and as Solids", *Journal of Biomaterial Science Polymer Edition.*

        J Caix, G Janvier , B Legault, L Bordenave , F Rouais, B Basse-Cathalinat, C Baquey " A canine *ex vivo* shunt for isotopic hemocompatibility evaluation of a NHLBI DTB primary reference material and of a IUPAC reference material ".

101.   G Bartelena, Y Loosli, T Zambelli, J G Snedeker, "Biomaterial surface modifications can dominate cell-substrate mechanics : the impact of PDMS plasma treatment on a quantitative assay of cell stiffness ", *Royal Society of Chemistry , 2012, 8, 673-681.*

102. S Bhat, Ashok Kumar, "Biomaterials and Bioengineering tomorrow's healthcare", *Landes Bioscience special review, Biomatter 3:3, e24717, 2013.*

103. C Hassler, T Boretius, T Stieglitz , "Polymers for Neural implants", *Journal of Polymer Science : Part B : Polymer Physics 2011,49,18-33.*

List of Publications

[A]   Published international Journal Papers:

(1)   **Seema D.Yardi**, Ankur Gupta, Poonam Saundriyal, Geeta Bhatt, Rishi Kant, D. Boolchandani, Shantanu Bhattacharya, "High efficiency coupling of optical fibres with SU8 micro-droplet using laser welding process ", *Laser in Manufacturing and materials Processing*, DOI:10.1007/s40516-016-0027-6, 2016.

[B]   Refereed International Conference Proceedings:

[1]   **Seema Yardi,** D. Boolchandani, Shantanu Bhattacharya, "Polymer Waveguide and Optical Fiber Coupling Using Whispering Gallery Modes in an Elliptical Micro- Sleeve", *Optics in Lifesciences*, Optical Society of America, Hawaii, USA, 2013 [JT2A.12].

[C]   International Conference Paper

[1]   **Seema Yardi,** D. Boolchandani, Shantanu Bhattacharya, "Porous Polydimethyl Siloxane (PDMS)- Acridine Orange (AO) as a biomaterial in opto-biosensing", International Symposium for Research Scholars (ISRS) – (11th -13th December) 2014, IC & SR Auditorium, IIT, Madras, India .

Bio-Data

Seema D. Yardi has nearly 30 years of teaching experience. She is working as Lecturer in Electronics, Department of Technical Education, Maharashtra State, since September 1992 with current posting at Government Polytechnic, Aurangabad. She obtained Bachelor's degree in Electronics and Telecommunications [E & T/C] from Government College of Engineering, Pune, M.S. [COEP], Master's degree in Electronics Engineering from Government College of Engineering, Aurangabad, M.S., India. She is currently pursuing Ph.D. at Malaviya National Institute of Technology, Jaipur, India, in the field of Optical signal Coupling & Bio-Sensing under the AICTE QIP (Poly) scheme of Government of Maharashtra. Besides teaching, she has carried out all the administrative responsibilities entrusted on her by the department. She is currently member of IEEE, USA, life member of IETE India, IMAPS India, ISTE India, OSA USA.

APPENDIX:

Data on Design of Experiments [DOE]:

ANOVA mathematical model

RSM: Response Surface methodology

Factors and final equations of Laser heat transfer bonding / fabrication:

Factors: Lasing speed, Lasing power

Objective: Single: Transmitance

Final Equation in terms of coded factors:

$Sqrt (Transmission) =$

$+0.046$

$+0.27 * A$

$-0.085 * B$

$-0.017 * A * B$

$+0.21 * A^2$

$+0.24 * B^2$

Final Equation in terms of Actual Factors:

$t (Transmission) =$

$+11.12031$

$-0.48362 * Power$

$-0.90516 * Speed$

$-2.83637E\text{-}003 * Power * Speed$

$-5.80923E\text{-}003 * Power^2$

$-0.23772 * Speed^2$